Falkland Islands Fisheries Department

Vessel Units

Allowable Effort

Allowable Catch

2017

Part 2

Stock assessments

Contributors

Alexander Arkhipkin	*Foreword, Editor*
Michaël Gras, Brendon Lee	*Rock cod, hake and other finfish*
Andreas Winter	*Loligo, Toothfish, Skates*

For citation purposes this publication should be referenced as follows:

FIFD (2016) Vessel Units, Allowable Effort, and Allowable Catch 2017. Fisheries Department, Directorate of Natural Resources, Falkland Islands Government.

Contents

1. Foreword

The Licensing Advice 2017 consists of two parts.

The brief report (Part 1) contains summaries of licensing advices for all regulated fisheries in Falkland Islands Conservation Zones for 2016 apart from the B-licensed *Illex*-fishery. It has been done using the data collected up to December 2015, and for Falkland calamari and finfish up to April 2016. Summary tables are presented at the end of the report.

The present full report (Part 2) contains a more detailed description of main assumptions, methods and stock assessments for those fisheries in 2015, and recommendations for their management in terms of calculated effort (vessel units) and total allowable catch (where applicable).

2. *Doryteuthis gahi* (*Loligo*) – Falkland calamari

2.1. Summary

1) The 2016 first season Falkland calamari fishery (C license) was open from February 24th, and closed as scheduled on April 28th. A sub-area of the Loligo Box was closed from April 7th to the end of the season to conserve small (younger) calamari, west of 57°15' W and between 51°00' and 51°30' N.
2) 22,616 tonnes of calamari catch were reported in the C-license fishery; giving an average CPUE of 22.17 tonnes vessel-day^{-1}. Throughout the season 49.0% of calamari catch and 48.7% of fishing effort were taken north of 52º S; vs. 51.0% of calamari catch and 51.3% of fishing effort taken south of 52º S. These are the most even north / south catch and effort partitions of any recent 1st season, with higher concentration towards the centre of the Loligo Box than usual.
3) Sub-areas north and south of 52°S were depletion-modelled separately. In the north sub-area, seven depletion periods / immigrations were inferred to have started on March 2nd, March 5th, March 21st, March 28th, April 4th, April 11th, and April 17th. In the south sub-area, five depletion periods / immigrations were inferred to have started on February 24th, March 10th, March 25th, March 30th, and April 4th.
4) Approximately 43,874 tonnes of calamari (95% confidence interval: [38,489 to 82,768] tonnes) were estimated to have immigrated into the Loligo Box during 1st season 2016, of which 13,290 t north of 52º S and 30,584 t south of 52º S.
5) The biomass estimate for calamari remaining in the Loligo Box at the end of 1st season 2016 was:
   Maximum likelihood of 24,868 tonnes, with a 95% confidence interval of [20,723 to 61,272] tonnes. With the bulk of calamari biomass entering the fishing zone as late immigrations, this season was unusual in having higher estimated calamari abundance at the end of the season than at the beginning of the season.
   The risk of calamari escapement biomass at the end of the season being less than 10,000 tonnes was estimated at effectively zero.

2.2. Introduction

The first season of the 2016 Falkland calamari fishery (*Doryteuthis gahi* – Patagonian longfin squid – colloquially *Loligo*) opened on February 24th with 16 C-licensed vessels participating; none having taken the flex option to start later. Early in March one vessel suffered mechanical failure and was towed to port by a sister ship. The tow vessel and damaged vessel were allocated extensions of 2 and 3 days respectively at the end of the season for time missed from the fishery, equivalent to the flex option. A different vessel suffered mechanical failure in late March and was replaced by a sister ship for 14 days from March to early April. On April 7th, a sub-area of the Loligo Box was excluded until the end of the season to conserve small (younger) calamari, consisting of grid XNAN in its entirety and grids XNAP and XPAP west of 57°15' W. The first season ended by directed closure on April 28th, plus respectively on April 30th and May 1st for the two flex-allocated vessels.

Total reported Falkland calamari catch under first season C license was 22,616 tonnes, corresponding to a CPUE of 22616 / 1020 = 22.17 tonnes vessel-day^{-1} (Table 1). This CPUE was the lowest in a first season since 2011, and the lowest in a first season not closed by emergency order since 2009.

As in previous seasons, the Falkland calamari stock assessment was conducted with depletion time-series models (Agnew et al., 1998; Roa-Ureta and Arkhipkin, 2007; Arkhipkin et al., 2008). Because calamari has an annual life cycle (Patterson, 1988), stock cannot be derived from a standing biomass carried over from prior years (Rosenberg et al., 1990). The depletion model instead calculates an estimate of population abundance over time by evaluating what levels of abundance and catchability must be extant to sustain the observed rate of catch. Depletion modelling is used both in-season and for the post-season summary, with the objective of maintaining an escapement biomass of 10,000 tonnes calamari at the end of each season as a conservation threshold (Agnew et al., 2002; Barton, 2002).

Table 2.1. Falkland calamari season comparisons since 2004. Days: total number of calendar days open to licensed calamari fishing including (since 1st season 2013) optional extension days; V-Days: aggregate number of licensed calamari fishing days reported by all vessels for the season.

	Season 1			Season 2		
	Catch (t)	Days	V-Days	Catch (t)	Days	V-Days
2004				17,559	78	1271
2005	24,605	45	576	29,659	78	1210
2006	19,056	50	704	23,238	53	883
2007	17,229	50	680	24,171	63	1063
2008	24,752	51	780	26,996	78	1189
2009	12,764	50	773	17,836	59	923
2010	28,754	50	765	36,993	78	1169
2011	15,271	50	771	18,725	70	1099
2012	34,767	51	770	35,026	78	1095
2013	19,908	53	782	19,614	78	1195
2014	28,119	59	872	19,630	71	1099
2015	19,383*	57*	871*	10,190	42	665
2016	22,616	68	1020			

* Does not include C-license catch or effort after the C-license target for that season was switched from calamari to *Illex*.

2.3. Methods

The depletion model formulated for the Falkland calamari stock is based on the equivalence:

$$C_{day} = q \times E_{day} \times N_{day} \times e^{-M/2} \quad \textbf{(1)}$$

where q is the catchability coefficient, M is the natural mortality rate (considered constant at 0.0133 day^{-1}; Roa-Ureta and Arkhipkin, 2007), and C_{day}, E_{day}, N_{day} are catch (numbers of calamari), fishing effort (numbers of vessels), and abundance (numbers of calamari) per day. In its basic form (DeLury, 1947) the depletion model

assumes a closed population in a fixed area for the duration of the assessment. However, the assumption of a closed population is imperfectly met in the Falkland Islands fishery, where stock analyses have often shown that calamari groups arrive in successive waves after the start of the season (Roa-Ureta, 2012; Winter and Arkhipkin, 2015). Arrivals of successive groups are inferred from discontinuities in the catch data. Fishing on a single, closed cohort would be expected to yield gradually decreasing CPUE, but gradually increasing average individual sizes, as the squid grow. When instead these data change suddenly, or in contrast to expectation, the immigration of a new group to the population is indicated (Winter and Arkhipkin 2015).

In the event of a new group arrival, the depletion calculation must be modified to account for this influx. This was done using a simultaneous algorithm (Roa-Ureta, 2012) that adds new arrivals on top of the stock previously present, and posits a common catchability coefficient for the entire depletion time-series. If two depletions are included in the same model (i.e., the stock present from the start plus a new group arrival), then:

$$C_{day} = q \times E_{day} \times (N1_{day} + (N2_{day} \times i2|_0^1)) \times e^{-M/2} \quad \textbf{(2)}$$

where i2 is a dummy variable taking the values 0 or 1 if 'day' is before or after the start day of the second depletion. For more than two depletions, $N3_{day}$, i3, $N4_{day}$, i4, etc., would be included following the same pattern.

The Falkland calamari stock assessment was calculated in a Bayesian framework (Punt and Hilborn, 1997), whereby results of the season depletion model are conditioned by prior information on the stock; in this case the information from the pre-season survey. The season depletion likelihood function was calculated as the difference between actual catch numbers reported and catch numbers predicted from the model (equation **2**), statistically corrected by a factor relating to the number of days of the depletion period (Roa-Ureta, 2012):

$$((n\text{Days} - 2)/2) \times \log\left(\sum_{days} \left(\log(\text{predicted } C_{day}) - \log(\text{actual } C_{day})\right)^2 \right) \quad \textbf{(3)}$$

The survey prior likelihood function was calculated as the normal distribution of the difference between catchability (q) derived from the survey abundance estimate, and catchability derived from the season depletion model:

$$\frac{1}{\sqrt{2\pi \cdot SD_{q\,survey}{}^2}} \times \exp\left(-\frac{(q_{model} - q_{survey})^2}{2 \cdot SD_{q\,survey}{}^2} \right) \quad \textbf{(4)}$$

Catchability q, rather than abundance N, was used for calculating the survey prior likelihood because catchability informs the entire season time series; whereas N from the survey only informs the first season depletion period – subsequent immigrations and depletions are independent of the abundance that was present during the survey.

Bayesian optimization of the depletion was calculated by jointly minimizing equations **3** and **4**, using the Nelder-Mead algorithm in R programming package 'optimx' (Nash and Varadhan, 2011). Relative weights in the joint optimization were assigned to equations **3** and **4** as the converse of their coefficients of variation (CV), i.e., the CV of the prior became the weight of the depletion model and the CV of the

depletion model became the weight of the prior. Calculations of the CVs are described in the Appendix. Because a complex model with multiple depletions may converge on a local rather than a global minimum, the optimization was stabilized by running a feed-back loop that set the q and N parameter outputs of the Bayesian joint optimization back into the in-season-only minimization (equation **3**), re-calculated this minimization and the CV resulting from it, then re-calculated the Bayesian joint optimization, and continued this process until both the in-season minimization and the joint optimization remained unchanged.

With C_{day}, E_{day} and M being fixed parameters, the optimization of equation **2** using **3** and **4** produces estimates of q and N1, N2, …, etc. Numbers of calamari on the final day (or any other day) of a time series are then calculated as the numbers N of the depletion start days discounted for natural mortality during the intervening period, and subtracting cumulative catch also discounted for natural mortality (CNMD). Taking for example a two-depletion period:

$$\begin{aligned} N_{\text{final day}} = {} & N1_{\text{start day 1}} \times e^{-M\,(\text{final day} - \text{start day 1})} \\ & + N2_{\text{start day 2}} \times e^{-M\,(\text{final day} - \text{start day 2})} \\ & - CNMD_{\text{final day}} \end{aligned} \quad \textbf{(5)}$$

where

$$CNMD_{\text{day 1}} = 0$$

$$CNMD_{\text{day x}} = CNMD_{\text{day x-1}} \times e^{-M} + C_{\text{day x-1}} \times e^{-M/2} \quad \textbf{(6)}$$

$N_{\text{final day}}$ is then multiplied by the average individual weight of calamari on the final day to give biomass. Daily average individual weight is obtained from length / weight conversion of mantle lengths measured in-season by observers, and also derived from in-season commercial data as the proportion of product weight that vessels reported per market size category. Observer mantle lengths are scientifically precise, but restricted to 1-2 vessels at any one time that may or may not be representative of the entire fleet. Commercially proportioned mantle lengths are relatively less precise, but cover the entire fishing fleet. Therefore, both sources of data are used. Daily average individual weights are calculated by averaging observer size samples and commercial size categories where observer data are available, otherwise only commercial size categories. To smooth fluctuations, $N_{\text{final day}}$ (or N on any other day of interest) is multiplied by the expected value of the average individual weight from its GAM trend (see Appendix), rather than by the empirical value on each day.

Distributions of the likelihood estimates from joint optimization (i.e., measures of their statistical uncertainty) were computed using a Markov Chain Monte Carlo (MCMC) (Gamerman and Lopes, 2006), a method that is commonly employed for fisheries assessments (Magnusson et al., 2013). MCMC is an iterative process which generates random stepwise changes to the proposed outcome of a model (in this case, the q and N of calamari) and at each step, accepts or nullifies the change with a probability equivalent to how well the change fits the model parameters compared to the previous step. The resulting sequence of accepted or nullified changes (i.e., the 'chain') approximates the likelihood distribution of the model outcome. The MCMC of the depletion models were run for 200,000 iterations; the first 1000 iterations were discarded as burn-in sections (initial phases over which the algorithm stabilizes); and the chains were thinned by a factor equivalent to the maximum of either 5 or the inverse of the acceptance rate (e.g., if the acceptance rate was 12.5%, then every 8^{th} (0.125^{-1}) iteration was retained) to reduce serial correlation.

For each model three chains were run; one chain initiated with the parameter values obtained from the joint optimization of equations **3** and **4**, one chain initiated with these parameters ×2, and one chain initiated with these parameters ×¼. Convergence of the three chains was accepted if the variance among chains was less than 10% higher than the variance within chains (Brooks and Gelman, 1998). When convergence was satisfied the three chains were combined as one final set. Equations **5**, **6**, and the multiplication by average individual weight were applied to the CNMD and each iteration of N values in the final set, and the biomass outcomes from these calculations represent the distribution of the estimate. The peaks of the MCMC histograms were compared to the empirical optimizations of the N values.

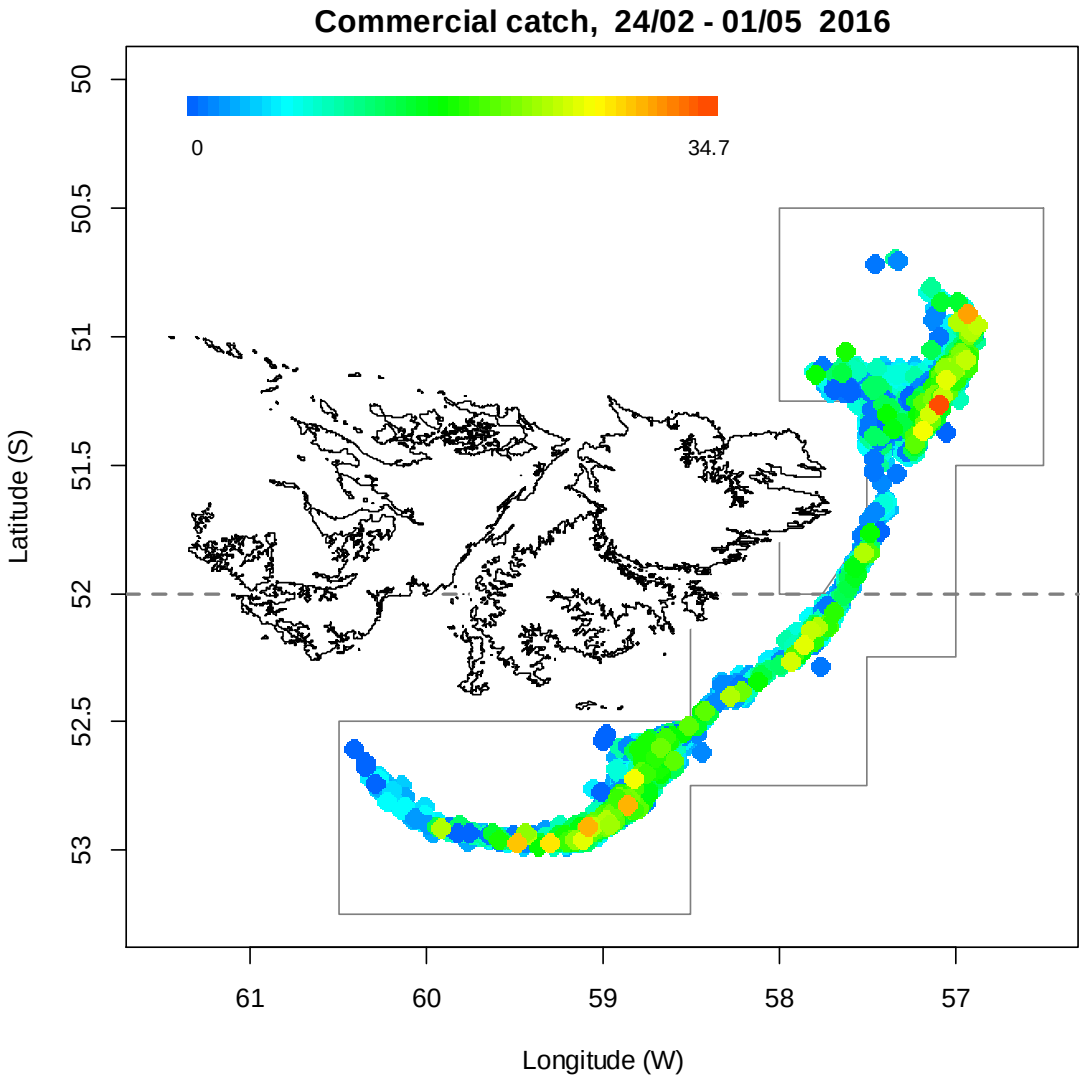

Figure 2.1. Spatial distribution of Falkland calamari 1st-season 2016 commercial catches, colour-scaled to catch weight (maximum = 34.7 tonnes). 3143 trawl catches were taken during the season. The Loligo Box fishing zone, as well as the 52 ºS parallel delineating the boundary between north and south assessment sub-areas, are shown in grey.

Total escapement biomass is defined as the aggregate biomass of calamari on the last day of the season for north and south sub-areas combined. Calamari sub-stocks emigrate from different spawning grounds and remain to an extent segregated

(Arkhipkin and Middleton, 2002). However, north and south biomasses are not assumed to be uncorrelated (Shaw et al., 2004), and therefore north and south likelihood distributions were added semi-randomly in proportion to the strength of their day-to-day correlation (semi-randomization algorithm in Winter, 2014b).

2.4. Stock assessment

2.4.1. Data

Falkland calamari catches were characterized in this season by an uncommonly even concentration throughout the Loligo Box (Figure 1). 7.3% of the catch by weight and 11.8% of vessel-days were taken in what was previously defined as the centre sub-area, between 52º S and 52.5º S (Payá, 2009; Roa-Ureta and Arkhipkin, 2007). By comparison, in first seasons of 2011, 2012, 2013, 2014, and 2015, percentages of catch taken in the centre were 0.8%, 2.4%, 0.07%, 0.05%, and 0.8%; percentages of vessel-days taken in the centre were 2.5%, 5.5%, 1.2%, 0.6%, and 5.9% (Winter, 2011; 2012; 2013; 2014a; 2015).

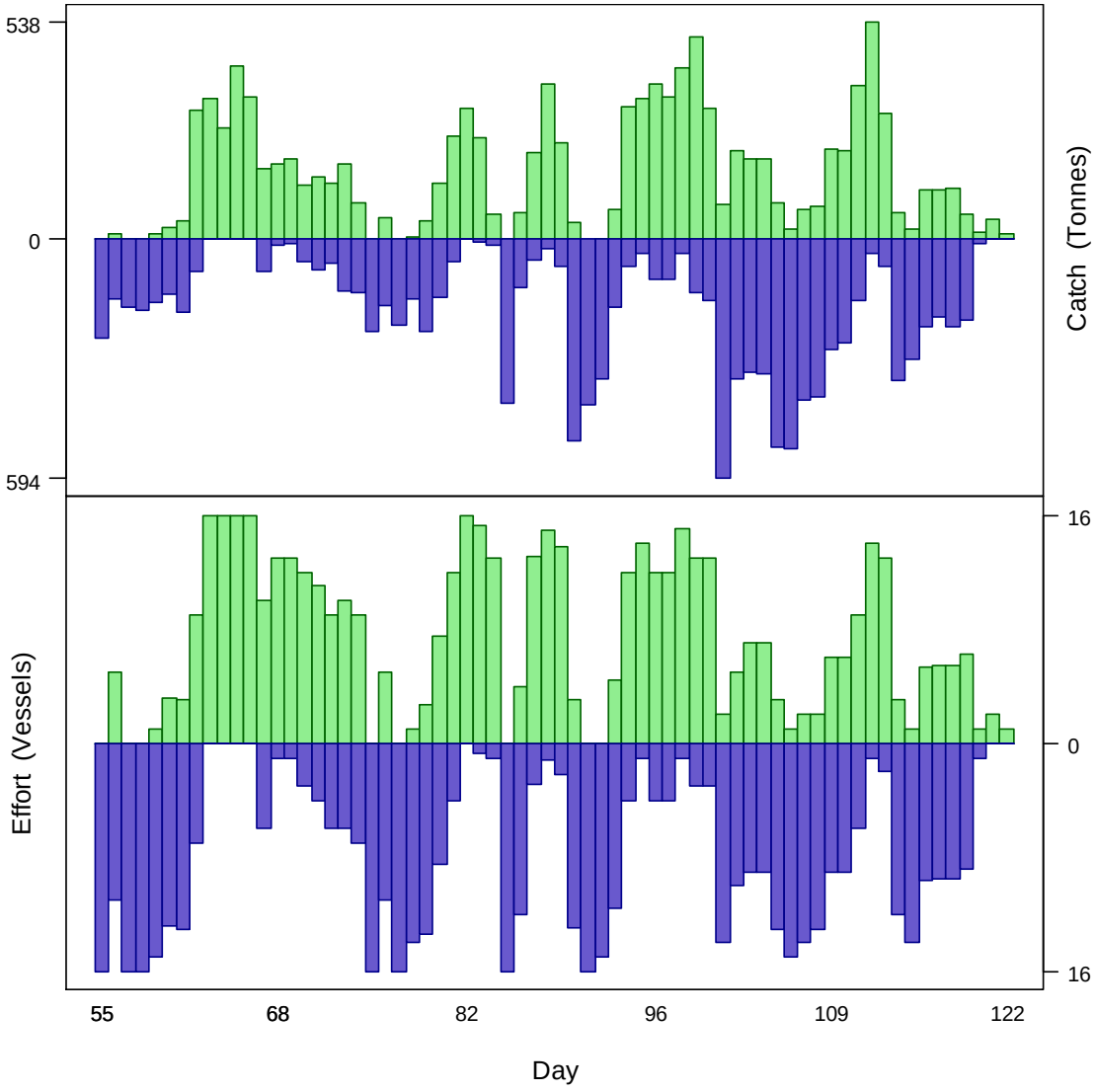

Figure 2.2. Daily total Falkland calamari catch and effort distribution by assessment sub-area north (green) and south (purple) of the 52º S parallel during 1st season 2016. The season was open from February 24th (chronological day 55) to April 28th (chronological day 119), plus flex days for two vessels until day 121 and for one vessel until day 122. As many as 16 vessels fished per day north of 52º S; as many as 16 vessels fished per day south of 52º S. As much as 538 tonnes calamari was caught per day north of 52º S; as much as 594 tonnes calamari was caught per day south of 52º S.

A total of 1020 vessel-days were fished during the season, with a median of 16 and no fewer than 14 vessels per day (except for the flex extensions). Vessels reported daily catch totals to the FIFD and electronic logbook data that included trawl start and end times, trawl positions, and product weight by market size categories. Two FIFD observers were deployed on three vessels in the fishery for a total of 72 observer-days (Bradley, 2016a; 2016b; Iriarte, 2016). Throughout the 68 days of the season, 4 days had no observer covering (3 of which were the extension days at the end), 56 days had 1 observer covering, and 8 days had two observers covering. Observers sampled an average of 417.3 calamari daily, and reported calamari maturity stages, sex, and mantle lengths to 0.5 cm. The length-weight relationship for converting both observer length data and commercially proportioned length data was taken from the pre-season survey (Winter et al, 2016):

$$\text{weight (kg)} = 0.112 \times \text{length (cm)}^{2.374} / 1000 \quad \textbf{(7)}$$

2.4.2. Group arrivals / depletion criteria

Start days of depletions - following arrivals of new calamari groups - were judged primarily with reference to daily changes in CPUE, with additional information from sex proportions, maturity, and average individual calamari sizes. CPUE was calculated as metric tonnes of calamari caught per vessel per day. Days were used rather than trawl hours as the basic unit of effort. Commercial vessels do not trawl standardized duration hours, but rather durations that best suit their daily processing requirements. An effort index of days is therefore more consistent.

Seven days in the north and five days in the south were identified that represented the onset of separate immigrations / depletions in the season. This exceptionally high number of immigrations (e.g., Winter and Arkhipkin, 2015) concurred with the outcome that catches and overall CPUE continued to increase in the fishery until three weeks before the end of the season (Figure 2), suggesting a generally late start to the out-migration.

- The first depletion north was identified on day 62 (March 2nd), one week after the start of the season but the first day that more than a third of the fleet fished north. Day 62 had the highest CPUE in the north until day 99 (April 8th) (Figure 3).
- The second depletion north was identified just three days later on day 65 (March 5th) with a rebound of CPUE after two days' decrease (Figure 3) and local minimal values of commercial and observer average weights, proportion of females, and average maturities (Figure 4).
- The third depletion north was identified on day 81 (March 21st) with a modest CPUE increase (Figure 3) but clear minima in commercial and observer average weights (Figure 4A & B).

- The fourth depletion north was identified on day 88 (March 28th) with a local CPUE peak (Figure 3) and one day after minima in average weights and proportion of females (Figure 4A, B & C).
- The fifth depletion north was identified on day 95 (April 4th) with steep minima in observer average weights and proportion of females (Figure 4B & C).
- The sixth depletion north was identified on day 102 (April 11th) with the highest CPUE north of the season (Figure 3), and minima in observer average weights and proportion of females (Figure 4B & C).
- The seventh depletion north was identified on day 108 (April 17th) with a local peak in CPUE (albeit taken by only two vessels, Figure 3), and the lowest minimum in commercial average weights until the end of the season (Figure 4A).
- The first depletion south was identified on day 55 (February 24th – the start of the commercial season) with 16 vessels starting the fishery in the south (Figure 2) and the highest CPUE in the south until day 70 (March 10th) (Figure 3).
- The second depletion south was identified on day 70. Besides the local CPUE peak that day (Figure 3), average weights had been at a local minimum the day before (Figure 4A & B).
- The third depletion south was identified on day 85 (March 25th) with the highest CPUE in the south up to that date (Figure 3). Average weights and maturity were not clearly associated with any time series minima (Figure 4A, B & D), resulting in this depletion start being questionable. However, the depletion model would have been difficult to execute without inferring a depletion start on this date.
- The fourth depletion south was identified on day 90 (March 30th). CPUE attained another season high (Figure 3), while average observer weight was near a local minimum (Figure 4B).
- The fifth depletion south was identified on day 95 (April 4th), when CPUE attained the second-highest peak of the season (Figure 3) and commercial average weight was at a steep local minimum (Figure 4A).

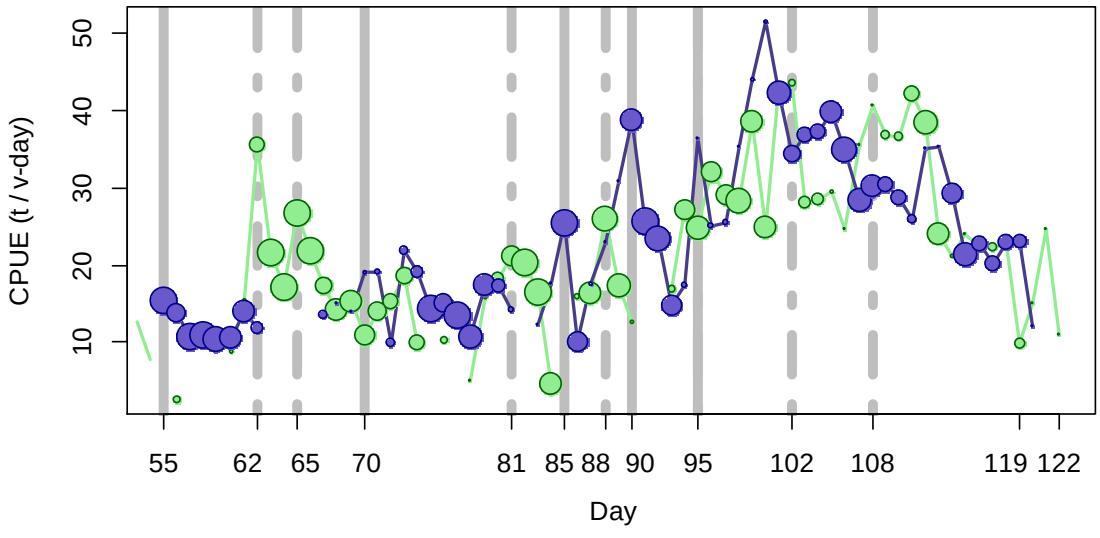

Figure 2.3. CPUE in metric tonnes per vessel per day, by assessment sub-area north (green) and south (purple) of 52º S latitude. Circle sizes are proportioned to the numbers of vessel fishing. Data from consecutive days are joined by line segments. Broken grey bars indicate the starts of in-season depletions north. Solid grey bars indicate the starts of in-season depletions south (day 95 was a depletion start both north and south).

Figure 2.4 (next page). A: Average individual calamari weights (kg) per day from commercial size categories. B: Average individual calamari weights (kg) by sex per day from observer sampling. C: Proportions of female calamari per day from observer sampling. D: Average maturity value by sex per day from observer sampling. In all graphs – Males: triangles, females: squares, unsexed: circles. North sub-area: green, south sub-area: purple. Data from consecutive days are joined by line segments. Broken grey bars indicate the starts of in-season depletions north. Solid grey bars indicate the starts of in-season depletions south (day 95 was a depletion start both north and south).

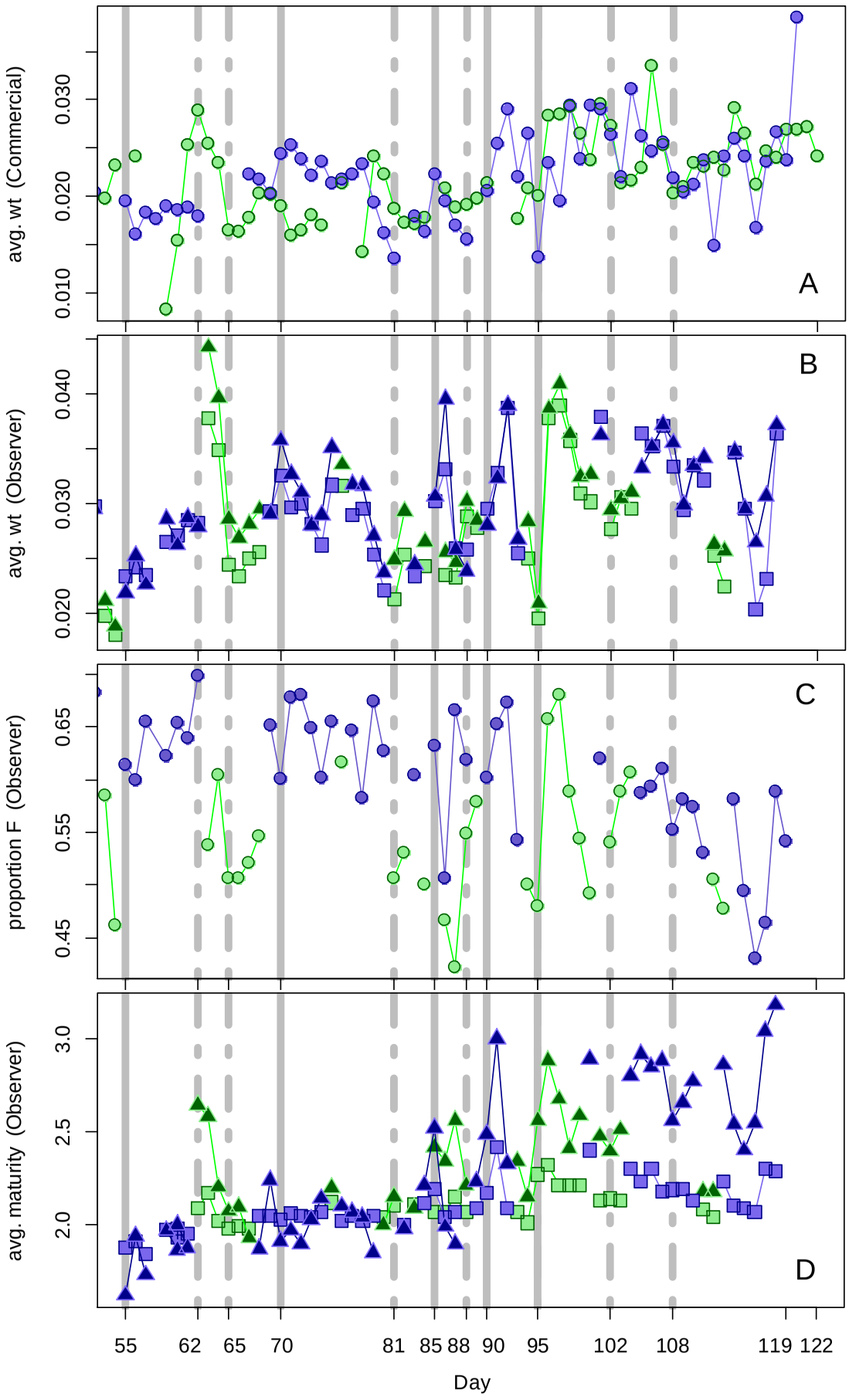
avg. wt (Commercial)
0.010
0.020
0.030
A
avg. wt (Observer)
0.020
0.030
0.040
B
proportion F (Observer)
0.45
0.55
0.65
C
avg. maturity (Observer)
2.0
2.5
3.0
D
55
62
65
70
81
85
88
90
95
102
108
119
122
Day

2.4.3. Depletion analyses

2.4.3.1. North

In the north sub-area, Bayesian optimization on catchability (q) resulted in a posterior (maximum likelihood $_{Bayesian}$ $q_N = 3.870 \times 10^{-3}$; Figure 5, left, and Equation **A9-N**) that was closer to the pre-season prior ($_{prior}$ $q_N = 3.681 \times 10^{-3}$; Figure 5, left, and Equation **A4-N**) than to the in-season depletion ($_{depletion}$ $q_N = 5.460 \times 10^{-3}$; Figure 5, left, and **A6-N**). Respective weights in the Bayesian optimization (converse of the CVs) were 0.493 for the in-season depletion (**A5-N**) and 0.298 for the prior (**A8-N**).

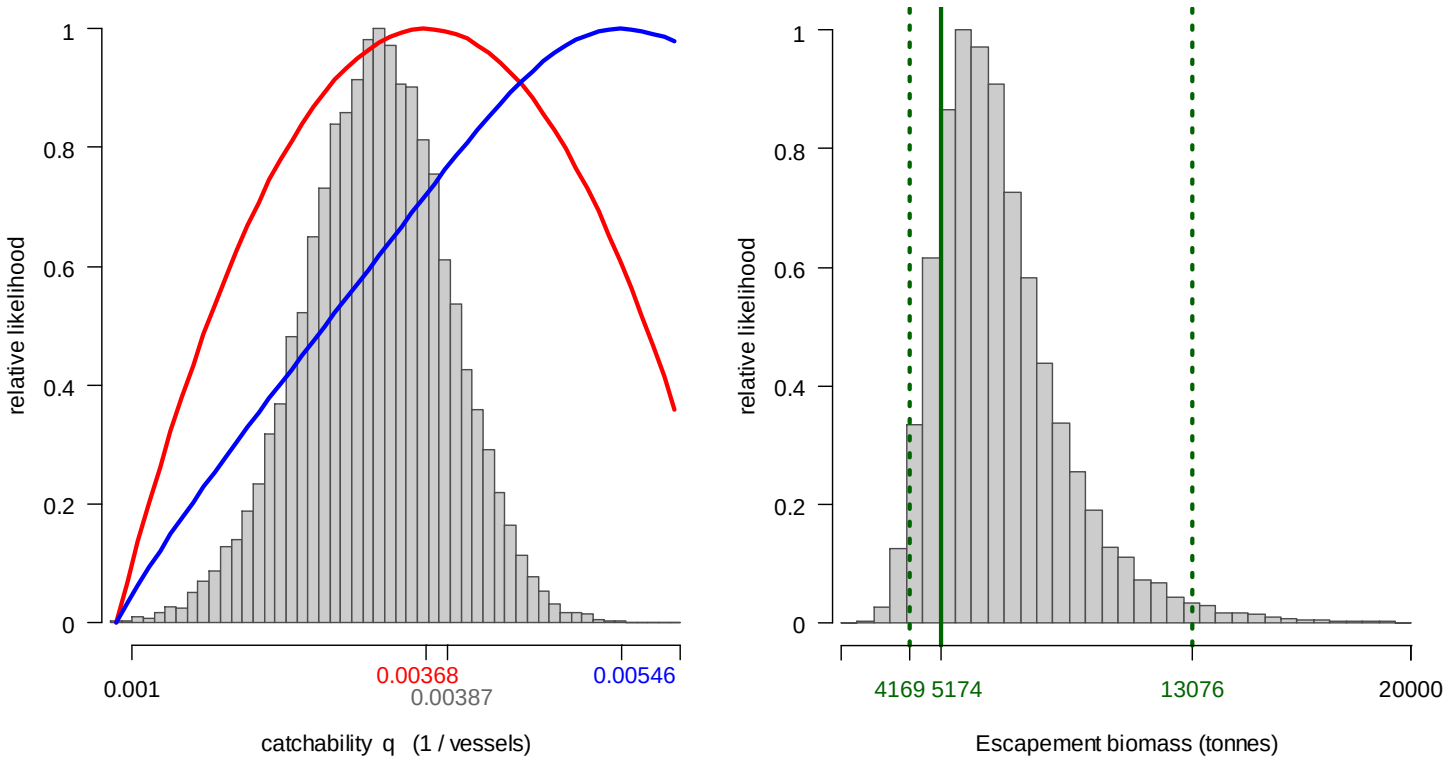

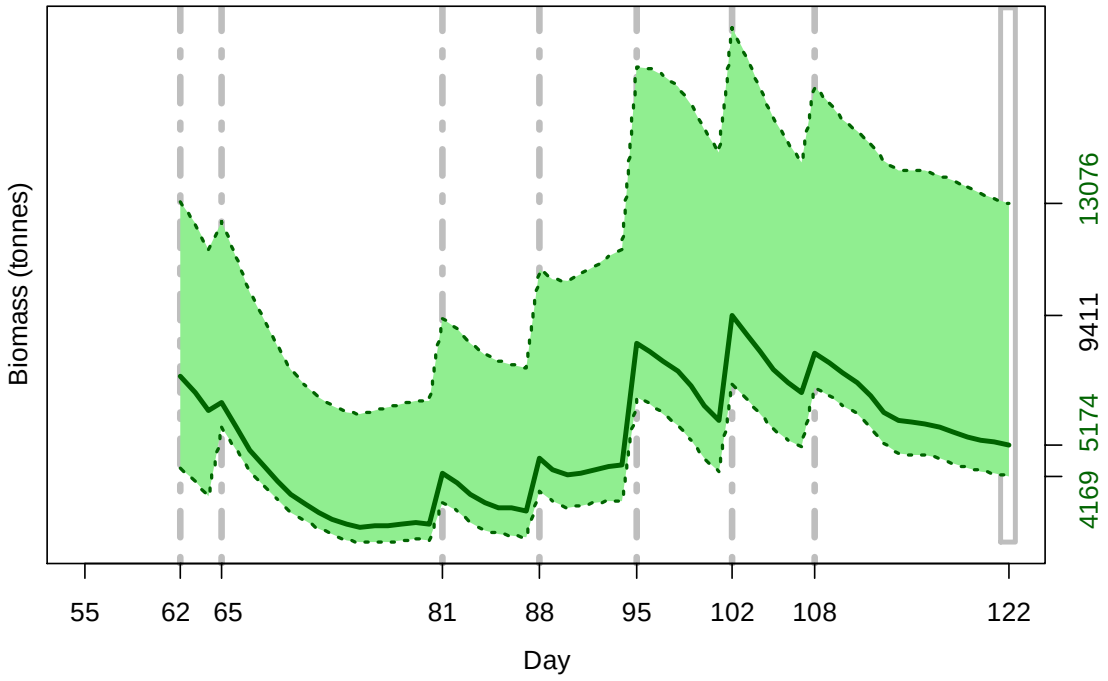

Figure 5 [previous page, upper]. North sub-area. Left: Likelihood distributions for calamari catchability. Red line: prior model (pre-season survey data), blue line: in-season depletion model, grey bars: combined Bayesian model. Right: Likelihood distribution (grey bars) of escapement biomass, from Bayesian posterior and average individual calamari weight at the end of the season. Green lines: maximum likelihood and 95% confidence interval. Note correspondence to Figure 6.

Figure 6 [previous page, lower]. North sub-area. Calamari biomass time series estimated from Bayesian posterior of the depletion model ± 95% confidence intervals. Broken grey bars indicate the start of in-season depletions north; days 62, 65, 81, 88, 95, 102 and 108. Note that the biomass 'footprint' on day 122 (May 1st) corresponds to the right-side plot of Figure 5.

The MCMC distribution of the Bayesian posterior multiplied by the GAM fit of average individual calamari weight (Figure A1-north) gave the likelihood distribution of calamari biomass on day 122 (May 1st) shown in Figure 5-right, with maximum likelihood and 95% confidence interval of:

$$B_{N\ day\ 122} = 5{,}174\ t \sim 95\%\ CI\ [4{,}169 – 13{,}076]\ t \quad \textbf{(8)}$$

At its highest point (penultimate depletion start: day 102 – April 11th), estimated calamari biomass north was 9,411 t ~ 95% CI [7,176 – 18,867] t (Figure 6).

2.4.3.2. South

In the south sub-area, relative ranks of catchability coefficients (q) were reversed from the north as the preseason prior $_{prior}q_S = 1.156 \times 10^{-3}$ (Figure 7 left, and equation **A4-S**) was higher than the Bayesian posterior maximum likelihood $q_S = 1.136 \times 10^{-3}$ (Figure 7, left, and equation **A9-S**), while the in-season depletion was lower $_{depletion}q_S = 0.824 \times 10^{-3}$ (Figure 7, left, and **A6-S**). Bayesian optimization was weighted 0.496 for in-season depletion (**A5-S**) vs. 0.235 for the prior (**A8-S**).

The MCMC distribution of the Bayesian posterior multiplied by the GAM fit of average individual calamari weight (Figure A1-south) gave the likelihood distribution of calamari biomass on day 122 (May 1st) shown in Figure 7-right, with maximum likelihood and 95% confidence interval of:

$$B_{S\ day\ 122} = 19{,}861\ t \sim 95\%\ CI\ [15{,}780 – 51{,}618]\ t \quad \textbf{(9)}$$

At its highest point (last depletion start day 95; April 4th), estimated calamari biomass south was 33,555 t ~ 95% CI [28,156 – 75,568] t (Figure 8).

Figure 7 [next page]. South sub-area. Left: Likelihood distributions for calamari catchability. Red line: prior model (pre-season survey data), blue line: in-season depletion model, grey bars: combined Bayesian model. Right: Likelihood distribution (grey bars) of escapement biomass, from Bayesian posterior and average individual calamari weight at the end of the season. Blue lines: max. likelihood and 95% conf. interval. Note correspondence to Fig. 8.

Figure 8 [next page, lower]. South sub-area. Calamari biomass time series estimated from Bayesian posterior of the depletion model ± 95% confidence intervals. Gray bars indicate the start of in-season depletions south; days 55, 70, 85, 90 and 95. Note that the biomass 'footprint' on day 122 (May 1st) corresponds to the right-side plot of Figure 7.

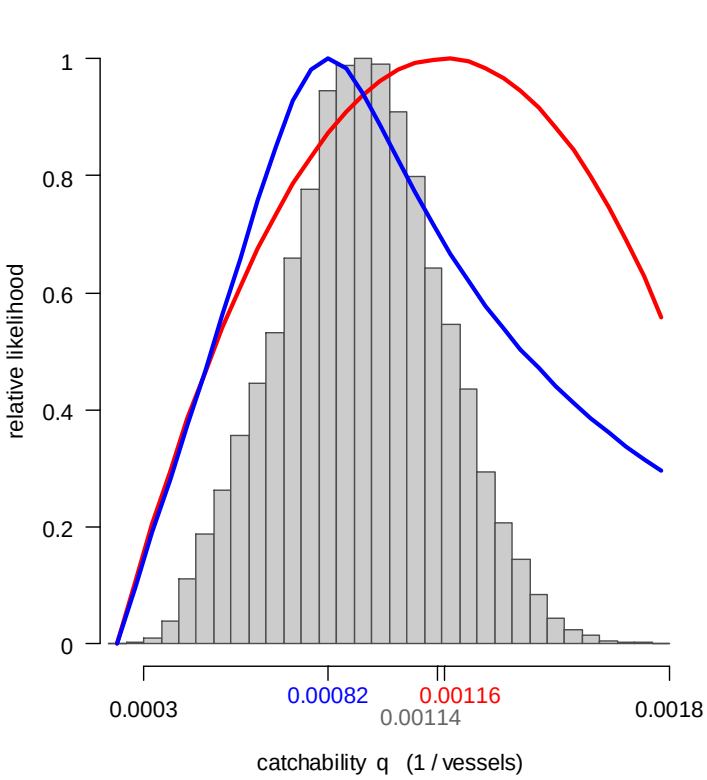
relative likelihood
1
0.8
0.6
0.4
0.2
0
0.0003
0.00082
0.00114
0.00116
0.0018
catchability q (1 / vessels)

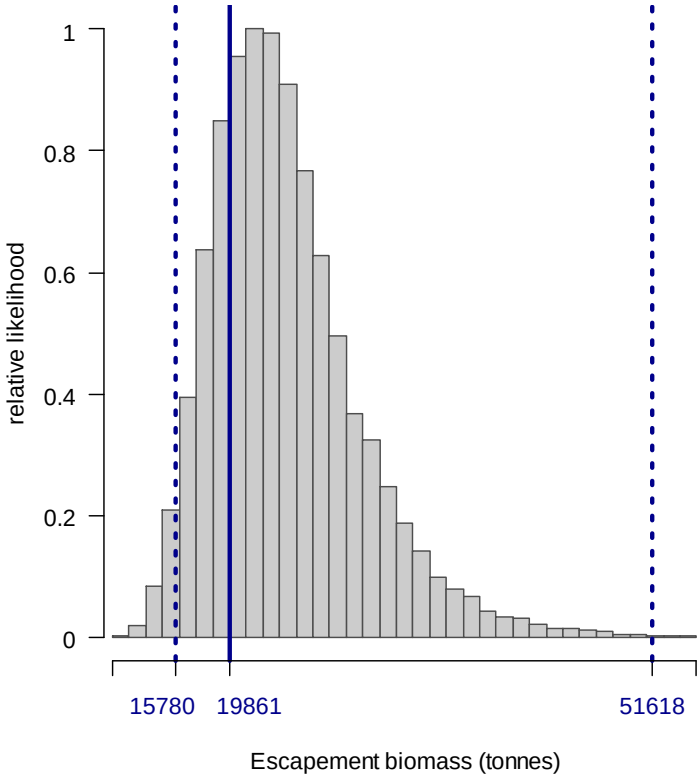
relative likelihood
1
0.8
0.6
0.4
0.2
0
15780
19861
51618
Escapement biomass (tonnes)

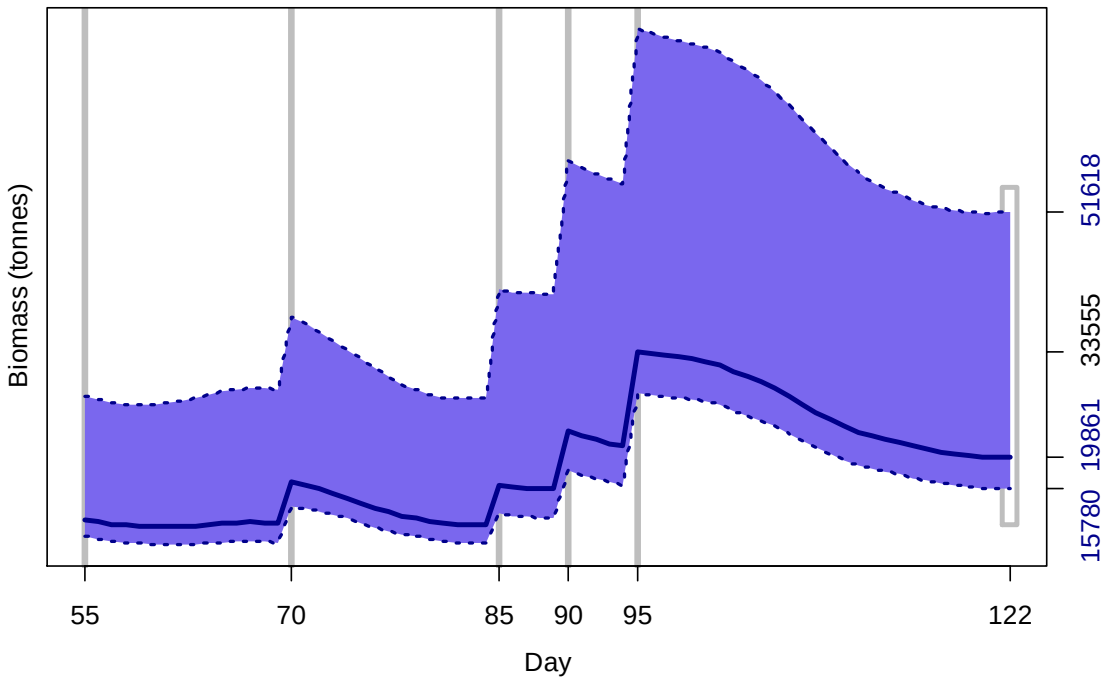

2.4.4. Escapement biomass

Total escapement biomass was defined as the aggregate biomass of Falkland calamari at the end of day 122 (May 1st) for north and south sub-areas combined (equations **8** and **9**). Depletion models are calculated on the inference that all fishing and natural mortality are gathered at mid-day, thus a half day of mortality ($e^{-M/2}$) was added to correspond to the closure of the fishery at 23:59 (mid-night) on May 1st for the final remaining vessel: equation **10**. Semi-randomized addition of the north and south biomass estimates gave the aggregate likelihood distribution of total escapement biomass shown in Figure 9.

$$B_{\text{Total day 122}} = (B_{\text{N day 122}} + B_{\text{S day 122}}) \times e^{-M/2}$$
$$= 24{,}868 \text{ t} \sim 95\% \text{ CI } [20{,}723 – 61{,}272] \text{ t} \quad \textbf{(10)}$$

This escapement biomass gave the uncommon result that a greater abundance of calamari was present at the end of the season than at the beginning of the season (21,729 t; Winter et al., 2016). Among both 1st and 2nd seasons since 2010, only in 1st season 2013 was a similar contrast obtained, when the pre-season survey biomass was estimated at a very low 5333 tonnes (Winter et al., 2013). Notably, the current pre-season survey biomass estimate of 21,729 t is the lowest since 1st season 2013.

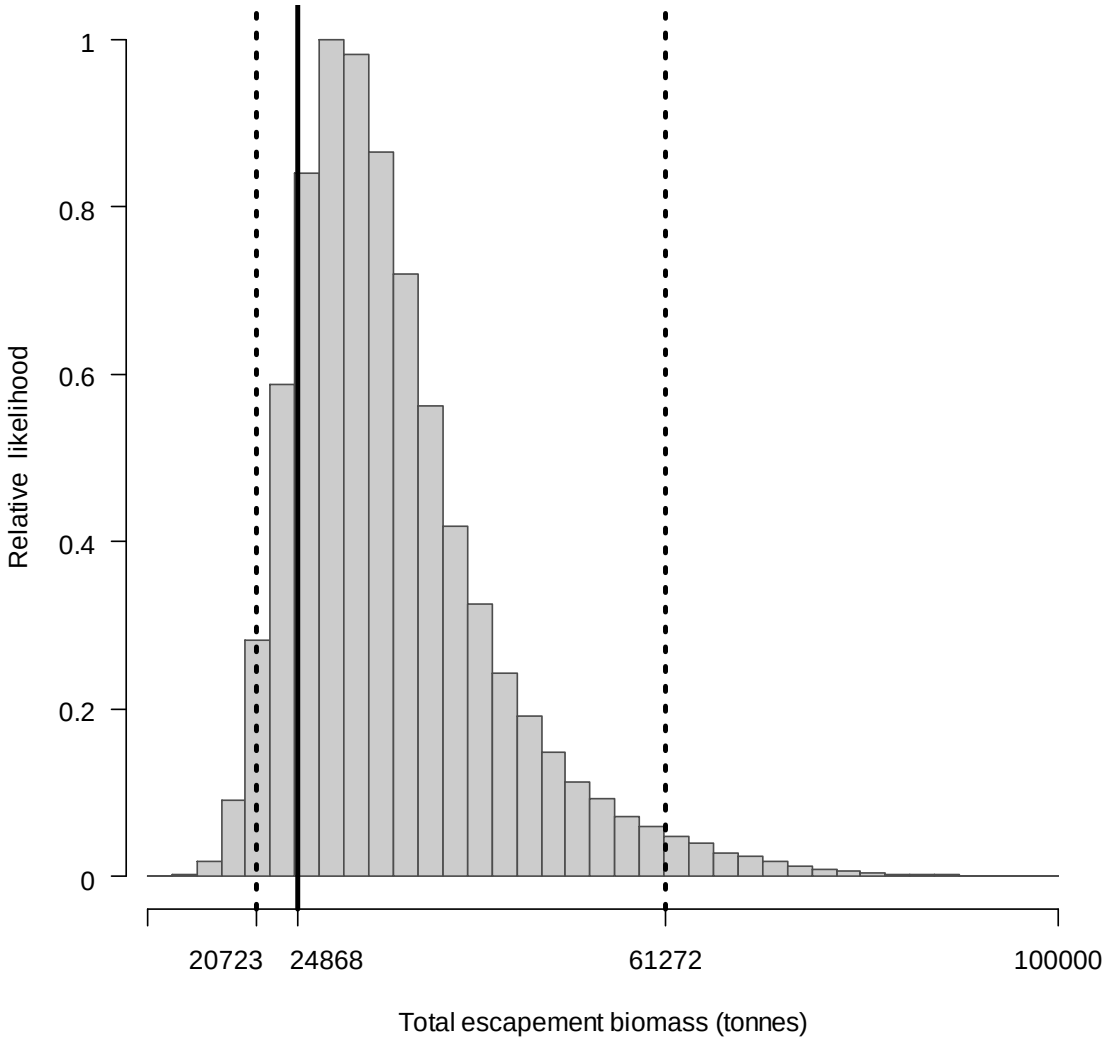

Figure 9. Likelihood distribution with 95% confidence intervals of total Falkland calamari escapement biomass corresponding to the season end (May 1st).

The risk of the fishery in the current season, defined as the proportion of the total escapement biomass distribution below the conservation limit of 10,000 tonnes (Agnew et al., 2002; Barton, 2002), was calculated as effectively zero.

2.4.5. Immigration

Falkland calamari immigration during the season was inferred on each day by how many more calamari were estimated present than the day before, minus the number caught and the number expected to have died naturally:

$$_{\text{Immigration}}N_{\text{day i}} = N_{\text{day i}} - (N_{\text{day i-1}} - C_{\text{day i-1}} - M_{\text{day i-1}})$$

where $N_{\text{day i-1}}$ are optimized in the depletion models, $C_{\text{day i-1}}$ calculated as in equation **2**, and $M_{\text{day i-1}}$ is:

$$M_{\text{day i-1}} = (N_{\text{day i-1}} - C_{\text{day i-1}}) \times (1 - e^{-M})$$

Immigration biomass per day was then calculated as the immigration number per day multiplied by predicted average individual weight from the GAM:

$$_{\text{Immigration}}B_{\text{day i}} = {}_{\text{Immigration}}N_{\text{day i}} \times {}_{\text{GAM}}Wt_{\text{day i}}$$

All numbers N are themselves derived from the daily average individual weights, so the estimation factors in that those calamari immigrating on a day would likely be smaller than average. Confidence intervals of the immigration estimates were calculated by applying the above algorithms to the MCMC iterations of the depletion models. Resulting total biomasses of calamari immigration north and south, up to season end (day 122), were:

$$_{\text{Immigration}}B_{\text{N day 62-122}} = 13{,}290 \text{ t} \sim 95\% \text{ CI } [11{,}906 – 22{,}803] \text{ t} \quad \textbf{(11-N)}$$

$$_{\text{Immigration}}B_{\text{S day 55-122}} = 30{,}584 \text{ t} \sim 95\% \text{ CI } [25{,}402 – 63{,}055] \text{ t} \quad \textbf{(11-S)}$$

Total immigration with semi-randomized addition of the confidence intervals was:

$$_{\text{Immigration}}B_{\text{Total 55-111}} = 43{,}874 \text{ t} \sim 95\% \text{ CI } [38{,}489 – 82{,}768] \text{ t} \quad \textbf{(11-T)}$$

In the north sub-area, the in-season peaks on days 65, 81, 88, 95, 102 and 108 accounted for 4.7%, 7.4%, 8.1%, 16.8%, 15.4% and 6.9% of in-season immigration (start day 55 was de facto not an in-season immigration), consistent with the variation in the time series biomass shown on Figure 6. In the south sub-area, the in-season peaks on days 70, 85, 90 and 95 accounted for 13.5%, 12.8%, 18.9% and 30.6% of in-season immigration, consistent with the variation in the time series biomass shown on Figure 8.

2.4.6. Size ranges

Concurrent with the bulk of calamari biomass having entered the fishing zone only late in the season, calamari catch individual size distributions during the 2016 1st season were small compared to previous 1st seasons. The median mantle length of both male and female calamari, north and south of 52°S, was 9.5 - 10 cm in the 2016 1st season. In the 2013 1st season, median mantle lengths south were similar at 9.5 - 10 cm, but bigger north at 11.5 cm. No other 1st seasons since at least 2009 had size distributions this small (Figure 10).

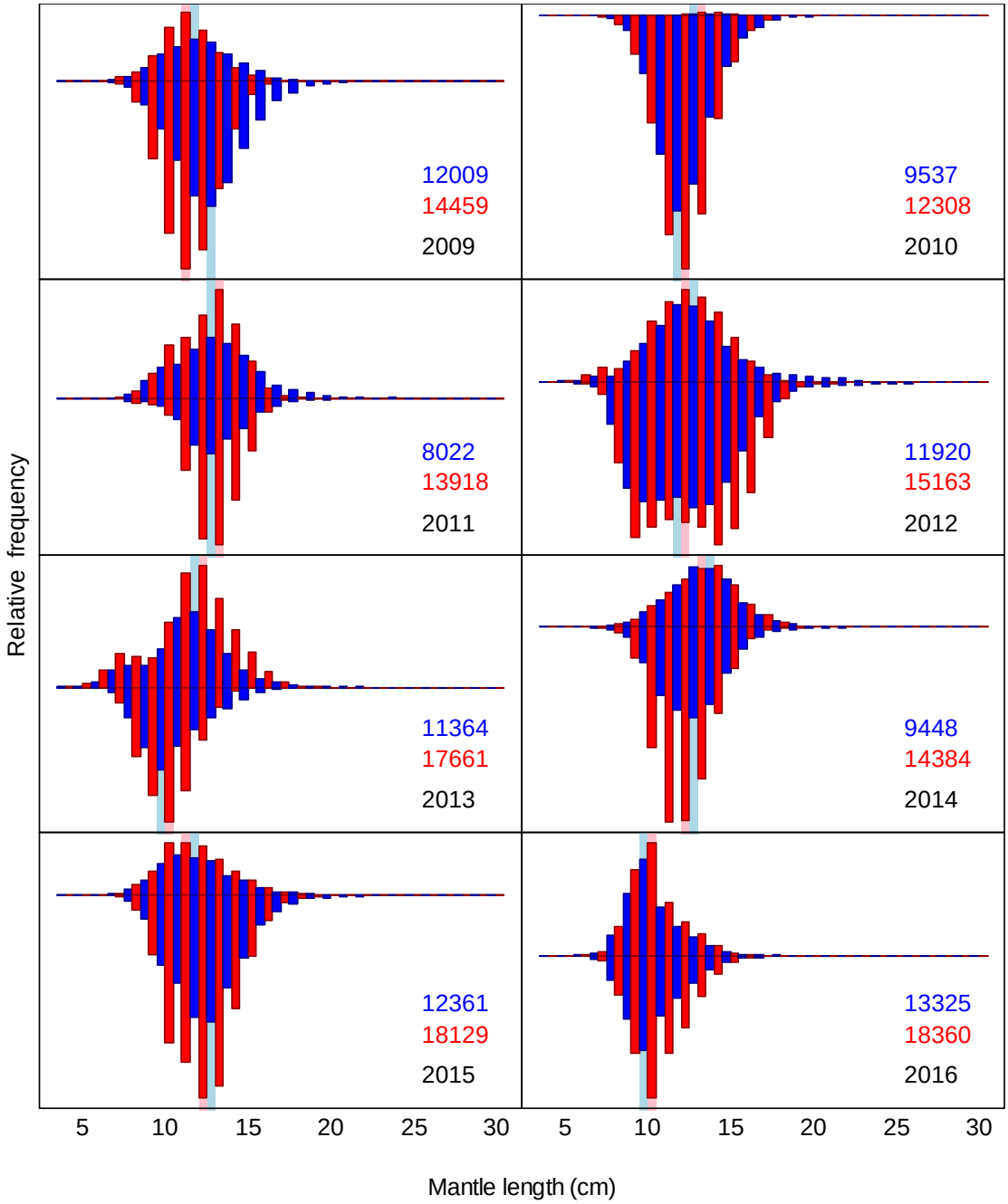

Figure 10. Falkland calamari mantle-length distributions from in-season observer random samples, 1st seasons 2009 – 2016. Distributions are partitioned north (up) and south (down) of latitude 52°S, males (blue) and females (red). Median lengths in light blue and pink are underlaid on the plots. Numbers of male and female calamari sampled each season are noted on each plot.

2.4.7. Bycatch

Figure 11 [below]. Distributions of the eight principal bycatches during 1st calamari season 2016. Thickness of grid lines is proportional to the number of vessel-days (1 to 242). Gray-scale is proportional to the bycatch biomass; maximum (tonnes) indicated on each plot.

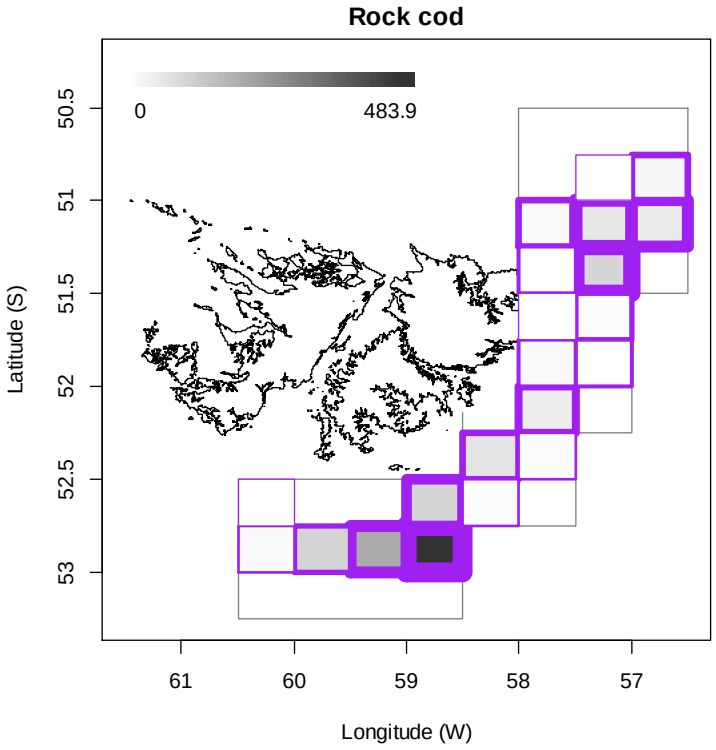
Rock cod
0
483.9
Latitude (S)
50.5
51
51.5
52
52.5
53
61
60
59
58
57
Longitude (W)

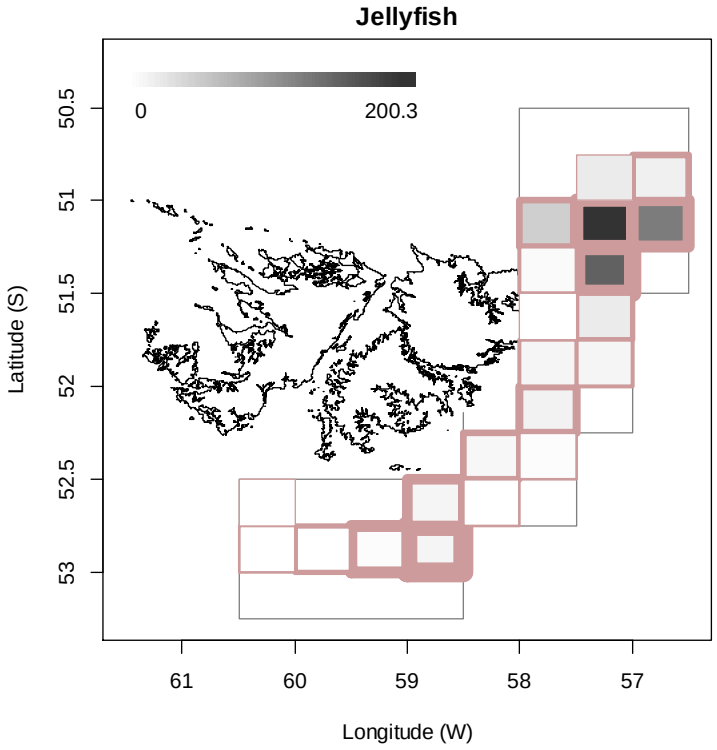
Jellyfish
0
200.3
Latitude (S)
50.5
51
51.5
52
52.5
53
61
60
59
58
57
Longitude (W)

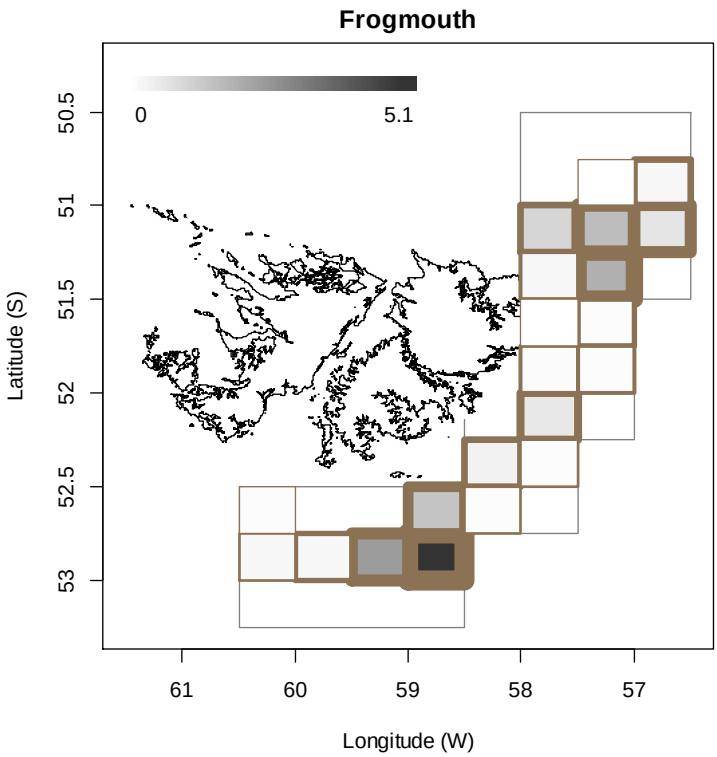
Frogmouth
0
5.1
Latitude (S)
50.5
51
51.5
52
52.5
53
61
60
59
58
57
Longitude (W)

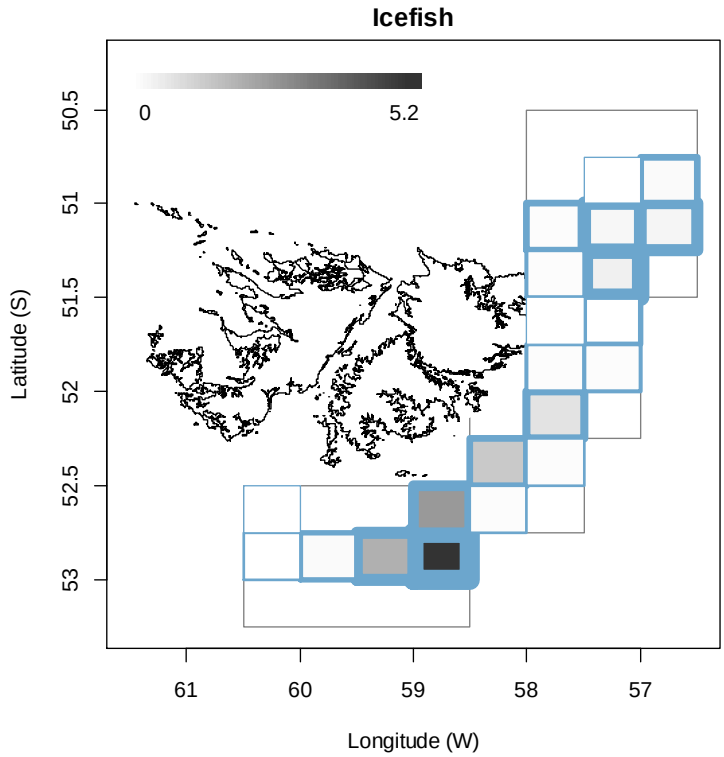
Icefish
0
5.2
Latitude (S)
50.5
51
51.5
52
52.5
53
61
60
59
58
57
Longitude (W)

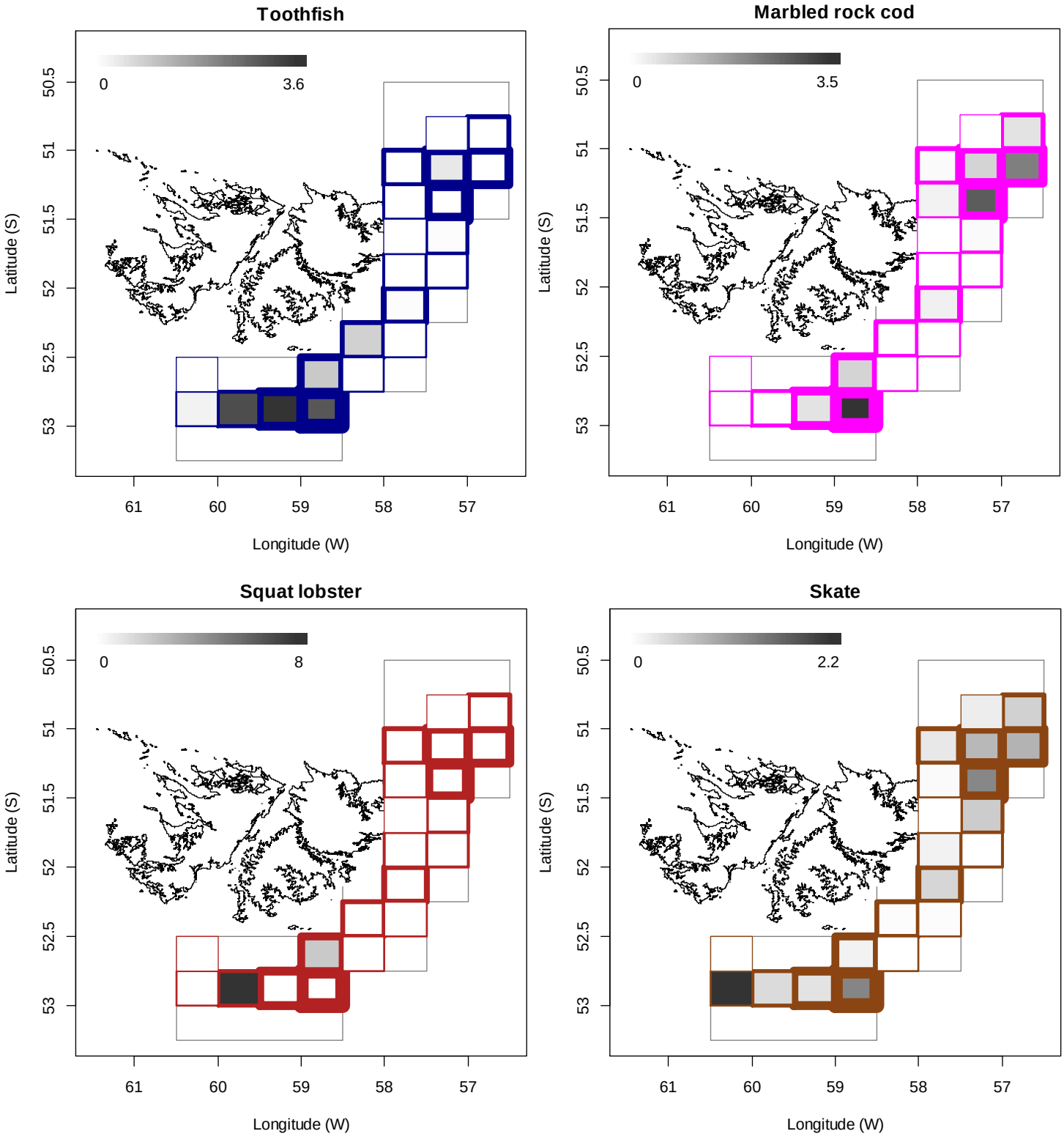

Of the 1020 calamari-target vessel-days in total (Table 1), only 3 vessel-days reported a primary catch other than calamari, which were 50.2%, 50.7%, and 54.4% rock cod (*Patagonotothen ramsayi*). The most common bycatches reported overall for the Falkland calamari season were rock cod (1296 t, reported from 969 vessel-days), jellyfish (Medusae) (654 t, 540 vessel-days), frogmouth (*Cottoperca gobio*) (17 t, 296

vessel-days), icefish (*Champsocephalus esox*) (13 t, 285 vessel-days), Patagonian toothfish (*Dissostichus eleginoides*) (12 t, 116 vessel-days), marbled rock cod (*Patagonotothen tessellata*) (12 t, 86 vessel-days), squat lobster (*Munida* spp.) (10 t, 9 vessel-days) and skate (Rajidae) (10 t, 167 vessel-days). Relative distributions by grid of these bycatches are shown in Figure 11.

2.5. References

Agnew, D.J., Baranowski, R., Beddington, J.R., des Clers, S., Nolan, C.P. 1998. Approaches to assessing stocks of *Loligo gahi* around the Falkland Islands. Fisheries Research 35: 155-169.

Agnew, D. J., Beddington, J. R., and Hill, S. 2002. The potential use of environmental information to manage squid stocks. Canadian Journal of Fisheries and Aquatic Sciences, 59: 1851–1857.

Arkhipkin, A.I., Middleton, D.A.J. 2002. Sexual segregation in ontogenetic migrations by the squid *Loligo gahi* around the Falkland Islands. Bulletin of Marine Science 71: 109-127.

Arkhipkin, A.I., Middleton, D.A.J., Barton, J. 2008. Management and conservation of a short-lived fishery resource: *Loligo gahi* around the Falkland Islands. American Fisheries Society Symposium 49: 1243-1252.

Barton, J. 2002. Fisheries and fisheries management in Falkland Islands Conservation Zones. Aquatic Conservation: Marine and Freshwater Ecosystems 12: 127–135.

Bradley, K. 2016a. Observer Report 1087. Technical Document, FIG Fisheries Department. 23 p.

Bradley, K. 2016b. Observer Report 1097. Technical Document, FIG Fisheries Department. 32 p.

Brooks, S.P., Gelman, A. 1998. General methods for monitoring convergence of iterative simulations. Journal of computational and graphical statistics 7:434-455.

DeLury, D.B. 1947. On the estimation of biological populations. Biometrics 3: 145-167.

Gamerman, D., Lopes, H.F. 2006. Markov Chain Monte Carlo. Stochastic simulation for Bayesian inference. 2nd edition. Chapman & Hall/CRC.

Iriarte, V. 2016. Observer Report 1090. Technical Document, FIG Fisheries Department. 27 p.

Magnusson, A., Punt, A., Hilborn, R. 2013. Measuring uncertainty in fisheries stock assessment: the delta method, bootstrap, and MCMC. Fish and Fisheries 14: 325-342.

Nash, J.C., Varadhan, R. 2011. optimx: A replacement and extension of the optim() function. R package version 2011-2.27. http://CRAN.R-project.org/package=optimx

Patterson, K.R. 1988. Life history of Patagonian squid *Loligo gahi* and growth parameter estimates using least-squares fits to linear and von Bertalanffy models. Marine Ecology Progress Series 47: 65-74.

Payá, I. 2009. Fishery Report. *Loligo gahi*, First Season 2009. Fishery statistics, biological trends, stock assessment and risk analysis. Technical Document, Falkland Islands Fisheries Department. 41 p.

Payá, I. 2010. Fishery Report. *Loligo gahi*, Second Season 2009. Fishery statistics, biological trends, stock assessment and risk analysis. Technical Document, Falkland Islands Fisheries Department. 54 p.

Punt, A.E., Hilborn, R. 1997. Fisheries stock assessment and decision analysis: the Bayesian approach. Reviews in Fish Biology and Fisheries 7:35-63.

Roa-Ureta, R. 2012. Modelling in-season pulses of recruitment and hyperstability-hyperdepletion in the *Loligo gahi* fishery around the Falkland Islands with generalized depletion models. ICES Journal of Marine Science 69: 1403–1415.

Roa-Ureta, R., Arkhipkin, A.I. 2007. Short-term stock assessment of *Loligo gahi* at the Falkland Islands: sequential use of stochastic biomass projection and stock depletion models. ICES Journal of Marine Science 64: 3-17.

Rosenberg, A.A., Kirkwood, G.P., Crombie, J.A., Beddington, J.R. 1990. The assessment of stocks of annual squid species. Fisheries Research 8: 335-350.

Shaw, P.W., Arkhipkin, A.I., Adcock, G.J., Burnett, W.J., Carvalho, G.R., Scherbich, J.N., Villegas, P.A. 2004. DNA markers indicate that distinct spawning cohorts and aggregations of Patagonian squid, *Loligo gahi*, do not represent genetically discrete subpopulations. Marine Biology, 144: 961-970.

Winter, A. 2011. *Loligo gahi* stock assessment, first season 2011. Technical Document, Falkland Islands Fisheries Department. 23 p.

Winter, A. 2012. *Loligo gahi* stock assessment, first season 2012. Technical Document, Falkland Islands Fisheries Department. 27 p.

Winter, A. 2013. *Loligo* stock assessment, first season 2013. Technical Document, Falkland Islands Fisheries Department. 23 p.

Winter, A. 2014a. *Loligo* stock assessment, first season 2014. Technical Document, Falkland Islands Fisheries Department. 28 p.

Winter, A. 2014b. *Loligo* stock assessment, second season 2014. Technical Document, Falkland Islands Fisheries Department. 30 p.

Winter, A., Arkhipkin, A. 2015. Environmental impacts on recruitment migrations of Patagonian longfin squid (*Doryteuthis gahi*) in the Falkland Islands with reference to stock assessment. Fisheries Research 172: 85-95.

Winter, A., Jürgens, L., Monllor, A. 2013. Loligo stock assessment survey, 1st season 2013. Technical Document, Falkland Islands Fisheries Department. 15 p.

Winter, A., Zawadowski, T., Shcherbich, Z., Bradley, K., Kuepfer, A. 2016. Falkland calamari stock assessment survey, 1st season 2016. Technical Document, Falkland Islands Fisheries Department. 19 p.

2.6. Appendix

2.6.1. Falkland calamari individual weights

A generalized additive model (GAM) was calculated from the daily observer data (both sexes combined) and commercial size category data of average individual daily weights of calamari. North and south sub-areas were calculated separately. For continuity, the GAMs were calculated using all pre-season survey and in-season data contiguously. GAM plots of the north and south sub-areas are shown in Figure A1.

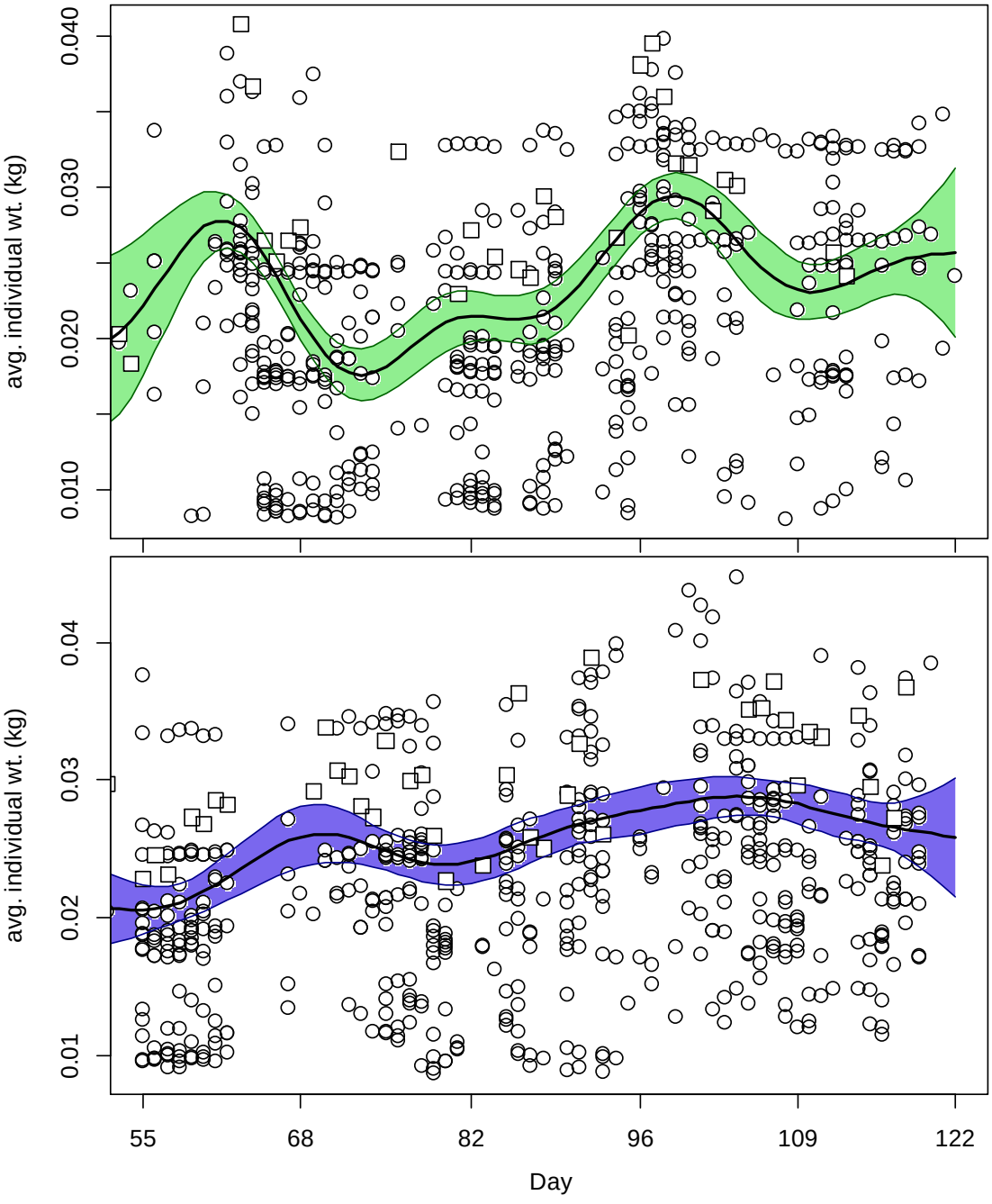

Figure A1. North (top) and south (bottom) sub-area daily average individual calamari weights from commercial size categories per vessel (circles) and observer measurements (squares). GAMs of the daily trends ± 95% confidence intervals (centre lines and colour under-shading).

2.6.2. Prior estimates and CV

The pre-season survey (Winter et al., 2016) had estimated Falkland calamari biomasses of 8,520 t (standard deviation: ± 1,404 t) north of 52º S and 13,209 t (standard deviation: 1,767 t) south of 52º S. From modelled survey catchability, Payá (2010) had estimated average net escapement of up to 22%, which was added to the standard deviation:

$$8{,}520 \pm \left(\frac{1{,}404}{8{,}520} + .22 \right) = 8{,}520 \pm 38.5\% = 8{,}520 \pm 3{,}278 \text{ t} \quad \textbf{(A1-N)}$$

$$13{,}209 \pm \left(\frac{1{,}767}{13{,}209} + .22 \right) = 13{,}209 \pm 35.4\% = 13{,}209 \pm 4{,}673 \text{ t} \quad \textbf{(A1-S)}$$

The 22% was added as a linear increase in the variability, but was not used to reduce the total estimate, because calamari that escape one trawl are likely to be part of the biomass concentration that is available to the next trawl.

Calamari numbers at the start of the season, day 55, were estimated as the survey biomasses divided by the GAM-predicted individual weight averages for the survey: 0.022 kg north and 0.021 kg south (Figure A1). Average coefficients of variation (CV) of the GAM over the duration of the pre-season survey were 12.69% north and 8.46% south, and CV of the length-weight conversion relationship (equation **8**) were 6.6% north and 6.9% south. Combining all sources of variation with the pre-season survey biomass estimates and average individual weight averages gave estimated calamari numbers at season start (February 24th; day 55) of:

$$_{\text{prior}}N_{\text{N day 55}} = \frac{8{,}520 \times 1000}{0.022} \pm \sqrt{38.5\%^2 + 12.69\%^2 + 6.6\%^2}$$

$$= 0.384 \times 10^9 \pm 41.1\% \quad \textbf{(A2-N)}$$

$$_{\text{prior}}N_{\text{S day 55}} = \frac{13{,}209 \times 1000}{0.021} \pm \sqrt{35.4\%^2 + 8.46\%^2 + 6.9\%^2}$$

$$= 0.645 \times 10^9 \pm 37.0\% \quad \textbf{(A2-S)}$$

The catchability coefficient (q) prior for the north sub-area was taken on day 62, when 9 vessels were fishing north and the 1st depletion period north started. The abundance prior (N) on day 62 was calculated as survey abundance on start day 55 discounted for 7 days of natural mortality (as no catch had been taken in those 2 days):

$$_{\text{prior}}N_{\text{N day 62}} = {}_{\text{prior}}N_{\text{N day 55}} \times e^{-M \cdot (62-55)} - \text{CNMD}_{\text{day 62}} = 0.347 \times 10^9 \quad \textbf{(A3-N)}$$

$$_{\text{prior}}q_{\text{N}} = C(N)_{\text{N day 62}} / ({}_{\text{prior}}N_{\text{N day 62}} \times E_{\text{N day 62}})$$

$$= (C(B)_{N\ day\ 62} / Wt_{N\ day\ 62}) / ({}_{prior}N_{N\ day\ 62} \times E_{N\ day\ 62})$$

$$= (318.9\ t / 0.028\ kg) / (0.347 \times 10^{9} \times 9\ vessel\text{-}days)$$

$$= 3.681 \times 10^{-3}\ vessels^{-1}\ ^{1} \qquad \textbf{(A4-N)}$$

The catchability coefficient (q) prior for the south sub-area was taken on day 55, when all 16 vessels were fishing south. As this was the first scheduled day of the season, no discount was applicable for either natural mortality or catch.

$${}_{prior}q_{S} = C(N)_{S\ day\ 55} / ({}_{prior}N_{S\ day\ 55} \times E_{S\ day\ 55})$$

$$= (C(B)_{S\ day\ 55} / Wt_{S\ day\ 55}) / ({}_{prior}N_{S\ day\ 55} \times E_{S\ day\ 55})$$

$$= (245.7\ t / 0.021\ kg) / (0.645 \times 10^{9} \times 16\ vessel\text{-}days)$$

$$= 1.156 \times 10^{-3}\ vessels^{-1}\ ^{2} \qquad \textbf{(A4-S)}$$

CVs of the priors were calculated as the sums of variability in ${}_{prior}N$ (equations **A2**) plus variability in the catches of vessels on the start days (day 62 N and day 55 S):

$$CV_{\ prior\ N} = \sqrt{41.1\%^{2} + \left(\frac{SD\left(C(B)_{N\ vessels\ day\ 62}\right)}{mean\left(C(B)_{N\ vessels\ day\ 62}\right)}\right)^{2}}$$

$$= \sqrt{41.1\%^{2} + 27.3\%^{2}} = 49.3\% \qquad \textbf{(A5-N)}$$

$$CV_{\ prior\ S} = \sqrt{37.0\%^{2} + \left(\frac{SD\left(C(B)_{S\ vessels\ day\ 55}\right)}{mean\left(C(B)_{S\ vessels\ day\ 55}\right)}\right)^{2}}$$

$$= \sqrt{37.0\%^{2} + 33.0\%^{2}} = 49.6\% \qquad \textbf{(A5-S)}$$

2.6.3. Depletion model estimates and CV

For the north sub-area, the equivalent of equation **2** with seven N_{day} was optimized on the difference between predicted catches and actual catches (equation **3**), resulting in parameters values:

${}_{depletion}N1_{N\ day\ 62}$	$= 0.191 \times 10^{9}$;	${}_{depletion}N2_{N\ day\ 65}$	$= 0.057 \times 10^{9}$
${}_{depletion}N3_{N\ day\ 81}$	$= 0.074 \times 10^{9}$;	${}_{depletion}N4_{N\ day\ 88}$	$= 0.077 \times 10^{9}$
${}_{depletion}N5_{N\ day\ 95}$	$= 0.127 \times 10^{9}$;	${}_{depletion}N6_{N\ day\ 102}$	$= 0.111 \times 10^{9}$
${}_{depletion}N7_{N\ day\ 108}$	$= 0.073 \times 10^{9}$		
${}_{depletion}q_{N}$	$= 5.460 \times 10^{-3}$ [3]		

(A6-N)

[1] On Figure 5-left.
[2] On Figure 7-left.
[C] On Figure 5-left.

The root-mean-square deviation of predicted vs. actual catches was calculated as the CV of the model:

$$CV_{\text{rmsd N}} = \frac{\sqrt{\sum_{i=1}^{n}\left({}_{\text{predicted}}C(N)_{\text{N day i}} - {}_{\text{actual}}C(N)_{\text{N day i}}\right)^2 / n}}{\text{mean}\left({}_{\text{actual}}C(N)_{\text{N day i}}\right)}$$

$$= 2.395 \times 10^6 / 8.107 \times 10^6 = 29.5\% \qquad \textbf{(A7-N)}$$

$CV_{\text{rmsd N}}$ was added to the variability of the GAM-predicted individual weight averages for the season (Figure A1-N); equal to a CV of 4.0% north. CVs of the depletion were then calculated as the sum:

$$CV_{\text{depletion N}} = \sqrt{CV_{\text{rmsd N}}^2 + CV_{\text{GAM Wt N}}^2} = \sqrt{29.5\%^2 + 4.0\%^2}$$

$$= 29.8\% \qquad \textbf{(A8-N)}$$

For the south sub-area, the equivalent of equation **2** with five N_{day} was optimized on the difference between predicted catches and actual catches (equation **3**), resulting in parameters values:

$${}_{\text{depletion}}N1_{\text{S day 55}} = 0.767 \times 10^9; \quad {}_{\text{depletion}}N2_{\text{S day 70}} = 0.260 \times 10^9$$

$${}_{\text{depletion}}N3_{\text{S day 85}} = 0.268 \times 10^9; \quad {}_{\text{depletion}}N4_{\text{S day 90}} = 0.391 \times 10^9$$

$${}_{\text{depletion}}N5_{\text{S day 95}} = 0.566 \times 10^9$$

$${}_{\text{depletion}}q_{\text{S}} = 0.824 \times 10^{-3}\ [4] \qquad \textbf{(A6-S)}$$

The normalized root-mean-square deviation of predicted vs. actual catches was calculated as the CV of the model:

$$CV_{\text{rmsd S}} = \frac{\sqrt{\sum_{i=1}^{n}\left({}_{\text{predicted}}C(N)_{\text{S day i}} - {}_{\text{actual}}C(N)_{\text{S day i}}\right)^2 / n}}{\text{mean}\left({}_{\text{actual}}C(N)_{\text{S day i}}\right)}$$

$$= 1.673 \times 10^6 / 7.179 \times 10^6 = 23.3\% \qquad \textbf{(A7-S)}$$

$CV_{\text{rmsd S}}$ was added to the variability of the GAM-predicted individual weight averages for the season (Figure A1-S); equal to a CV of 3.2% south. CVs of the depletion were then calculated as the sum:

$$CV_{\text{depletion S}} = \sqrt{CV_{\text{rmsd S}}^2 + CV_{\text{GAM Wt S}}^2} = \sqrt{23.3\%^2 + 3.2\%^2}$$

$$= 23.5\% \qquad \textbf{(A8-S)}$$

[4] On Figure 7-left.

2.6.4. Combined Bayesian models

For the north sub-area, the joint optimization of equations **3** and **4** resulted in parameters values:

$_{\text{Bayesian}}N1_{\text{N day 62}} = 0.268 \times 10^9$; $_{\text{Bayesian}}N2_{\text{N day 65}} = 0.036 \times 10^9$
$_{\text{Bayesian}}N3_{\text{N day 81}} = 0.082 \times 10^9$; $_{\text{Bayesian}}N4_{\text{N day 88}} = 0.089 \times 10^9$
$_{\text{Bayesian}}N5_{\text{N day 95}} = 0.152 \times 10^9$; $_{\text{Bayesian}}N6_{\text{N day 102}} = 0.133 \times 10^9$
$_{\text{Bayesian}}N7_{\text{N day 108}} = 0.067 \times 10^9$

$_{\text{Bayesian}}q_{\text{N}} = 3.870 \times 10^{-3}$ [5] **(A9-N)**

These parameters produced the fit between predicted and actual catches shown in Figure A2-N.

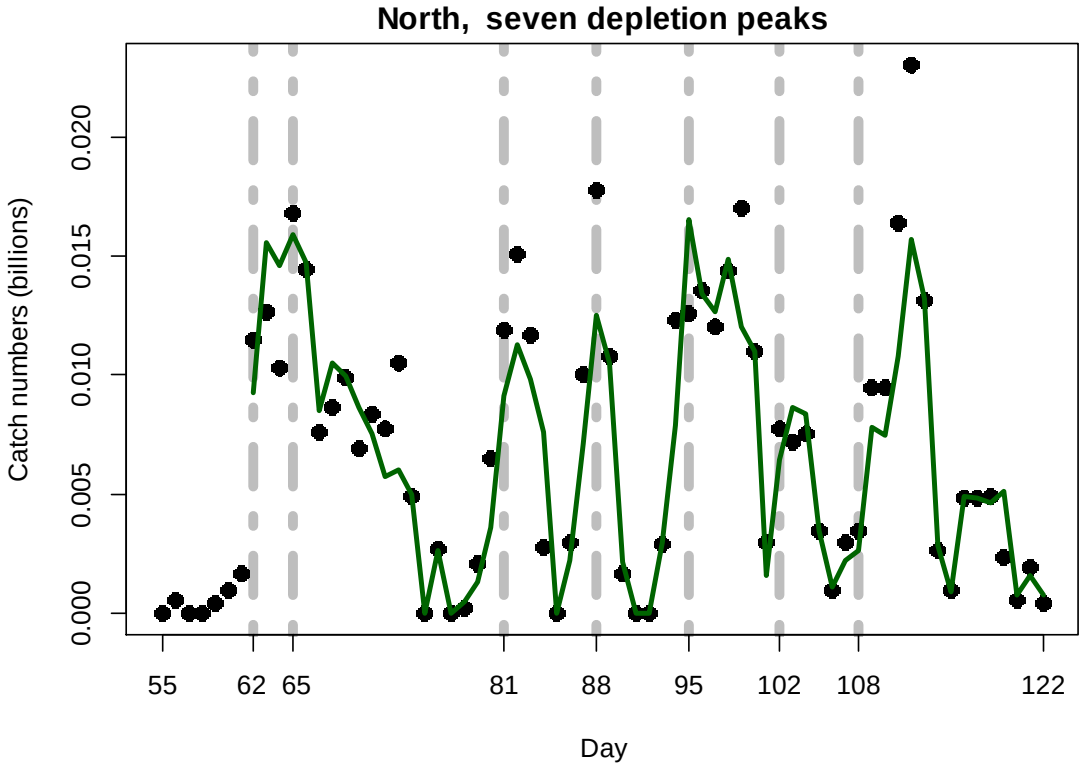

Figure A2-N. Daily catch numbers estimated from actual catch (black points) and predicted from the depletion model (green line) in the north sub-area.

For the south sub-area, the joint optimization of equations **3** and **4** resulted in parameters values:

$_{\text{Bayesian}}N1_{\text{S day 55}} = 0.568 \times 10^9$; $_{\text{Bayesian}}N2_{\text{S day 70}} = 0.204 \times 10^9$
$_{\text{Bayesian}}N3_{\text{S day 85}} = 0.207 \times 10^9$; $_{\text{Bayesian}}N4_{\text{S day 90}} = 0.292 \times 10^9$
$_{\text{Bayesian}}N3_{\text{S day 95}} = 0.458 \times 10^9$

[5] On Figure 5-left.

$$\text{Bayesian } q_S = 1.136 \times 10^{-3}\ ^{6} \quad \textbf{(A9-S)}$$

These parameters produced the fit between predicted and actual catches shown in Figure A2-S.

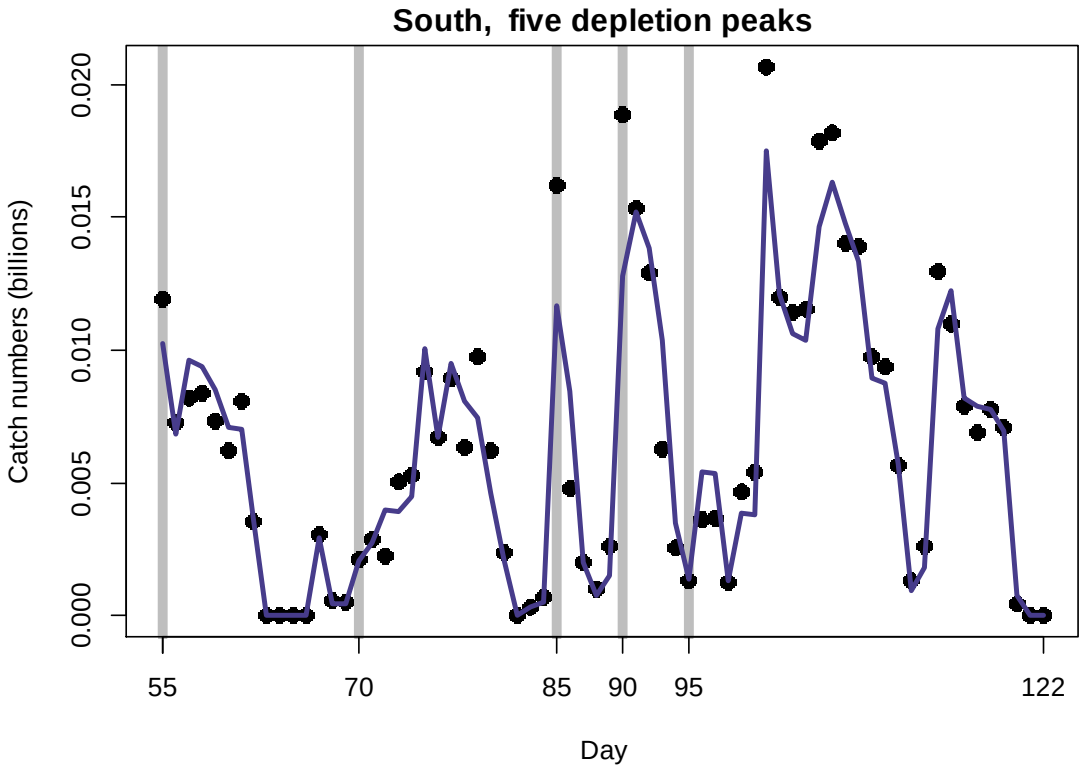

Figure A2-S. Daily catch numbers estimated from actual catch (black points) and predicted from the depletion model (blue line) in the south sub-area.

[6] On Figure 7-left.

3. Finfish Fisheries based on Rock Cod, *Patagonotothen ramsayi*

3.1. Introduction

The finfish fishery of the Falkland Islands is regulated using both a total allowable catch (TAC) and a total allowable effort (TAE). Various finfish species are exploited by the finfish fleet. The TAC/TAE was firstly based on the southern blue whiting (*Micromesistius a. australis*) stock which was the most important finfish species exploited by the trawlers. However, the decrease of this resource in years 2004–2007 (Laptikhovsky et al., 2013) has led the Directorate of Natural Resources – Fisheries Department (DNR-F) to rebuild its licensing system based on the rock cod (*Patagonotothen ramsayi*) stock which became, from 2007, the most abundant finfish species.

Fishing activity is known to impact the life history traits and abundance of targeted species. Biological data collected by fishery observers and during the research cruises has been used to investigate if targeted trawling has impacted rock cod life history traits. Variation in abundance can be explored using fishery independent and fishery dependent data (Hilborn and Walters, 1992; Maunder and Punt, 2004).

The objective of this report is firstly to analyse biological data collected by the DNR-F to highlight if the targeted trawling fishery that started in 2007 has induced modifications in rock cod life history traits. Secondly, rock cod abundance estimations based on fishery independent data will be compared to standardized fishery dependent relative abundance indices. These last data will also be used as input data in a biomass dynamic model. Based on reported catch and effort, the methodology to estimate suggested VUM and fishing times for 2016 will be applied and results presented and discussed.

3.2. Material and methods

3.2.1. Length frequency

Rock cod biological data are collected by observers during commercial fishing trips on board finfish bottom trawlers operating in the finfish zone (i.e. north of 52°S, west of 59°30'W and south of 48°15'S) and during research cruises conducted by the DNR-F in the same area. Total length of sampled fish was measured to the nearest cm after determining sex and maturity stage. Random and sub–sampled data were selected to plot annual histograms for each sex and highlight trends in average total length and length modes from 2003 through to 2015.

3.2.2. Length–at–maturity

Maturity stage is determined using an 8 maturity stage scale (Brickle et al., 2006; see also observer manual). A specimen was considered to be mature when it was between the early developing stage (maturity stage 3) and the recovering spent stage (maturity stage 8) during the reproduction period (from June through to August; Brickle et al., 2006). For each year, the percentage of mature specimens sampled in the finfish zone was estimated for each length class. These data were then modelled using a binomial error Generalised Linear Model (GLM) and the length at 50% maturity (also called

length–at–maturity, the length where 50% of the population is mature) was finally estimated using the model parameters.

3.2.3. Age–length relationship modelling

Otoliths of rock cod are collected during research cruises and observer trips throughout the year. Associated data are total length, weight, sex and maturity stage for each specimen. Ageing was carried by the DNR-F in 2003–2004, Gdnya (Poland) in 2008–2010 and again by DNR-F since 2011. To be aged, rock cod otoliths are transversally sectioned and annual rings are counted under microscope. At the time of writing up this report, ageing was carried out up to the 2014 data collection.
The objective of this analysis is to show how parameters of these models have changed between years as the fishing effort targeting rock cod increased. In the von Bertalanffy model, the predicted length–at–time t ($E\left[\frac{L}{t}\right]$) is estimated as:

$$E\left[\frac{L}{t}\right] = L_{\infty}\left(1 - e^{K(t-t_0)}\right)$$

Where L_{∞} is the asymptotic average length, K is the Brody growth rate coefficient and t_0 is the length at age 0. The model was fitted by minimising the negative log likelihood. A likelihood ratio test (Haddon, 2011) was performed to statistically compare the three estimated parameters of the annual von Bertalanffy curves. The time series of each parameter was drawn to highlight if a trend in length–at–age appears after the fishery started to target rock cod in 2007. However, as the von Bertalanffy curve parameters are correlated, a growth performance index (P) combining two (K and L_{∞}) of the three parameters in one was estimated as (Pauly, 1979):

$$P = \log(K) + \log(L_{\infty})$$

3.2.4. Biomass surveys

In February 2016, the F/V Castelo (ZDLT1) was chartered by the DNR-F for a survey covering a significant part of the finfish area (see Figure 1 in Gras et al., 2016). This survey was conducted from 2 to 22 February 2016. A total of 90 one hour–trawls were assessed in 86 grid squares. During each station, start and end positions of the trawl on the bottom were recorded as well as the horizontal net opening. These parameters were used to derive the swept area surface. Every time it was possible, the entire catch was weighed by species or higher taxonomic level for invertebrates and a conversion factor was used when the catch was too big to be weighed. The swept area and catch weight were used to estimate the density of rock cod at each station. These observed data were finally used to estimate the total biomass in the surveyed zone (auto–correlation of the data was taken into account using geostatistic methods). A time series of rock cod biomass was drawn using results from surveys conducted in February 2010–2011, October 2014, February 2015–2016.

3.2.5. Standardized CPUE

Another source of data to estimate rock cod abundance, called fishery dependent data, uses Catch Per Unit Effort (CPUE) of fishing vessels during commercial trips. Fishery dependent data have the advantage to be available throughout the time but the disadvantages to be distributed according to the targeted stock, incomplete and/or

inaccurate. As a result, before using them as an index of abundance, extraneous factors have to be removed from raw CPUE by standardizing them. Various methods have been developed during the last decades and the most powerful one is based on Generalized Linear Models (Hilborn and Walters, 1992; Maunder and Punt, 2004). In the case of the rock cod of the FICZ, a delta–GLM was fitted. It combines two GLMs, a binomial error GLM which models the presence/absence $(U^{obs}_{y,m,c,t})_{0/1}$ and a Gaussian error GLM which models the log–transformed CPUE $\ln(U^{obs}_{y,m,c,t})_{>0}$ using four variables: year y, month m, callsign c and target species t (defined as the most prevalent species in the net) which are introduced in both models as:

$$\text{logit}\left(U^{obs}_{y,m,c,t}\right)_{0/1} = \alpha_y + \beta_m + \gamma_c + \delta_t + \omega_{y,m,c,t}$$

And

$$\log\left(U^{obs}_{y,m,c,t}\right)_{>0} = \alpha_y + \beta_m + \gamma_c + \delta_t + \varepsilon_{y,m,c,t}$$

3.2.6. Biomass dynamic model

The standardized CPUE derived from catch reporting data were used as input data in a stock assessment model. As the time series of CPUE is short (11 years) and rock cod could live up to 15 years, over–parametrisation problems would probably be encountered with an age structured model. The simpler Schaefer biomass dynamic model was therefore chosen (Hilborn and Walters, 1992). In this model, the biomass at time $t+1 (B_{t+1})$ is estimated using the biomass at time t (B_t) and taking into account the population growth rate r, the population carrying capacity (K) and the catch occurring at time t:

$$B_{t+1} = B_t + rB_t\left(1 - \frac{B_t}{K}\right) - C_t$$

The model was fitted by minimizing the negative log likelihood and the biomass estimation confidence interval was estimated using a Markov Chain Monte Carlo algorithm that implements survey biomass as a penalty function.

3.2.7. Q–values and Vessel Units estimation

Catches ($C_{v,y}$) and effort ($E_{v,y}$) of each active vessel v for the year y during the last 5 years (2011–2015 for the purpose of the 2017 licence advice) are used to estimate the Catch Per Unit Effort ($CPUE_{v,y}$ in kg.h^{-1}) for each vessel and year as:

$$CPUE_{v,y} = \frac{C_{v,y}}{E_{v,y}}$$

Using $CPUE_{v,y}$ and the unexploited fishable biomass estimation derived from survey data for the year y (B_y), the rock cod catchability ($q_{v,y}$) for the vessel v during the year y can be derived as

$$CPUE_{v,y} = q_{v,y} \times B_y \Leftrightarrow q_{v,y} = \frac{CPUE_{v,y}}{B_y}$$

The average monthly effort ($E^m_{v,y}$) of each vessel v for the year y is estimated as:

$$E^m_{v,y} = \frac{E_{v,y}}{D_{v,y}} \times 30.5$$

Where $D_{v,y}$ is the number of fishing days for the vessel v during the year y. Monthly effort $E^m_{v,y}$ is then averaged over the preceding 5 years for each vessel v. Catchability $q^m_{v,y}$ is estimated for each year y and each vessel v as

$$q^m_{v,y} = \frac{C_{v,y}}{E^m_{v,y} \times B_y}$$

Both $E^m_{v,y}$ and $q^m_{v,y}$ are then averaged over the preceding 5 years to become $\bar{E}^m_v$ and $\bar{q}^m_v$ and both are used to estimate the vessel units month (VUM_v) of each vessel v using the rock cod abundance (B_y) of the year y which is the last biomass estimation ($y = 2016$) in the purpose of the 2017 licence advice as:

$$VUM_v = \frac{\bar{q}^m_v \times E^y_v \times B_y}{1000}$$

As VUM_v is often proportional to the GRT, a linear regression is fitted for each licence to estimate the associated intercept (a) and slope (b) values. If this linear relationship is statistically significant, suggestions for 2017 VUM_{GRT} are then made as the median calculated for particular 500 mt–GRT band interval as

$$VUM_{GRT} = a + b \times GRT$$

If the linear relationship is not statistically significant, VUM are then equal to the intercept

$$VUM_{GRT} = a$$

Finally the fishing time is estimated as

$$FT = \frac{VU}{VUM_{GRT}}$$

Where VU is the proportion of TAC (60 for the 60,000 t used during the last years) allocated to the licence type (12.2 for the 12,200 t allocated to A–licensed vessels, 18 for the 18,000 t allocated to G–licensed vessels and 20.1 for the 20,100 t allocated to W–licensed vessels were defined in the framework of the 2015 licence advice based on historical catches of each licence type).

3.3. Results

3.3.1. Length frequency

Total length data of rock cod were collected for length frequency distribution from 2003 to 2015. Each year, between 1,500 and 25,500 fish have been measured after sex and maturity determination. Length frequency histograms (**Figure 3.1**) showed that catches were bimodal during the first two years. Starting from 2005, one mode was

identified for each year. Mean total length first increased from 2003 to 2008 when it reached its maximum value, then decreased until 2013 and finally increased again during the last two years of the time series (**Figure 3.2**). No significant differences were found between average total length of 2003 and 2015. The onset of the targeted fishery in 2007 is probably at the origin of the decreasing trend starting in 2008, a phenomenon already observed in other fisheries. The fishery does not seem to have impacted the average length of fish caught as no significant difference was found between the start and the end of the time series.

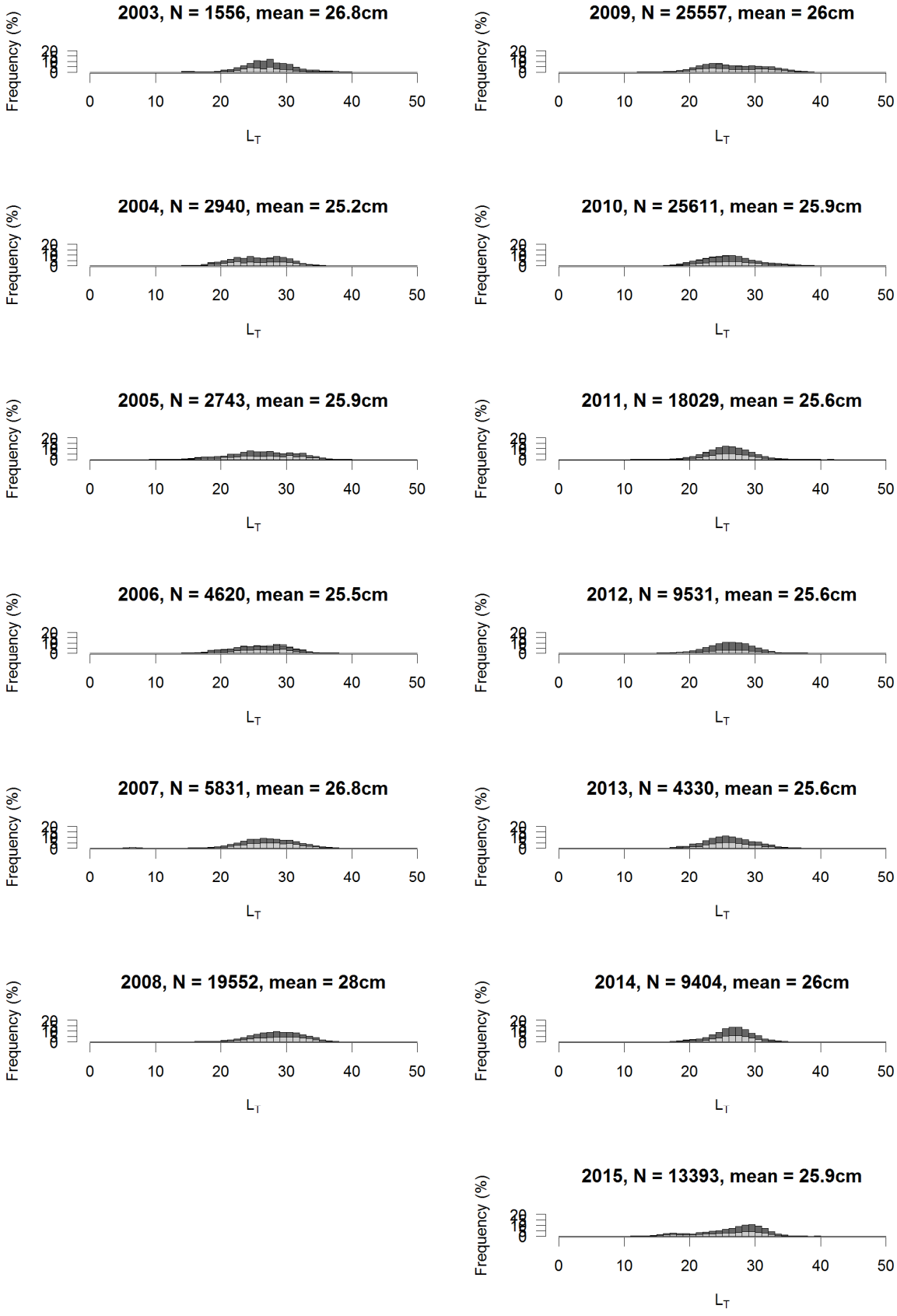

Figure 3.1: Annual length frequencies of female (dark grey) and male (light grey) rock cod sampled during observer trips and research cruises from 2003 to 2015 in the finfish area. N is the number of fish sampled per year and mean is the average length.

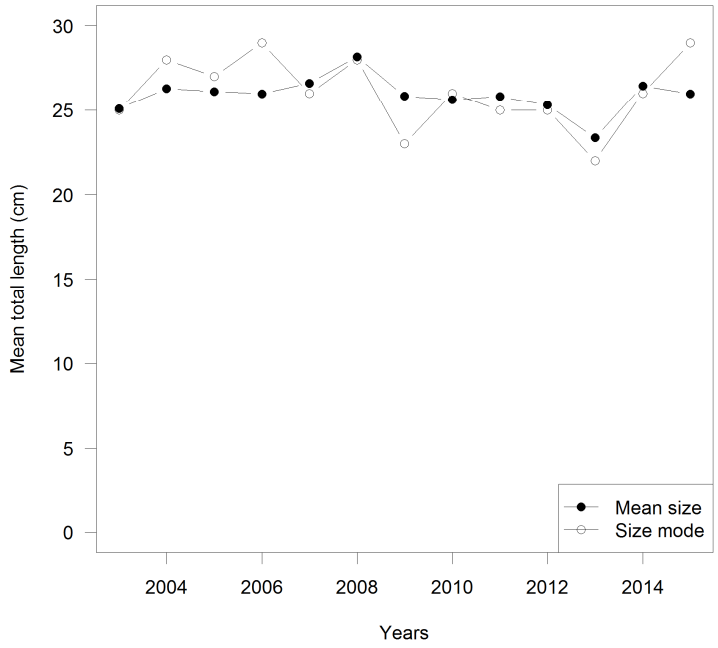

Figure 3.2: Annual mean and mode of rock cod total length. Specimens were collected by observers during commercial trip or during surveys.

3.3.2. Length–at–maturity

Rock cod maturity data were fitted to binomial GLMs from 2003 to 2015. Throughout this period, the length–at–maturity (**Figure 3.3**) first varied without trend from 2003 to 2007 and then followed a decreasing trend until 2013 from 27.65 to 24.24 cm. This decrease occurred in two steps, a first one at the onset of the fishery between 2007 and 2008 and the second one from 2011 to 2012. Finally, from 2013 to 2015 length–at–maturity followed an increasing trend.

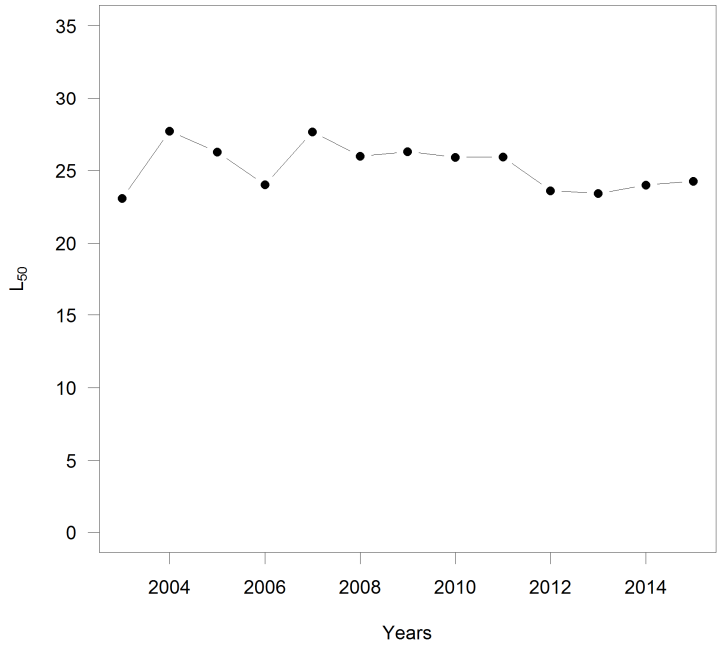

Figure 3.3: Length–at–maturity time series using data collected in June, July and August.

3.3.3. Age–length relationship

The DNR-F otolith collection started in 1994 and was continuous from 2002 to 2015 (**Table 3.1**). Depending on the year, ageing was carried out by an ageing lab in Gdnya (Poland) or by DNR-F staff scientists. A first set of otolith was aged by DNR-F in 2003–2004 before the targeted fishery started in order to have a better insight of the rock cod population dynamic. Ageing started to be carried out on a regular basis from 2008, first by Gdnya ageing lab until 2010 and then by two different agers in DNR-F.

Age–length relationships were modelled in 2003–2004 and from 2008 through to 2014 (**Figure 3.4**). The likelihood ratio test revealed that von Bertalanffy curves were all significantly different from year to year. However, the time series of the 3 parameters and of the growth performance index did not show any significant trend throughout the studied period (**Figure 3.5** and **Figure 3.6**). Moreover, the age distribution does not appear to have changed much and the sampled fish still cover the full age distribution 0 – ±15 years.

Table 3.1: Annual number of otoliths collected and aged and name of the ager for rock cod.

Year	Number of otoliths collected	Number of Otoliths aged	Ager
1994	223	0	
1995	417	0	
1997	1	0	
1999	15	0	
2000	23	3	GDY
2001	3	3	GDY
2002	618	0	
2003	1552	705	PB
2004	1787	467	PB
2005	216	0	
2006	78	0	
2007	196	0	
2008	764	641	GDY
2009	1113	1042	GDY
2010	1144	531	GDY
2011	1295	518	EB
2012	1067	484	EB
2013	1208	452	BL
2014	1208	446	BL
2015	1276	0	

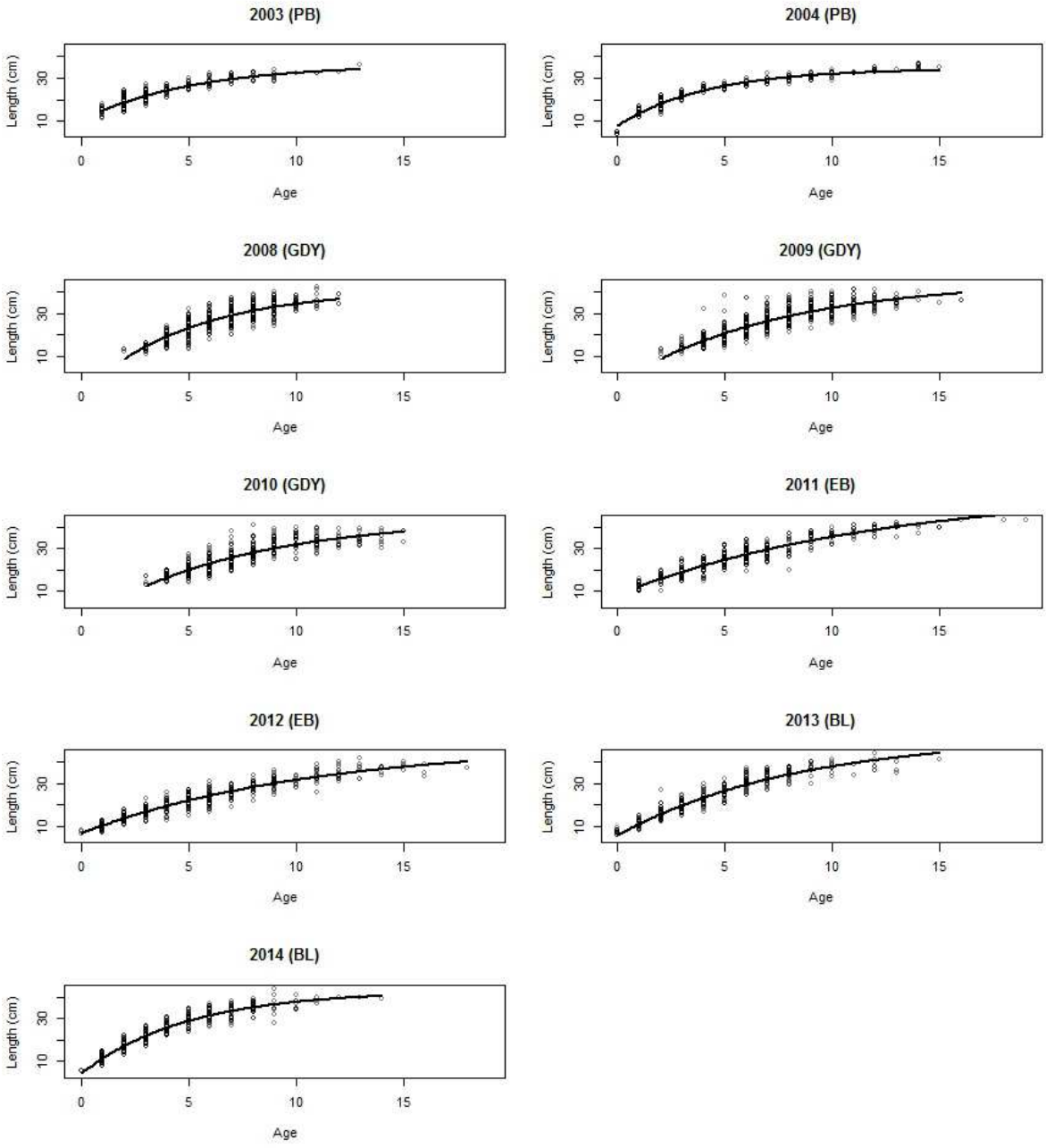

Figure 3.4: Annual age–length relationships modelled using a von Bertalanffy growth model fitted to age data collected by the DNR-F.

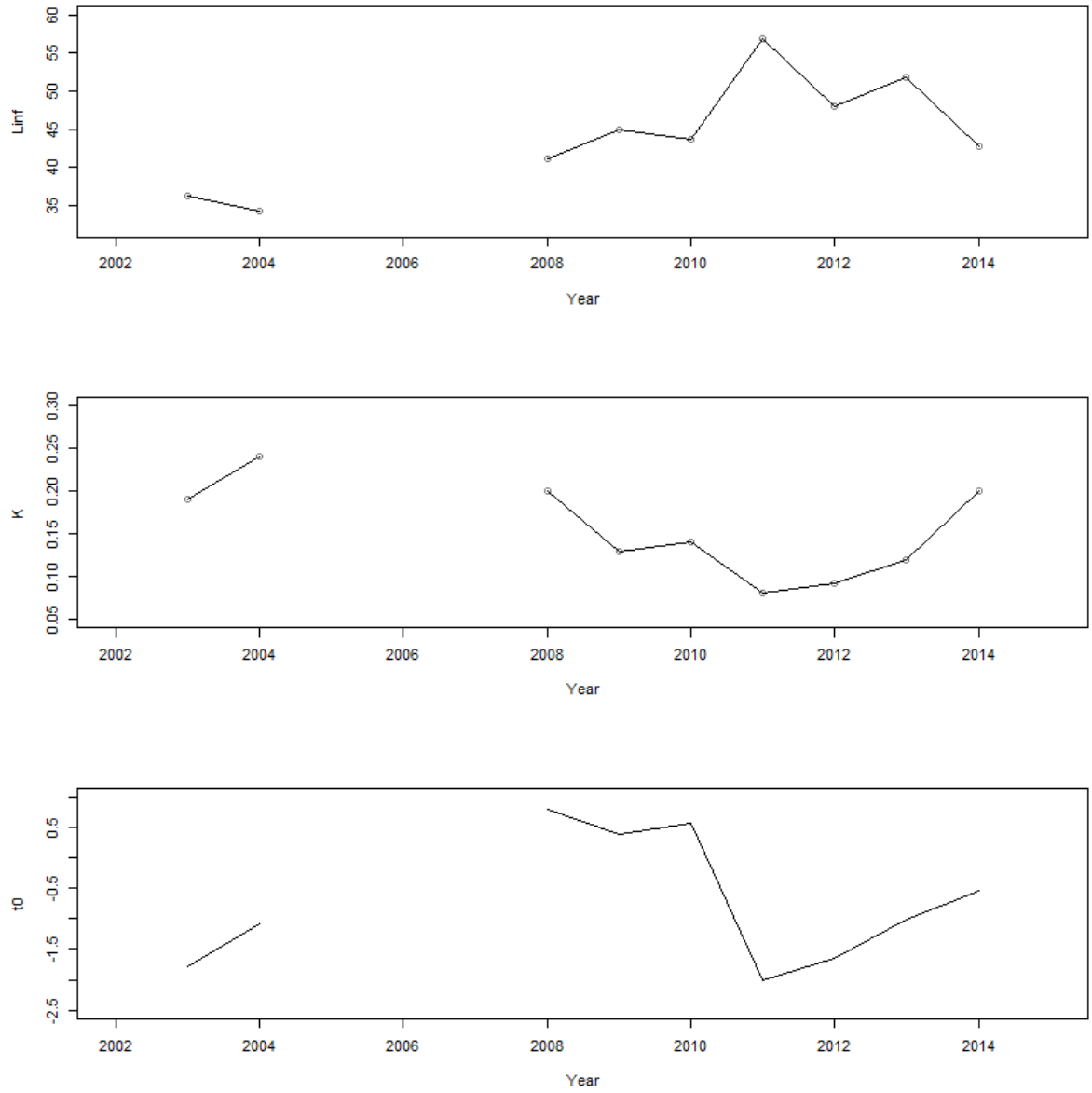

Figure 3.5: Time series of the 3 parameters of the von Bertalanffy growth models fitted to age data collected in 2003–2004 and from 2008 through to 2014.

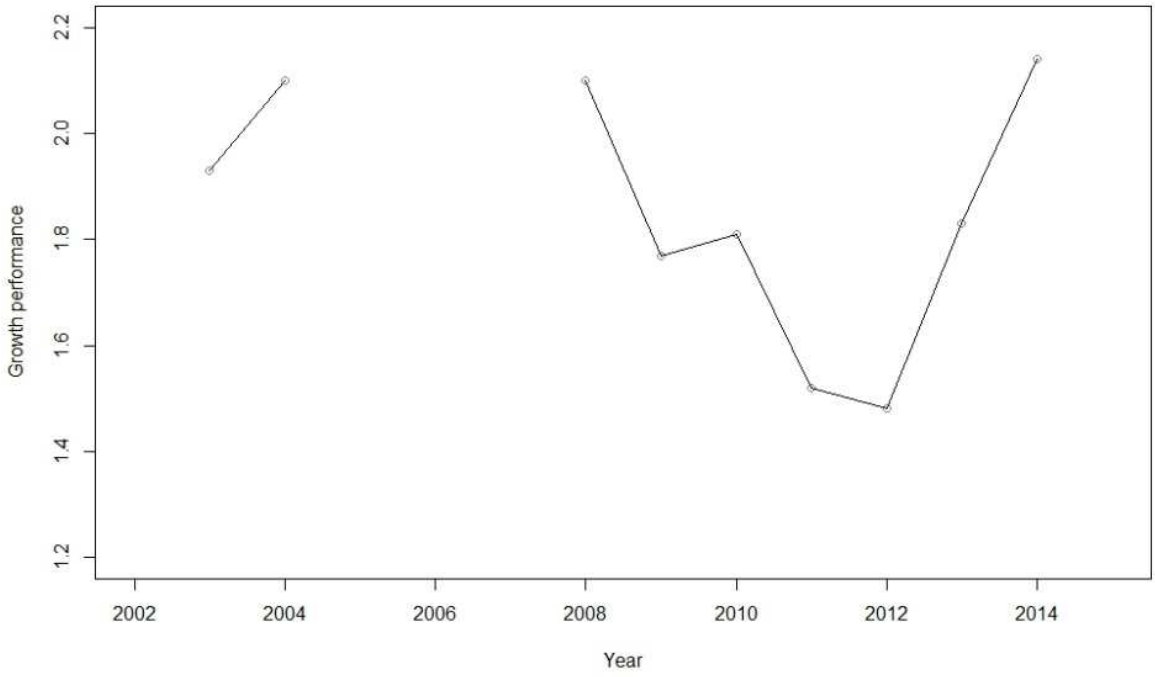

Figure 3.6: Time series of the growth performance index derived from von Bertalanffy growth model parameters.

3.3.4. Biomass survey

From 2016, the DNR-F has used two sensors to measure the horizontal net opening of the DNR-F's bottom trawl during research cruises (Gras et al., 2016). As significant differences were noted between estimated and measured horizontal net opening, two models were developed to correct historical research cruise data and estimate new comparable biomasses (Gras, 2016). The first biomass estimation for rock cod was carried out in February 2010 and revealed that 653,009 t of rock cod were present in the finfish area (**Figure 3.7**). When this survey was repeated in February 2011, the biomass increased to 803,955 t. In 2014 the survey was conducted in October and the biomass was estimated at 262,415 t. In order to carry out a seasonal comparison, the survey was repeated in February 2015 showing a decrease of the biomass to 206,485 t. Finally, the biomass estimation based on February 2016 survey revealed a slight decrease of the biomass at 195,693 t. Highest concentrations were identified every time in the northwest and in the northeast of the finfish area where large and small rock cod were caught respectively (**Figure 3.7**).

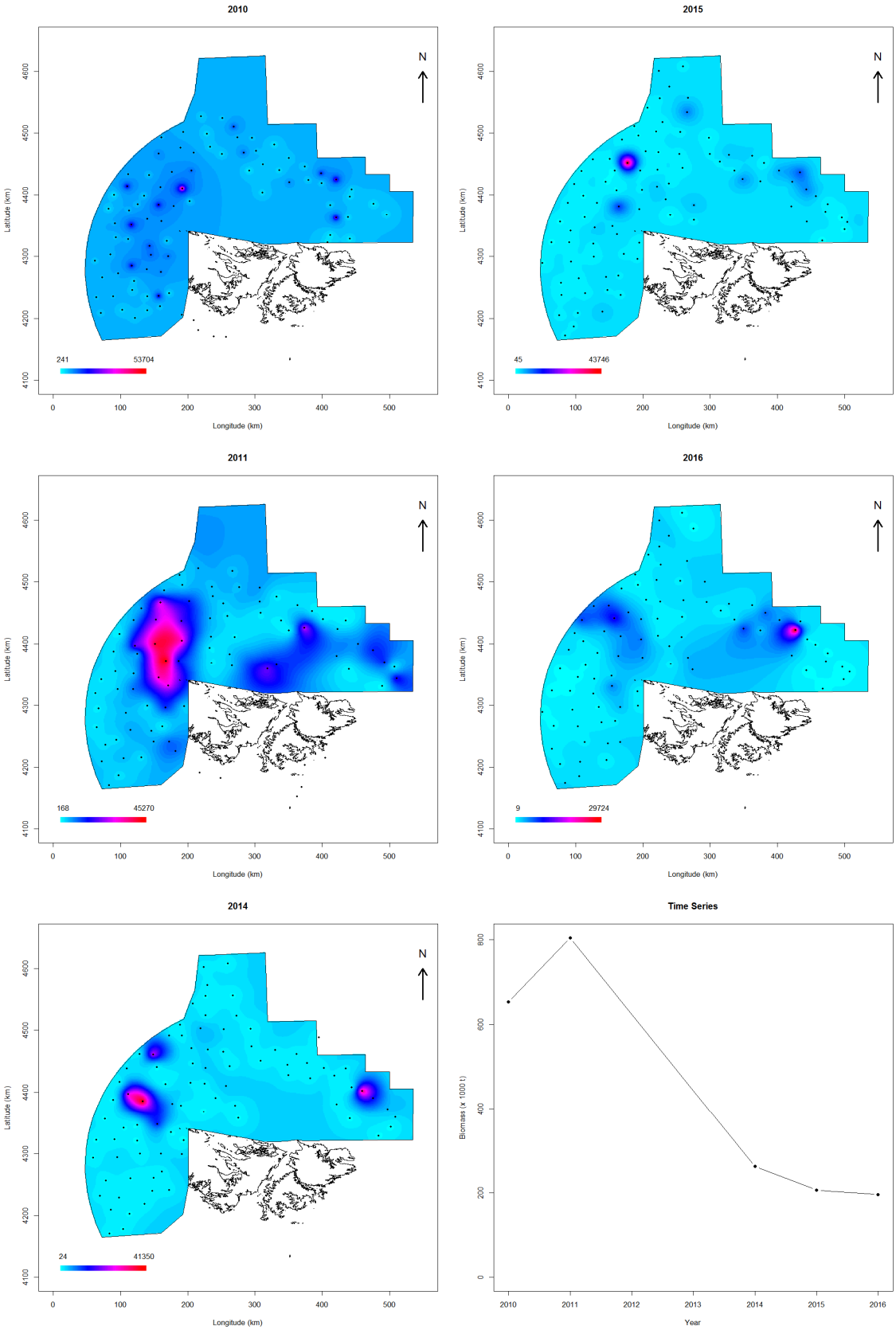

Figure 3.7: Kriged maps of rock cod abundance in the surveyed area based on catch data collected during the surveys conducted in February 2010, 2011, 2014, 2015 and 2016.

3.3.5. Catches and fisheries dependent index of abundance

Reported catches by trawlers operating in Falkland waters (**Figure 3.8** left) increased from 2005 (8620 t) to 2010 when a maximum of 76,458 t was achieved. From 2010 to 2013 catches decreased to 32,436 t. In 2014, catches increased again to 56,686 t and finally dropped again in 2015 to 29,038 t which was the lowest annual catch observed since 2006 (prior to the onset of the fishery).

Index of relative abundance derived from fisheries dependent data increased from 2005 to 2010 and then exhibited a high variance without showing any increasing or decreasing trend (**Figure 3.8** right).

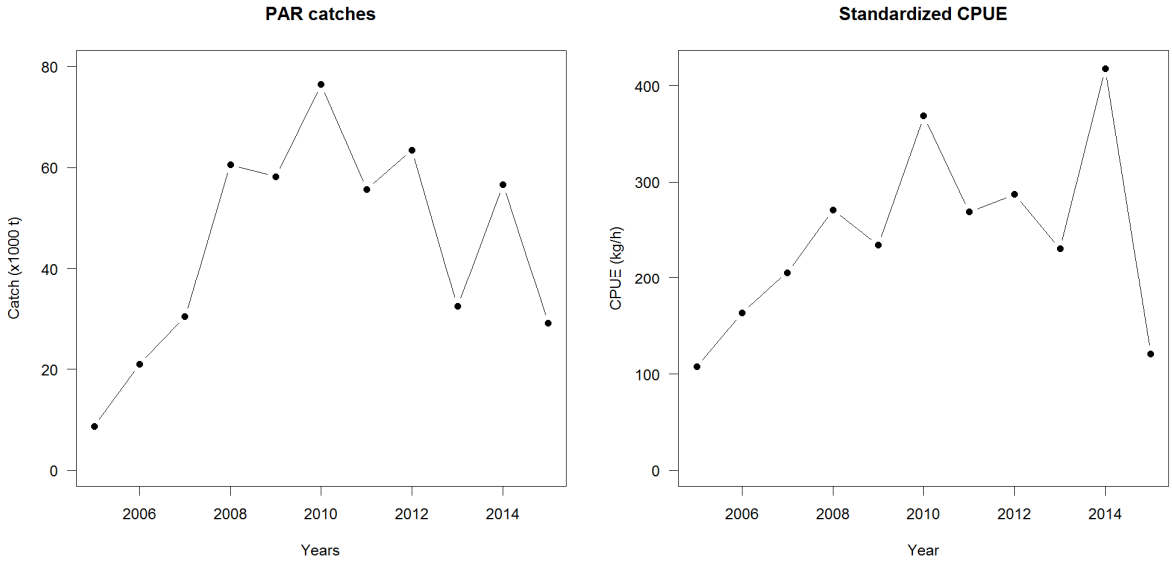

Figure 3.8: Annual total catches in Falkland waters (left) and time series of the standardized CPUE (right) from 2005 to 2015

3.3.6. Biomass dynamic model

The biomass dynamic model was fitted to the index of relative abundance (**Figure 3.9**). The model shows an increase of rock cod abundance from 2005 to 2008. The biomass seems then to be stable until the end of the time series. However, the model does not reflect the variance observed in the index of relative abundance at the end of the time series.

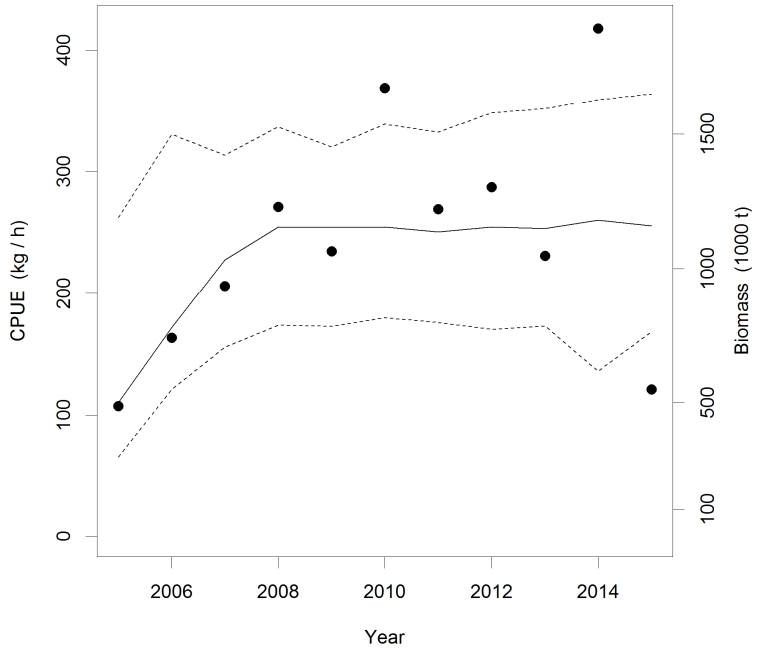

Figure 3.9: Schaefer biomass dynamic model (solid line) fitted using the standardized CPUE (dots) derived from the finfish fleet operating in Falkland waters. The confidence interval of the estimation (dashed line) was estimated using a Markov Chain Monte Carlo procedure.

3.4. Conclusion

Although annual catches of rock cod were stable between 2008 and 2012, they became more variable between 2013 and 2015. Especially in 2013 and 2015, vessels did not target rock cod and catches were on average 30,000 t. Analyses of biological data showed that the rock cod stock does not exhibit any sign of overexploitation. Moreover, the biomass dynamic model which was fitted using the fishery dependent index of relative abundance showed that the rock cod biomass, after experiencing an increase from 2005 to 2008 remained stable until 2015. However, data collected during surveys in 2010–2011 and 2014–2016, which are the most reliable sources of information to monitor the rock cod stock abundance, showed that rock cod biomass decreased from 650,000 to less than 200,000 (–70%) between 2010 and 2015.

3.5. Recommendation

Although two of the three sources of information showed that rock cod abundance was stable since the onset of the fishery in 2007, the most reliable source (fishery independent) showed that biomass in 2015 and 2016 was only 30% of the biomass estimated in 2010. Using this new biomass estimation and the last 5 years of catch and effort (including 2013 and 2015 when vessels did not target rock cod) as input data in the vessel unit months (VUM) estimation led to significant decrease of VUM and significant increase of fishing time, sometimes up to 300%. Allowing such an increase of effort would not be sustainable for the finfish fishery and might lead to an overexploitation of the finfish resources. Following a precautionary approach, the DNR–F decided to reduce the VUM of G, W licences and bycatch by 10%. The VU

used to estimate the allocated fishing effort for 2017 are in Table 3.1 of the licence advice part 1 (FIFD, 2016).

On top of the TAE historically used to regulate the finfish fishery and because the rock cod biomass drop observed in February 2015 was confirmed in February 2016, **a precautionary TAC for rock cod will be set up for 2017 at 30,000 t**. The TAC corresponds to the average of the two lowest annual catches (2013 and 2015) observed since the onset of the fishery in 2007. Vessels will be allowed to target rock cod as long as the total catch of 2017 will be <30,000 t. As soon as the TAC of 30,000 t will be achieved, vessels will be asked not to target rock cod anymore and target other stocks. The same enforcement will be applied for restricted finfish licensed vessels with hake, i.e. vessels catching more than 10% of rock cod will be asked to change the fishing area.

3.6. Perspectives

During the last decade, the DNR-F has put an effort into gaining a better insight of the rock cod biology and population dynamics (Brickle et al, 2006a; Brickle et al, 2006b; Laptikhovsky et al., 2013; Arkhipkin et al., 2013). At the same time, a series of surveys has been carried out throughout the finfish area to estimate the available biomass in the finfish area (Brickle and Laptikhovsky, 2010; Arkhipkin et al., 2011; Pompert et al., 2014; Gras et al., 2015; Gras et al., 2016). It was shown that this biomass significantly decreased from 2010 to 2016.

In this report, it has been shown that von Bertalanffy parameters of rock cod age–length relationships are significantly different from year to year but time series of parameters do not indicate that rock cod stock is declining. However, as calibration is not yet available, year and agers effects are not separated. In the near future, a calibration between all agers will be set up. Moreover, some years of the rock cod otolith collection has not been aged and the time series from 2003 could be completed to date.

During the last years, the Vessel Unit method has shown several limits. First, the method is valid only when fishers target rock cod. When fishers try to avoid this stock like in years 2013 and 2015, VUM significantly decreased leading to a significant increase of the fishing time, a non–sustainable situation on the long term for the Falkland fisheries stocks. Improvements of the method will be tested in the near future to try to avoid annual adjustments to the methodology.

3.7. References

Arkhipkin, A. I., Bakanev, S., & Laptikhovsky, V. V. (2011). *Rock cod biomass survey*. Stanley, Falkland Islands.

Arkhipkin, A. I., Jurgens E., Howes, P.N. (2013). Spawning, egg development and early ontogenesis in rock cod *Patagonotothen ramsayi* (Regan, 1913) caught on the Patagonian Shelf and maintained in captivity. *Polar Biology*, *36*(8), 1195–1204.

Brickle, P., Arkhipkin, A. I., & Shcherbich, Z. (2006a). Age and growth of a sub-Antarctic notothenioid , Patagonotothen ramsayi (Regan 1913), from the Falkland Islands. *Polar Biology*, *29*(8), 633–639.

Brickle, P., & Laptikhovsky, V. V. (2010). *Rock cod biomass survey*. Stanley, Falkland Islands.

Brickle, P., Laptikhovsky, V., Arkhipkin, A. I., Portela, J. (2006b). Reproductive biology of *Patagonotothen ramsayi* (Regan, 1913) (Pisces: Nototheniidae) around the Falkland Islands. *Polar Biology, 29*, 570–580.

FIFD (2016) Vessel Units, Allowable Effort, and Allowable Catch 2017. Fisheries Department, Directorate of Natural Resources, Falkland Islands Government.

Gras, M. (2016). *A linear model to predict horizontal net opening of the DNR Fisheries Department bottom trawl*. Stanley, Falkland Islands.

Gras, M., Blake, A., Pompert, J., Jürgens, L., Visauta, E., Busbridge, T., Rushton, H., Zawadowski, T. (2015). *Report of the 2015 rock cod biomass survey ZDLT1–02–2015*. Stanley, Falkland Islands.

Gras, M., Pompert, J., Blake, A., Boag, T., Grimmer, A., Iriarte, V. & Sanchez, B. (2016). *Report of the 2016 finfish and rock cod biomass survey ZDLT1–02–2016*. Stanley, Falkland Islands.

Haddon, M. (2010). *Modelling and quantitative methods in fisheries*. CRC press.

Hilborn, R., & Walters, C. J. (1992). *Quantitative Fisheries Stock Assessment Choice, Dynamics and Uncertainty*. (R. Hilborn & C. J. Walters, Eds.). Springer.

Laptikhovsky, V., Arkhipkin, A. I., & Brickle, P. (2013). From small bycatch to main commercial species: Explosion of stocks of rock cod Patagonotothen ramsayi (Regan) in the Southwest Atlantic. *Fisheries Research*, *147*, 399–403.

Maunder, M. N., & Punt, A. E. (2004). Standardizing catch and effort data: a review of recent approaches. *Fisheries Research*, *70*(2-3), 141–159.

Pauly, D. (1979). *Gill size and temperature as governing factors in fish growth: a generalization of von Bertalanffy's growth formula*.

Pompert, J., Gras, M., Blake, A., & Visauta, E. (2014). *Rock cod biomass and biological survey*. Stanley, Falkland Islands.

4. Toothfish

4.1. Summary

1. Toothfish stock assessment was calculated using an age-structured production model in CASAL software. The stock assessment model was revised for 2015 by: a) including out-of-zone catch reports, b) optimizing natural mortality within the model and c) empirically evaluating the best-fit umbrella factor.

2. The revised and updated model obtained a natural mortality of M = 0.184 year^{-1} and a best-fit umbrella factor of 0.38.

3. The stock assessment calculated toothfish total biomass of 24,243 tonnes and spawning stock biomass of 7079 tonnes in 2015. The ratio of SSB_{2015} : SSB_0 (current spawning stock biomass to unfished spawning stock biomass) was 0.445. Maximum sustainable yield was estimated by the stock assessment model at 1579 tonnes, of which 1276.5 tonnes allocable to the longline fishery after deductions for finfish and *Loligo* bycatch.

4. The recommendation for the toothfish longline fishery is to maintain total allowable catch (TAC) at 1040 tonnes, same as last year. The recommendation is based on proximity of the SSB_{2015} : SSB_0 ratio to the threshold reference point, plus evidence of the toothfish population rebuilding from retrospective analysis of the data.

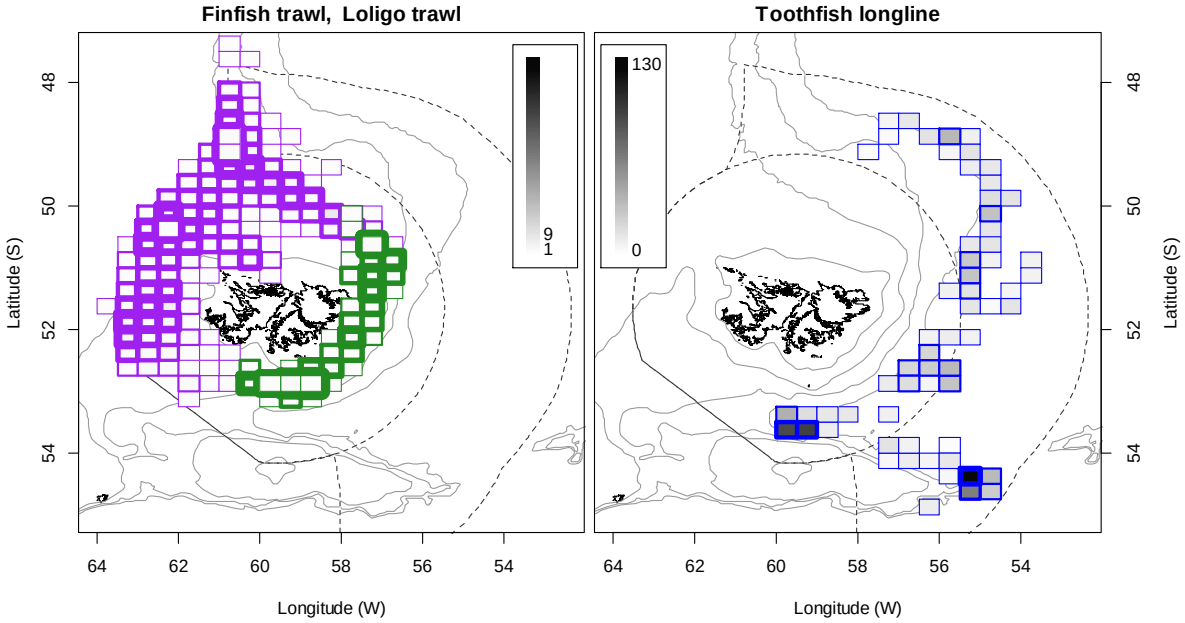

Figure 4.1. Distribution of toothfish catches in 2015 by Falkland zone grid. Thickness of grid lines is proportional to the number of vessel-days; grey-scale is proportional to the toothfish catch biomass. Left: finfish trawls (purple); maximum 200 vessel-days and maximum 9 tonnes toothfish in one grid, *Loligo* trawls (green); maximum 256 vessel-days and maximum 1 tonne toothfish in one grid. Right: toothfish longline (blue); maximum 26 vessel-days and maximum 130 tonnes toothfish in one grid.

4.2. Introduction

A commercial longline fishery targeting Patagonian toothfish (*Dissostichus eleginoides*) has been operating in Falkland Islands waters since 1994 (des Clers et al. 1996, Laptikhovsky and Brickle 2005). Important quantities of toothfish are also caught in two other Falklands fisheries: finfish trawl, of which it is not a target but commercially valuable bycatch, and *Loligo* (*Doryteuthis gahi*) squid trawl, of which it is also bycatch, but individuals caught in this fishery are too small to be commercially valuable. The fisheries access different parts of the toothfish population in different areas: longlining occurs on the slope and in deep water, finfish trawling on the shelf primarily north and west of the Falkland Islands, and *Loligo* trawling also on the shelf, east of the Falkland Islands (Figure 1).

The current stock assessment of Falkland Islands toothfish was calculated with updated catch and effort through 2015, and with 679 additional age / size metrics from otoliths sampled in 2014. In 2015, reported toothfish catch totalled 1232.2 tonnes, the lowest since 1997. Of the total toothfish catch in 2015, 91.1% by weight was taken by longline license, 8.4% by finfish trawl, and 0.5% by *Loligo* trawl. Longline fishing was undertaken during 216 days in 2015, the lowest effort since 1993.

4.3. Methods

The stock assessment was calculated as an age-structured production model in CASAL software (C++ Algorithmic Stock Assessment Laboratory; Bull et al. 2012). As previously (FIFD 2014), this stock assessment was based on the objective function comprising one relative annual abundance index (longline CPUE), and catch-at-age distributions of the toothfish longline, finfish trawl (including skate and surimi licenses), and *Loligo* trawl fisheries. Jig and pot fisheries catch negligible quantities of toothfish and have no toothfish observer data to determine catch-at-age distributions. Finfish trawl and *Loligo* squid trawl were modelled separately because the small mesh permitted solely for *Loligo* fishing results in different toothfish catch-at-age distributions. The two *Loligo* seasons were combined. The use of only longline CPUE as a relative abundance index was motivated by the inconsistency of CPUE in fisheries where toothfish is a bycatch and not a target; toothfish bycatch may change just because those fisheries are switching targets, areas, or seasonality, rather than by any factors related to the toothfish stock.

Yearly index values were weighted for the CASAL optimization using Francis' (2011) two-stage approach. First, to address observation error an effective sample size (N) of age-class data per year in each fishery was calculated based on data fit to the multinomial distribution, using the function 'Neff.obs' in R package 'DataWeighting' (Francis 2013). Second, to address process error, effective sample sizes were multiplied by a weighting factor calculated as the inverse of the variance of difference between observed and expected mean age classes, standardized for the variance of the expected age distributions (Method TA1.8 in Table A.1, Francis 2011).

The age-structured production model was calculated with a Beverton-Holt stock-recruitment function (Bull et al. 2012). The steepness parameter of the stock-

recruitment function (the fraction of recruitment from the unfished population when spawning stock biomass declines to 20% of its unfished level; Mangel et al. 2013) was set to the commonly used reference value of 0.75 (Brandão and Butterworth 2009, Day et al. 2014, Mormede et al. 2014). Recruitment variability was set to 0.6 (Mormede et al. 2014). The variability distributions of optimized quantities such as total biomass and spawning stock biomass in the age-structured production model were calculated by Monte-Carlo Markov Chain (MCMC).

4.3.1. Data

Longline CPUE data were restricted to catch reports of ≥500 m set depth and ≥1 kg toothfish catch weight, as the contrary were presumed to represent erroneous entries or broken line sets. The longline CPUE index was also restricted to years since 1996. Earlier years were considered compromised by high levels of IUU fishing (Payne et al. 2005), and the composition of the longline fishing fleet changed from 1996 onwards. Before 1996, longline fishing was conducted mostly by Chilean vessels, after 1996, mostly by Falklands and Korean vessels; a difference which would have caused a disproportionate vessel effect in the standardization model.

However, catch totals and catch-at-age proportions were used from all available years. Catch reports that list fishing effort as "trawl and jig time" (used under various licenses until 1996) were considered trawls if the unit effort was ≤1440; the number of minutes in 24 hours. Trawl catch reports under experimental license were considered *Loligo* trawls if >50% of the catch was *Loligo*, or if the report was within 7 days of a report by the same vessel that did catch >50% *Loligo*. Otherwise, experimental-license trawls were considered finfish.

Toothfish age and maturity data were restricted to measurements that had been processed by FIFD staff and observers, and restricted to ages >0. Length data were restricted to measurements that had been sampled randomly. Age / length distributions were summarized for the longline, finfish trawl, and *Loligo* trawl fisheries separately. As far as possible[7], observer age / length data were matched to catch reports, and the same criteria as above were used to distinguish between finfish trawls and *Loligo* trawls.

4.3.2. Input analyses

For the age-structured production model, catch proportions-at-age in the longline, finfish and *Loligo* fisheries were calculated by assigning ages to all length measurements by conditional probability of the age-at-length distributions. Ages ≥31 years were assigned to a '31+' class. Longline CPUE (kg / 1000 hooks) was standardized as described in Appendix 1. Catch selectivity-at-age was modelled as a logistic function in the longline fishery, but as a double-normal function in the finfish and *Loligo* fisheries because toothfish bycatches in these fisheries first increase then decrease with age. Maturity was scored on an 8-point scale, and toothfish are considered mature from stage 3 (Laptikhovsky et al. 2006, 2008). A maturity ogive (proportion ≥stage 3 per age) was fitted by a generalized additive model instead of the more typical logistic function because even the oldest ages had maturity proportions significantly less than 1 (Figure 2); an outcome that is likely related to skipped spawning (Collins et al. 2010, Brendon Lee FIFD pers. comm.). The length-weight

[7] Based on date and vessel call sign. Catch reports and observer data entries do not use cross-referenced identification codes.

relationship was calculated in the format $W = a \cdot L^b$ (Froese 2006), and length-at-age was modelled by the von Bertalanffy equation $L = L_{inf} \times (1 - e^{-K(t - t0)})$ in R package 'fishmethods' (Nelson 2015). Length-weight and size-at-age distributions are plotted in Figure 3; parameters are summarized in Appendix 2.

Figure 4.2. Proportion of toothfish mature (maturity stage ≥3) by age, from FIFD observer data. Fitted by a generalized additive model up to age 30, then the average of ages 31+ (red lines).

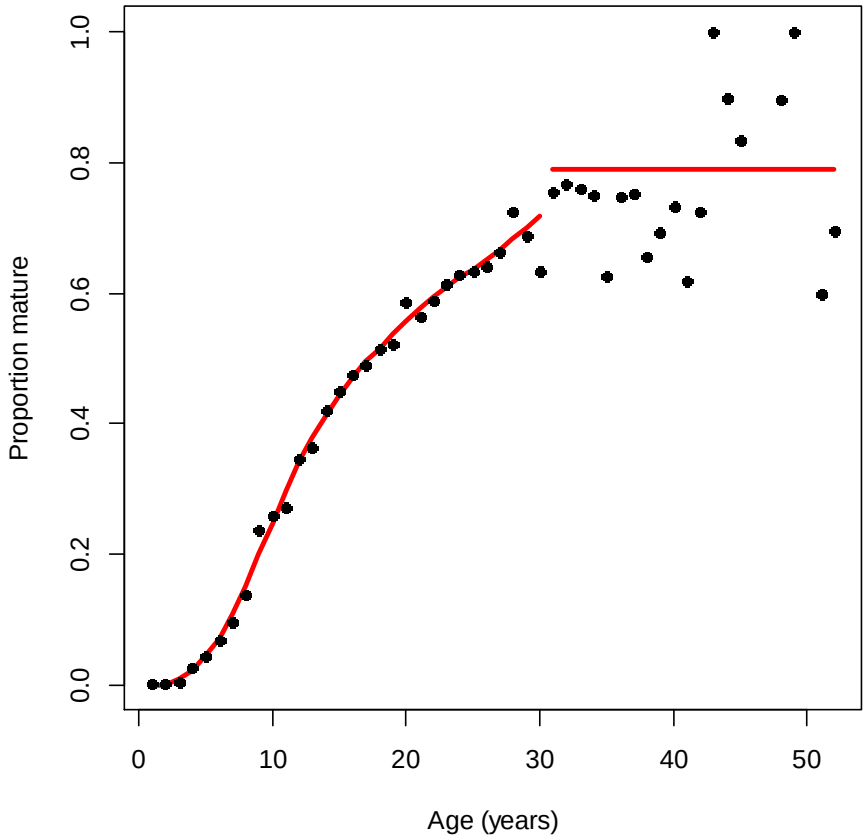

Figure 3 [below]. Length-weight (left) and length-at-age (right) relationships calculated from observer data. Equation parameters are summarized in Appendix 2.

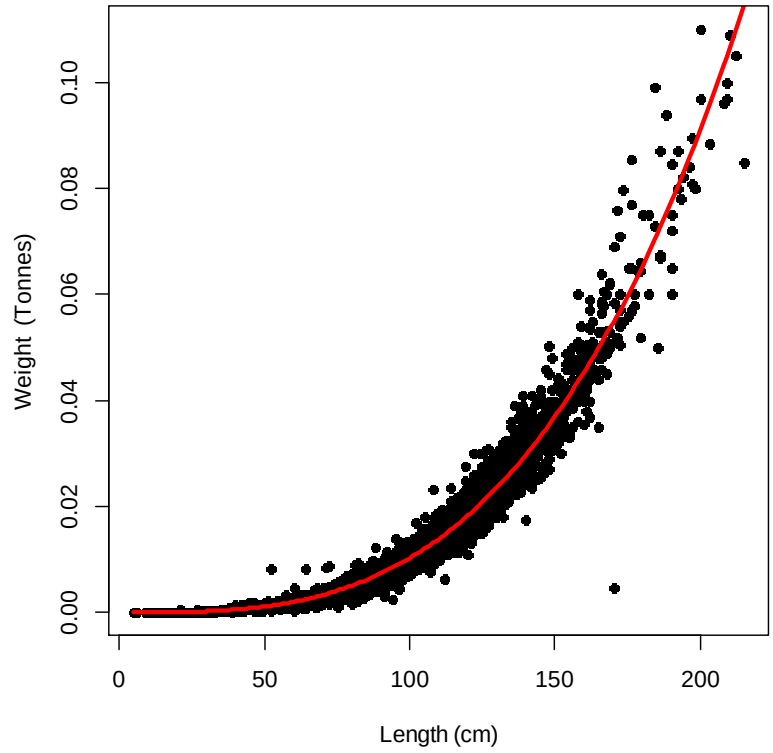

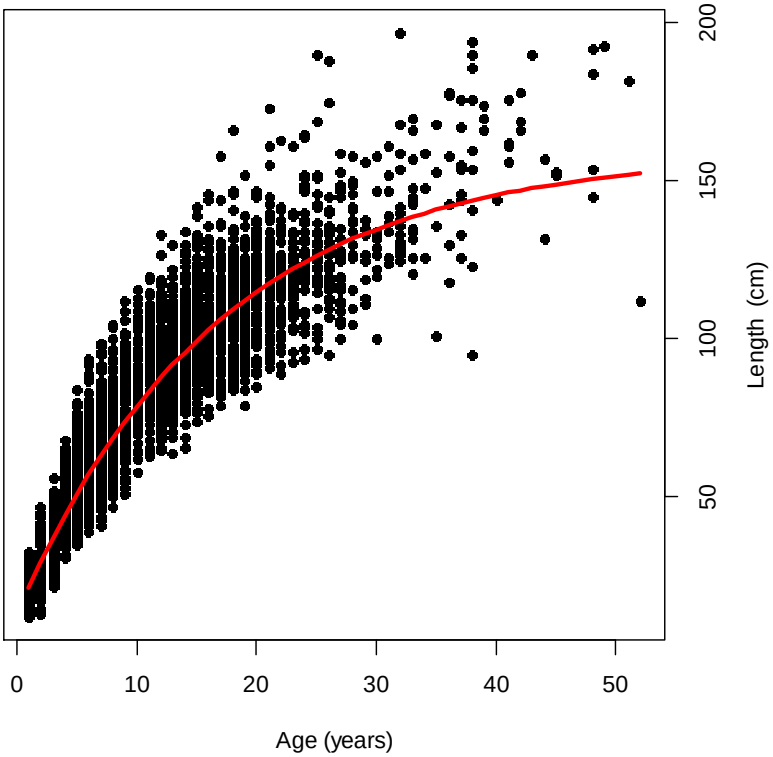

4.3.3. Model changes

Three changes from last year were effected in modelling the toothfish stock:

1. Out-of-zone catch reports were no longer excluded, as catches close to the zone impact the same toothfish population.

   Out-of-zone catch reports comprised 13.6% to 24.8% of longline toothfish catch weight in the three years 1998-2000, otherwise annually <10% of longline toothfish catch weight and 0% in the past four years; 0% to 7.8% of finfish trawl toothfish catch weight, and 0% of *Loligo* trawl toothfish catch weight. Given this inter-annual variability in out-of-zone catch percentage, not including the out-of-zone catches could potentially bias the relative annual abundance index.

2. Natural mortality of toothfish was estimated by optimization within the age-structured production model.

   A previous stock assessment (Payá and Brickle 2008) had estimated natural mortality at 0.13 from Hoenig's (1983) empirical equation ($\ln(M) = 1.44 - 0.982 \times \ln(t_{max})$) and assuming maximum longevity (t_{max}) of 35 years. This estimate was subsequently used as a fixed parameter in age-structured production models (Payá and Brickle 2008, FIFD 2013, FIFD 2014). However, the FIFD toothfish aging database by now includes 46 entries older than 35 years, taken between 2008 and 2013. Payne et al. (2005) used natural mortality 0.165 by averaging estimates calculated from the South Georgia toothfish stock. Because of the deficiency of natural mortality information specific to the Falkland Islands stock, the choice was made to optimize this parameter within the model. Variability of natural mortality was also calculated by MCMC.

3. The 'umbrella' factor was empirically evaluated.

   The 'umbrella' or 'cachalotera' longline method (Moreno et al. 2008) has been used in the Falkland Islands since July 2007 to reduce toothfish depredation by whales (Brown et al. 2010). Average improvement in toothfish CPUE has been estimated as 0.263^{-1} by the distribution mode of 'umbrella' to 'non-umbrella' catch ratios (Brown et al. 2010), and as 0.3125^{-1} by comparing same-day longline sets (Payá and Brickle 2008). Both analyses had obtained highly variable results on the basis of relatively restricted data sets. Subsequent stock assessments (FIFD 2013, 2014) used the factor of ×0.263 to scale toothfish CPUE under the 'umbrella' method since July 2007 to the putative equivalent CPUE without umbrellas before July 2007.

   For the current stock assessment, a range of umbrella factors from ×0.1 to ×0.5 was tested by calculating the age-structured production model with each umbrella factor in turn. The fitness of the umbrella factors was compared by the normalized root-mean-square deviation between each yearly CPUE index and its corresponding yearly total biomass from the age-structured production model. The umbrella factor with the best fit was then implemented for the final stock assessment.

Given these changes in the stock assessment model, a within-model retrospective analysis was calculated for three years prior to the latest year of the model (2015), using the same parameters and structure but cutting the most recent year's data from each successive model run (Legault 2009). The retrospective analysis was applied in particular to the stock indicator of $SSB_{current}$: SSB_0; the ratio of current spawning stock biomass to unfished spawning stock biomass under average recruitment.

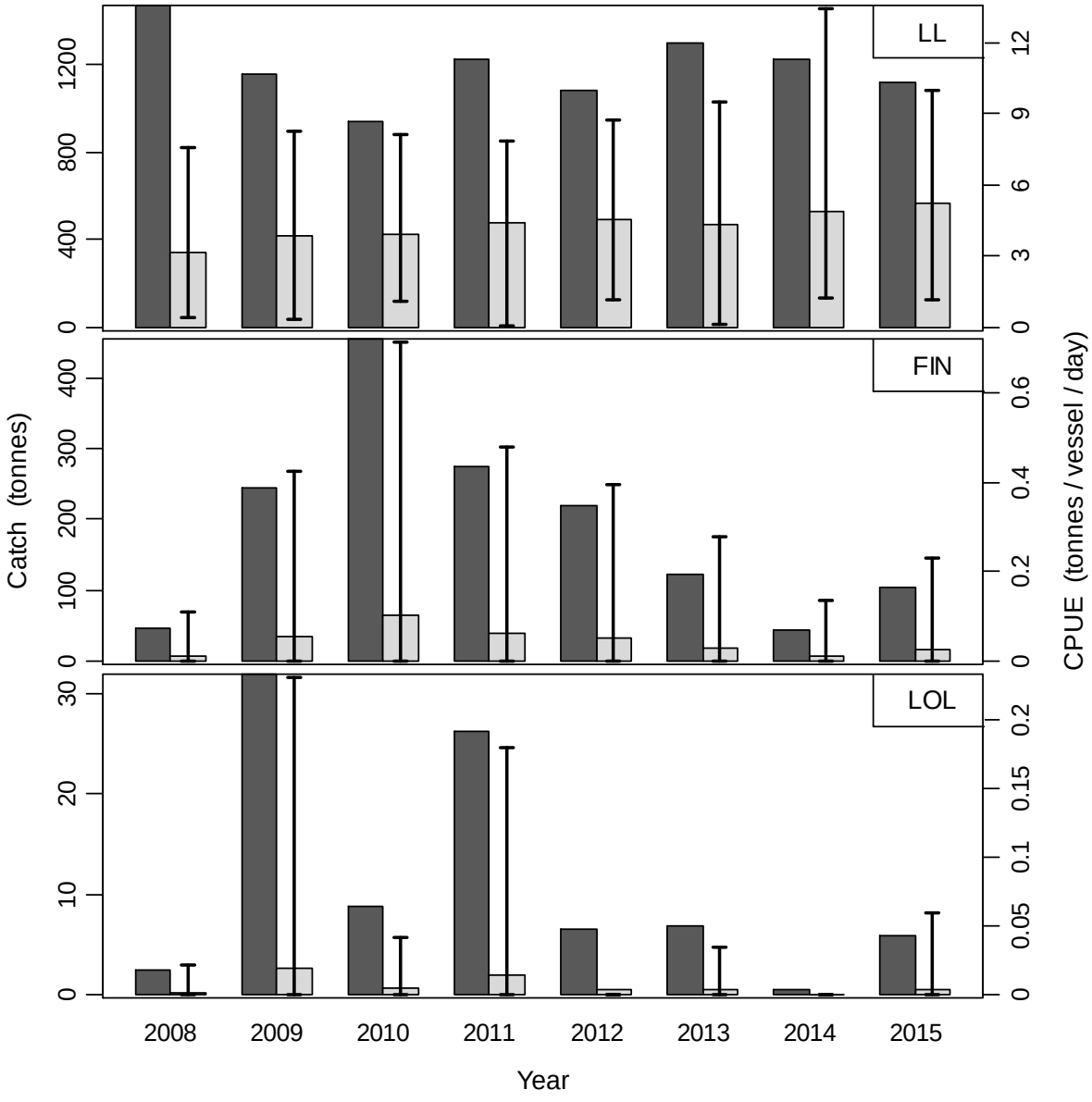

Figure 4.4. Annual catches (tonnes; dark bars) and unstandardized CPUE (tonnes / vessel / day; light bars with 95% intervals) of toothfish in each of the toothfish longline (LL), finfish trawl (FIN) and *Loligo* trawl (LOL) fisheries since 2008 (first full year of 'umbrella' longlining).

4.4. Results

4.4.1. Catches

Annual toothfish catches in the target longline fishery have ranged from 943 to 1469 tonnes since 2008, with a downward trend over the past three years. Average CPUE in the longline fishery increased significantly over the same period, from 3.1 to 5.2 t / vessel / day (Figure 4 - top panel). Annual toothfish catches and average CPUE in finfish trawls both reached their maximum in 2010, the year that rock cod (*Patagonotothen ramsayi*) first attained predominance in the finfish trawl fishery (FIG 2011). From 2010 toothfish catch and CPUE in finfish trawls declined annually until 2014, but increased again from 2014 to 2015 (Figure 4 - middle panel). Annual toothfish catches and CPUE in *Loligo* trawls were highest by large margins in 2009 and 2011 (Figure 4 - bottom panel), the two years which, except for the uncommon *Illex argentinus* ingression of 2015, had the lowest *Loligo* catches since 2008 (Winter 2015). That may comprise some bias as lower catches of one species can avail vessel crews to sort more carefully for another species, but bias is unlikely to represent the whole difference of toothfish bycatch being much higher in those two years. The contrast suggests that conditions resulting in poor *Loligo* abundance may be favourable to juvenile toothfish in the *Loligo* fishing zone.

4.4.2. Umbrella factor

Among iterations of the age-structured production model, the root-mean-square deviation of the CPUE index vs. total biomass minimized at an umbrella factor of 0.381 (smoothed by a LOESS function; Figure 5). Accordingly, the age-structured production model was calculated using the 0.38 umbrella factor.

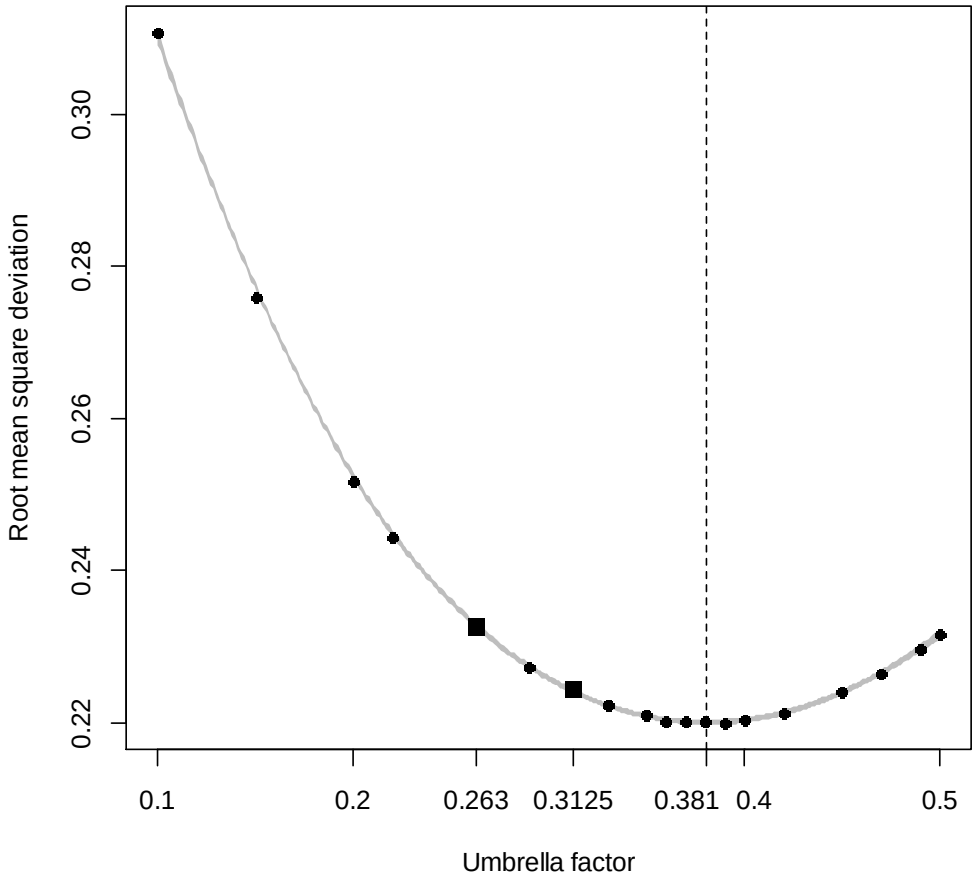

Figure 4.5. Normalized root-mean-square deviations between yearly CPUE indices and total biomass estimates, vs. the umbrella catch conversion factors they were calculated under. The two umbrella factors that were used in previous assessments are plotted as square symbols: 0.263 and 0.3125. A LOESS function of the root-mean-square deviations (grey trace) minimized at umbrella factor = 0.381.

4.4.3. Natural mortality

Natural mortality (M) optimized within the age-structured production model resulted in M = 0.184 year^{-1} with a 95% confidence interval of [0.171, 0.212] year^{-1}. This value is higher than the previous natural mortality parameter of M = 0.13 (Payá and Brickle 2008, FIFD 2014), which has likewise been used for toothfish in the Heard and McDonald Islands (Candy and Constable 2008) and Prince Edward Islands (Brandão and Butterworth 2009). The M = 0.184 year^{-1} model optimum is higher also than M = 0.165 used for toothfish in South Georgia (Hillary et al. 2006), and in the Falkland Islands as a composite average (Payne et al. 2005). This comparatively high M value produced by the current model optimization may potentially be an effect of invisible whale depredation; i.e. consumption of toothfish off a longline that leaves no trace and is therefore not quantified in the assessment. Research on the topic of longline depredation is currently in progress.

The practicality of estimating natural mortality within a stock assessment is a matter of some debate (Lee et al. 2011, Francis 2012, Lee et al. 2012). For toothfish, Candy et al. (2011) attempted to estimate natural mortality within the CASAL model

of the Heard and McDonald Islands fishery, but obtained boundary problems in optimizing parameters M and B_0 (unfished spawning stock biomass). In the current Falkland Islands stock assessment, boundary problems were not obtained and the relatively concise, realistic confidence interval indicates that the model estimate M = 0.184 $year^{-1}$ is appropriate.

4.4.4. Biomass and MSY

The standardized toothfish longline CPUE index decreased strongly from 1996 to 2006, and has shown a slowly increasing trend since 2006 (Figure 6 - top panel). Toothfish total biomass and spawning-stock biomass over the same period continued to decrease, as the long life-span of toothfish precludes rapid changes in population trends. However, the rate of biomass decrease has slowed (Figure 6 - bottom panel).

Estimated total toothfish biomass in 2015 was 24243 tonnes with a 95% confidence interval of [19239 to 58985 tonnes]. Estimated spawning stock biomass in 2015 was 7079 tonnes with a 95% confidence interval of [5400 to 16196 tonnes]. The ratio of $SSB_{current}$:SSB_0 was 7079 tonnes / 15915 tonnes = 0.445. Of the MCMC iterations, 7.7% of the distribution of SSBcurrent:SSB_0 ratios was <0.400, 24.9% of the distribution was <0.450, and 49.6% of the distribution was <0.500.

Maximum sustainable yield (MSY) calculated by the age-structured production model was 1579 tonnes. Spawning stock biomass corresponding to MSY was 3839 tonnes, and corresponding fishing mortality F_{MSY} = 0.35; i.e., the yield-per-recruit slope was 35% of the unfished yield-per-recruit slope.

MSY is based on toothfish catch of all fisheries. Allowable catch in the target longline fishery therefore deducts bycatches in the finfish and *Loligo* fisheries, factored by the loss of future spawning stock biomass from the bycatch in those fisheries. Calculations for the deductions are shown in Appendix 3. Finfish trawls took 103.1 tonnes toothfish in 2015, incurring a deduction of 103.1 × 2.60 = 268.0 t. *Loligo* trawls took 6.6 tonnes toothfish in 2015, incurring a deduction of 6.6 × 5.24 = 34.8 t. The multipliers represent finfish and *Loligo* trawls catching smaller, younger toothfish than the longline fishery, thereby removing larger numbers with higher potential for growth per unit catch weight. Based on MSY, maximum toothfish catch allowable to the longline fishery is thus 1579 – 268.0 – 34.8 = 1276.5 tonnes.

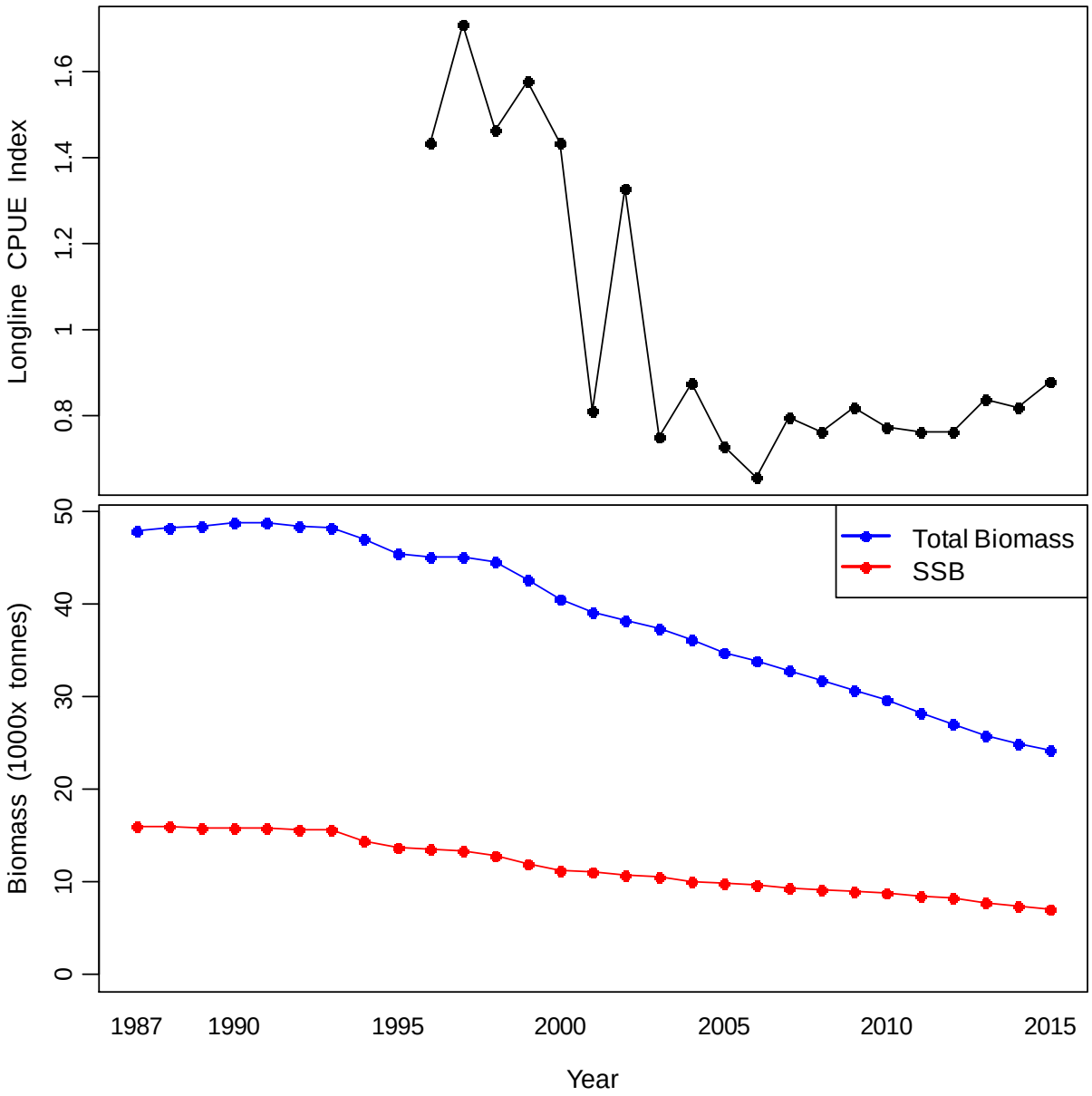

Figure 6. Standardized toothfish CPUE index in the longline fishery (top panel); toothfish annual total biomass and spawning stock biomass estimated with the age-structured production model, assuming an umbrella factor of 0.38 (bottom panel).

4.5. Recommendation

The Falkland Islands Fisheries toothfish harvest control rule prescribes that $SSB_{current}$:SSB_0 < 0.45 will result in reduction of total allowable catch (TAC) and increase in conservation measures (FIG 2014). The SSB_{2015}:SSB_0 ratio of the current stock assessment is 0.445 with 24.9% of the corresponding MCMC distribution < 0.45 (the distribution being right-skewed). Thus the $SSB_{current}$:SSB_0 ratio is just below the prescribed threshold reference point. However, the retrospective analysis of $SSB_{current}$:SSB_0 showed a continual improvement of the ratios with every yearly addition of data (Table 1). Accordingly, even though the historic depletion of the

toothfish stock has not been fully arrested as of 2015 (Figure 6, bottom panel), the trend is correcting itself along with increasing CPUE in the longline fishery (Figure 6, top panel).

Based on the evidence of a slowly recovering toothfish stock, the recommendation from this stock assessment is to maintain the TAC for longline fishing at its current level of 1040 tonnes.

Table 4.1. Retrospective analysis of $SSB_{current}$:SSB_0 ratios with toothfish stock assessment data from 2015 back to 2012.

Data	SSB_{2012}:SSB_0	SSB_{2013}:SSB_0	SSB_{2014}:SSB_0	SSB_{2015}:SSB_0
to 2012	0.453			
to 2013	0.477	0.453		
to 2014	0.507	0.483	0.461	
to 2015	0.514	0.489	0.466	0.445

4.6. References

Brandão A., Butterworth D.S. (2009) A proposed management procedure for the toothfish (*Dissostichus eleginoides*) resource in the Prince Edward Islands vicinity. *CCAMLR Science* 16, 33-69.

Brown J., Brickle P., Hearne S., French G. (2010) An experimental investigation of the 'umbrella' and 'Spanish' system of longline fishing for the Patagonian toothfish (*Dissostichus eleginoides*) in the Falkland Islands: Implications for stock assessment and seabird by-catch. *Fisheries Research* 106, 404-412.

Bull B., Francis R.I.C.C., Dunn A., McKenzie A., Gilbert D.J., Smith M.H., Bian R., Fu D. (2012) CASAL (C++ algorithmic stock assessment laboratory): CASAL user manual v2.30-2012/03/21. *NIWA Technical Report 135*, 280 pp.

Candy S.G., Constable A.J. (2008) An integrated stock assessment for the Patagonian toothfish (*Dissostichus eleginoides*) for the Heard and McDonald Islands using CASAL. *CCAMLR Science* 15, 1-34.

Candy S.G., Welsford D.C., Lamb T., Verdouw J.J., Hutchins J.J. (2011) Estimation of natural mortality for the Patagonian toothfish at Heard and McDonald Islands using catch-at-age and aged mark-recapture data from the main trawl ground. *CCAMLR Science* 18, 29-45.

Chen S., Watanabe S. (1989) Age dependence f natural mortality coefficient in fish population dynamics. *Nippon Suisan Gakkaishi* 55, 205-208.

Collins M.A., Brickle P., Brown J., Belchier M. (2010) The Patagonian toothfish: biology, ecology, and fishery. *Advances in Marine Biology* 58, 227-300.

Day J., Wayte S., Haddon M., Hillary R. (2014) Stock assessment of the Macquarie Island fishery for Patagonian toothfish (*Dissostichus eleginoides*) using data up to and including August 2013. *Report to SARAG* 48, 1 April 2014. CSIRO, Australia.

des Clers S., Nolan C.P., Baranowski R., Pompert J. (1996) Preliminary stock assessment of the Patagonian toothfish longline fishery around the Falkland Islands. *Journal of Fish Biology* 49, 145-156.

FIFD (2013) Toothfish stock assessment and TAC 2013-2014. *Vessel Units, Allowable Effort, and Allowable Catch 2014*. Fisheries Department, Directorate of Natural Resources, Falkland Islands Government, 49 pp.

FIFD (2014) Toothfish stock assessment and TAC 2014-2015. *Vessel Units, Allowable Effort, and Allowable Catch 2015*. Fisheries Department, Directorate of Natural Resources, Falkland Islands Government, 54 pp.

FIG (2011) Fisheries Department Fisheries Statistics. *Volume 15, 2010*. Fisheries Department, Directorate of Natural Resources, Falkland Islands Government, 72 pp.

FIG (2014) Sustainability measures 2014 – 2015. Patagonian toothfish (*Dissostichus eleginoides*). Fisheries Department, Directorate of Natural Resources, Falkland Islands Government, 15 pp.

Francis R.I.C.C. (2011) Data weighting in statistical fisheries stock assessment models. *Canadian Journal of Fisheries and Aquatic Sciences* 68, 1124-1138.

Francis R.I.C.C. (2012) The reliability of estimates of natural mortality from stock assessment models. *Fisheries Research* 119-120, 133-134.

Francis R.I.C.C. (2013) DataWeighting: A set of R functions for evaluating and calculating data weights for CASAL. R package version 1.0.

Francis R.I.C.C., Hurst R.J., Renwick J.A. (2003) Quantifying annual variation in catchability for commercial and research fishing. *Fishery Bulletin* 101, 293-304.

Froese R. (2006) Cube law, condition factor and weight–length relationships: history, meta-analysis and recommendations. *Journal of Applied Ichthyology* 22, 241-253.

Hillary R.M., Kirkwood G.P., Agnew D.J. (2006) An assessment of toothfish in subarea 48.3 using CASAL. *CCAMLR Science* 13, 65-95.

Hoenig J.M. (1983) Empirical use of longevity data to estimate mortality rates. *Fishery Bulletin* 82, 898-903.

Kenchington T.J. (2014) Natural mortality estimators for information-limited fisheries. *Fish and Fisheries* 15, 533-562.

Laptikhovsky V., Arkhipkin A., Brickle P. (2006) Distribution and reproduction of the Patagonian toothfish *Dissostichus eleginoides* Smitt around the Falkland Islands. *Journal of Fish Biology* 68, 849-861

Laptikhovsky V., Arkhipkin A., Brickle P. (2008) Life history, fishery, and stock conservation of the Patagonian toothfish around the Falkland Islands. *American Fisheries Society Symposium* 49, 1357-1363.

Laptikhovsky V., Brickle P. (2005) The Patagonian toothfish fishery in Falkland Islands' waters. *Fisheries Research* 74, 11-23.

Lee H.-H., Maunder M.N., Piner K.R., Methot R.D. (2011) Estimating natural mortality within a fisheries stock assessment model: An evaluation using simulation analysis based on twelve stock assessments. *Fisheries Research* 109, 89-94.

Lee H.-H., Maunder M.N., Piner K.R., Methot R.D. (2012) Reply to 'The reliability of estimates of natural mortality from stock assessment models'. *Fisheries Research* 119-120, 154-155.

Legault C.M. (2009) Report of the retrospective working group. *Northeast Fisheries Science Center Reference Document* 09-01, NOAA, U.S. Department of Commerce, 30 pp.

Mangel M., MacCall A.D., Brodziak J., Dick E.J., Forrest R.E., Pourzand R., Ralston S. (2013). A perspective on steepness, reference points, and stock assessment. *Canadian Journal of Fisheries and Aquatic Sciences* 70, 930-940.

Manning M. (2011) CPUE: A collection of functions for standardised CPUE analysis. R package version 1.1.

Maunder M.N., Punt A.E. (2004) Standardizing catch and effort data: A review of recent approaches. *Fisheries Research* 70, 141-159.

Maunder M.N., Starr P.J. (2003) Fitting fisheries models to standardised CPUE abundance indices. *Fisheries Research* 63, 43-50.

Moreno C.A., Castro R., Mujica L., Reyes P. (2008) Significant conservation benefits obtained from the use of a new fishing gear in the Chilean Patagonian toothfish fishery. *CCAMLR Science* 15, 79-91.

Mormede S., Dunn A., Hanchet S.M. (2014) A stock assessment model of Antarctic toothfish (*Dissostichus mawsoni*) in the Ross Sea region incorporating multi-year mark-recapture data. *CCAMLR Science* 21, 39-62.

Nelson G.A. (2015) Package 'fishmethods': Fishery science methods and models from published literature and contributions from colleagues. R package version 1.9-0.

Payá I., Brickle P. (2008) Stock assessment and total allowable catch of toothfish (*Dissostichus eleginoides*), 2008. *Fisheries Department Scientific Report*, Falkland Islands Government, 42pp.

Payne A.G., Agnew D.J., Brandão A. (2005) Preliminary assessment of the Falklands Patagonian toothfish (*Dissostichus eleginoides*) population: Use of recruitment indices and the estimation of unreported catches. *Fisheries Research* 76, 344-358.

Shono H. (2005) Is model selection using Akaike's information criterion appropriate for catch per unit effort standardization in large samples? *Fisheries Science* 71: 978-986.

Winter A. (2015) Falkland calamari stock assessment. *2nd season 2015*. Fisheries Department, Directorate of Natural Resources, Falkland Islands Government, 25 pp.

4.7. Appendix

4.7.1. CPUE standardization

Longline CPUE was standardized to remove the effect of co-variates other than yearly abundance (Maunder and Punt 2004). Co-variate effects were estimated by fitting longline CPUE to a generalized linear model (GLM) in log scale with normal error distribution, because CPUE is usually log-normally distributed (Maunder and Starr 2003). Significant co-variates were added to the year effect by forward selection using the function 'stepCPUE' in R package 'CPUE' (Manning 2011). Because AIC can bias co-variate effects (Shono 2005), the criterion for co-variate significance was set instead by the r^2 of the GLM fit, at an increase of 0.5%. Error of the indices was expressed as the coefficients of variation (cv) calculated from the covariance matrices, plus 20% to account for process error (Francis et al. 2003): $\sqrt{cv^2 + 0.20^2}$. Standardization co-variates tested were the individual vessel, month, soak duration of the reported catch, depth (expressed as a 3-degree polynomial function ($c + x + x^2 + x^3$) to relax the assumption that the relationship between CPUE and depth would have to be linear), and fishing region (3 regions: north or south of 53.5° within the Falklands zone, or outside the Falklands zone). The 53.5° S demarcation separates the Burdwood Bank spawning area from fishing further north (Payne et al. 2005).

4.7.2. Model input parameters

length-weight model ($W(t) = a \cdot L(cm)^b$):

a	5.165041×10^{-9}
b	3.149191
N	22,605

von Bertalanffy length-at-age model ($L(cm) = L_{inf} \times (1 - e^{-K(t - t0)})$):

K	0.059996
t_0	-1.399824
L_{inf}	158.833377
cv	0.154907
N	3,539

maturity proportions at age:

Age	N	Prop. Mature	Age	N	Prop. Mature
1	939	0.000	17	6363	0.494
2	6514	0.001	18	6484	0.516
3	4496	0.010	19	4729	0.537
4	3296	0.024	20	3617	0.557
5	4537	0.044	21	3582	0.576
6	3367	0.072	22	2414	0.593
7	4844	0.109	23	1529	0.609
8	4553	0.152	24	1222	0.623
9	4823	0.200	25	1312	0.637
10	4862	0.249	26	1078	0.651
11	5712	0.297	27	707	0.666
12	7331	0.341	28	566	0.683
13	7511	0.380	29	281	0.700
14	7737	0.414	30	262	0.717
15	7806	0.444	31+	1916	0.789
16	7336	0.470			

4.7.3. MSY deduction

Spawning stock biomass corresponding to the toothfish catch in each fishery in 2015 was projected forward for 51 years (starting age 1 to age 52, the maximum known age of Falklands toothfish), discounting each year for natural mortality[8] and incrementing the year for its gain in maturity per age distribution. Age distributions were taken from the observer-sampled random length distributions and the size-at-age measurements.

$$age\ W\ prop_{year\ i\ fishery\ f}|_1^{31+} = \left(age\ N\ prop_{year\ i\ fishery\ f} \times weight_{age}\right)|_1^{31+}$$

$${}_{catch}SSB_{year\ i\ fishery\ f} = \sum_{age\ =\ 1}^{31+} \left({}_{catch}B_{year\ i\ fishery\ f} \times age\ W\ prop|_1^{31+} \times maturity\ prop|_1^{31+}\right)$$

$${}_{catch}SSB_{year\ i+1\ fishery\ f} = {}_{catch}SSB_{year\ i\ fishery\ f} \times e^{-M}$$

where

${}_{catch}B_{year\ i\ =\ 2015\ fishery\ f\ =\ LL}$	=	1123.2 tonnes
${}_{catch}B_{year\ i\ =\ 2015\ fishery\ f\ =\ FLN}$	=	103.1 tonnes
${}_{catch}B_{year\ i\ =\ 2015\ fishery\ f\ =\ LOL}$	=	6.6 tonnes

and age proportions in 2015 :

[8] The age-invariant natural mortality optimized in the age-structured production model. Natural mortality actually decreases rapidly in the first few years then increases in late years as a fish approaches senescence (Chen and Watanabe 1989), but modelling this curve is rarely applied (Kenchington 2014).

Age	Catch Proportion N			Age	Catch Proportion N		
	LL	FIN	LOL		LL	FIN	LOL
1	0.00000	0.12771	0.41284	17	0.05946	0.00000	0.00000
2	0.00000	0.19036	0.37639	18	0.06354	0.00000	0.00000
3	0.00029	0.21783	0.13296	19	0.04809	0.00000	0.00000
4	0.00058	0.20048	0.04230	20	0.03060	0.00000	0.00000
5	0.01078	0.17060	0.02550	21	0.02507	0.00000	0.00000
6	0.02507	0.06602	0.00453	22	0.02390	0.00000	0.00000
7	0.04693	0.02024	0.00302	23	0.01224	0.00000	0.00000
8	0.03818	0.00048	0.00113	24	0.01049	0.00000	0.00000
9	0.05013	0.00145	0.00057	25	0.01282	0.00000	0.00000
10	0.04955	0.00145	0.00019	26	0.00758	0.00000	0.00000
11	0.05829	0.00145	0.00038	27	0.00816	0.00000	0.00000
12	0.08540	0.00048	0.00019	28	0.00466	0.00000	0.00000
13	0.07491	0.00048	0.00000	29	0.00291	0.00000	0.00000
14	0.08219	0.00048	0.00000	30	0.00262	0.00000	0.00000
15	0.08219	0.00048	0.00000	31+	0.01807	0.00000	0.00000
16	0.06529	0.00000	0.00000				

The forward projection calculated that the biomass of toothfish caught in the longline fishery in 2015 (1123.2 t), if not caught and subject only to natural mortality, would have yielded an average annual spawning stock biomass of 114.3 t between 2016 and 2067; thus 0.102 t per t caught in 2015. Equivalently for all three fisheries:

Fishery	TOO Catch 2015	Avg. SSB 2016-2067	Avg. SSB / 2015 Catch
LL	1123.2 t	114.3 t	0.102
FIN	103.1 t	27.3 t	0.264
LOL	6.6 t	3.5 t	0.533

Accordingly, toothfish bycatch in finfish trawls removes 0.264 / 0.102 = 2.60× more potential future growth per unit weight from the population than toothfish longline catch, and toothfish bycatch in *Loligo* trawls removes 0.264 / 0.102 = 5.24× more potential future growth per unit weight from the population than toothfish longline catch.

5. Skates

5.1. Summary

- In 2015, skate catch by skate-licensed trawlers was reported at 2365.3 tonnes, out of a total skate catch (all fisheries) of 6487.2 tonnes. The total skate catch in 2015 was the third-highest since 1993, after 2011 and 2012
- Stock assessment of the multi-species skate assemblage was calculated with a Schaefer production model. The model was optimized on CPUE indices of Korean and Spanish target trawl catches north of 51°S, with penalty functions for survey biomass estimates calculated in 2010 and 2013, carrying capacity ≥ initial biomass, and current biomass > maximum sustainable yield.
- The Schaefer production model estimated skate biomass north of 51°S in 2015 at 39,733 tonnes (95% confidence interval 33,838 to 81,133 tonnes) and maximum sustainable yield at 6,726 tonnes (95% confidence interval 5,907 to 60,079 tonnes).
- Among the four predominant species, individual species CPUE time series continued to show increasing trends for *Bathyraja albomaculata* and *Bathyraja brachyurops*. The CPUE time series for *Zearaja chilensis* showed a significant downturn for the past two years, and the CPUE trend for *Bathyraja griseocauda* levelled off with a non-significant decreasing trend.

5.2. Introduction

Skate catches (Rajiformes) have been reported in Falkland Islands waters since 1987. Skate catches were low until the stocks were commercially recognized by a Korean trawl fleet in the early 1990s (Wakeford et al. 2005), but rapidly increased >5000 tonnes year^{-1}. Given the strong targeted effort, skate trawling was licensed separately from other trawl fisheries starting in 1994 (Wakeford et al. 2005). Two skate fishing regions were identified: north and south of the Falkland Islands, and the southern region soon showed signs of decreasing catch (Agnew et al. 2000; Wakeford et al. 2005). As a conservation measure, directed fishing for skates was prohibited south of 51°S in 1996 (Agnew et al. 1999).

Directed fishing for skates in the north has continued annually. In 2015, skate catch by skate-licensed trawlers was 2365.3 tonnes (Table 1), taken in 54 grid units north of 51 ºS (Figure 1). Of these 54 grid units, 66.9% of skate catch and 48.6% of skate-license effort occurred in just 8 grid units that mainly followed the 200 m isobath (Figure 1). Skate bycatch by other commercial bottom trawls (licensed for finfish or Falkland calamari) was 3954.5 tonnes, taken in 142 grid units around the Falkland Islands. Of these 142 grid units, 47 were among the 54 grid units that had also been fished with skate license; and these accounted for 73.9% of the skate catch by other commercial bottom trawls. Of the total skate bycatch by other commercial bottom trawls, 21.7% was taken by vessels that had also held skate licenses during the year, while representing 14.9% of the effort. Additionally 27.6 tonnes of skate in 2015 were taken as bycatch under longline (L) license, and 0.3 tonnes under *Illex* (B) license. No skate bycatch was taken under surimi (S) license. Total experimental (E license) catch of skate in 2015 was 10.4 tonnes.

FIFD observers sampled skates on 19 fishing vessels in 2015, over a total of 145 sample stations. Fifteen skate species were identified, representing most of the known species in Falkland Islands waters (Arkhipkin et al. 2012). By specimen numbers, 34.7% of skate samples were *Bathyraja brachyurops*, 27.9% *Bathyraja albomaculata*, 18.4% *Zearaja chilensis*, 5.3% *Bathyraja griseocauda*, 4.4% *Bathyraja macloviana*, 3.3% *Amblyraja doellojuradoi*, 2.4% *Bathyraja scaphiops*, 1.3% *Psammobatis* spp., 0.9% *Bathyraja multispinis*, 0.5% *Bathyraja cousseauae*, 0.3% *Dipturus argentinensus*, 0.3% *Amblyraja cf. georgiana*, 0.1% *Bathyraja papilionifera*, 0.1% *Bathyraja magellanica*, 0.1% *Bathyraja meridionalis*.

Stock assessment for license allocation was again based on the multi-species skate complex, as species are not identified in vessel catch reports (Agnew et al. 2000, Wakeford et al. 2005, Winter et al. 2015). However, annual CPUE trends are reported for six major species of interest (Winter et al. 2015).

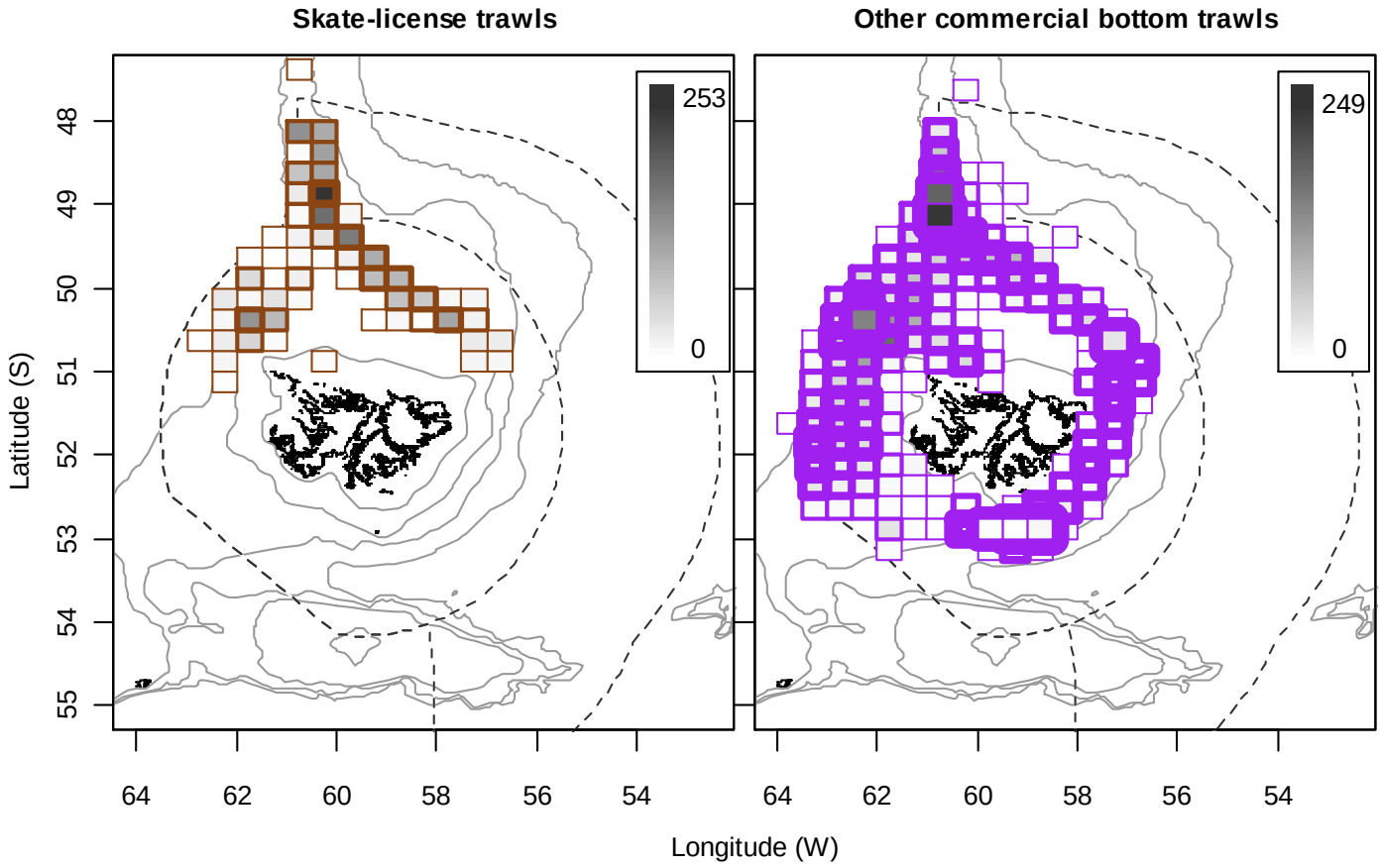

Figure 1. Distribution of skate catches by grid under skate license (left) and other bottom-trawl licenses (right) in 2015. Thickness of grid lines is proportional to the number of vessel-days (1 to 17 for skate license, left; 1 to 256 for other bottom-trawl licenses, right). Gray-scale is proportional to the skate catch biomass (maximum 253.3 tonnes in one grid unit for skate license, left; maximum of 248.8 tonnes for other bottom-trawl licenses, right).

5.3. Methods

The skate stock assessment calculated last year (Section 5 in FIFD, 2015) was updated with the most recent year's catch and effort report data. All skate catches from all years are entered according to the revised conversion factors (Winter and Pompert 2014). The current skate stock assessment was calculated as a Schaefer production model (Schaefer 1954), expressed as a difference equation:

$$B_{t+1} = B_t + rB_t\left(1 - \frac{B_t}{K}\right) - C_t$$

where B_t and C_t are the stock biomass and catch in year t; r is the intrinsic population growth rate and K is the carrying capacity. The Schaefer production model was optimized on time series indices of standardized CPUE. In previous years (e.g., FIFD 2015) the CPUE index of Korean skate-license trawls north of 51°S was used solely for optimization, as this CPUE index had been found to be the most consistent (Laptikhovsky et al. 2011). However, recent revelations of potential catch misreporting in the skate fishery (B. Meehan, FIFD, pers. comm.) have motivated an approach to mitigate reliance on one single index. For this assessment the Schaefer production model was instead optimized on an objective function comprising the negative log-likelihood functions of both Korean and Spanish skate-license CPUE trawl indices north of 51°S:

$$\mathbf{L}\{\mathbf{CPUE}_{Korea\,N}, \mathbf{CPUE}_{Spain\,N} \mid \mathbf{parameters}\} = \mathbf{L}\{\mathbf{CPUE}_{Korea\,N} \mid \mathbf{K}, \mathbf{B_1}, \mathbf{r}, \mathbf{q}_{Korea\,N}\} + \mathbf{L}\{\mathbf{CPUE}_{Spain\,N} \mid \mathbf{K}, \mathbf{B_1}, \mathbf{r}, \mathbf{q}_{Spain\,N}\}$$

where

$$\mathbf{L}\{\mathbf{CPUE}_{Korea\,N} \mid \mathbf{K}, \mathbf{B_1}, \mathbf{r}, \mathbf{q}_{Korea\,N}\} = \mathbf{n}\left(\log(\sigma_{Korea\,N}) + \frac{\log(2\pi)}{2}\right) + \frac{\sum_t\left(\log(B_t) - \log(\mathbf{CPUE}_{Korea\,N\,t} / \mathbf{q}_{Korea\,N})\right)^2}{2\sigma^2_{Korea\,N}}$$

Equivalently, substitute *Spain N* for *Korea N*; notation following Hilborn and Mangel (1997); n is the length of time series t observations, q is the catchability coefficient of the CPUE index expressed as kg of skate catch per trawl hour, and σ is the standard deviation between $\log(B_t)$ and $\log(CPUE_t / q_t)$:

$$\sigma_{Korea\,N} = \sqrt{\left(\log(B_t) - \log(\mathbf{CPUE}_{Korea\,N\,t} / \mathbf{q}_{Korea\,N})\right)^2}$$

$CPUE_{Korea\ N}$ and $CPUE_{Spain\ N}$ were standardized for latitude, longitude, month and depth using generalized additive models (GAM). Annual skate catch and effort data from 1989 through 2015 were included. Skate licenses have been implemented since 1994 (Wakeford et al. 2005), and a probabilistic algorithm (FIFD 2013) was used to infer which Korean trawls were actually targeting skates in the years 1989 to 1993, before the issuance of skate licenses. The two earliest years 1987 and 1988 were not

included because catch reporting did not yet distinguish trawls from jigging or longline. The same probabilistic assignment of 1989 to 1993 Korean skate target trawls as last year (FIFD 2015) was applied to the current assessment. The algorithm was not calculated to infer Spanish trawls targeting skates in 1989 to 1993, because in the following years 1994 to 1996, which are used as the template, only 12 days of skate license trawling were taken by a single Spanish vessel (during 1995).

Biomass in the first year of the fishery ($B_1 = B_{1989}$) was optimized as a free parameter in the Schaefer production model. B_1 is sometimes assumed to equal the carrying capacity K (Punt 1990, Hilborn and Mangel 1997), but as skate fishing in Falkland Islands waters was ongoing before 1989 the assumption is unreliable for this fishery, and K and B_1 were optimized separately along with r, $q_{Korea\ N}$, and $q_{Spain\ N}$.

Four penalty terms were added to the Schaefer production model to stabilize the optimization. The first two penalty terms related to skate biomass estimates from FIFD skate surveys conducted in 2010 (Arkhipkin et al. 2010) and 2013 (Pompert et al. 2014). In either survey the 26 grid units were occupied that represented the historic concentration of the skate target fishery (Payá et al. 2008). Because the actual commercial fishery can shift around in any year, the inference was made that the proportion of total commercial skate catch taken in the top 26 grids (not necessarily the exact same ones) should reflect the ratio of survey area biomass to total biomass north of 51 ºS (Laptikhovsky et al. 2011). Survey area biomasses in 2010 and 2013 were estimated from swept-area samples with variability distributions calculated by bootstrap re-sampling (Arkhipkin et al. 2010, Pompert et al. 2014). The proportions of total commercial skate catch taken in the top 26 grids in 2010 and 2013 likewise had variability distributions calculated by bootstrap re-sampling. Combining the two variability distributions, composite estimates of total skate biomass had 95% confidence limits of:

2010	17,832.7	to	50,198.3 tonnes
2013	14,494.1	to	82,840.4 tonnes

The penalty function was implemented as the log squared difference:

$$\mathbf{P}\{B_{survey\ 2010}, B_{2010} \mid K, B_1, r, q_{Korea\ N}\} = \emptyset \frac{\left(\log\left(B_{survey\ 2010\ min\ /\ max\ 95\%}\right) - \log\left(B_{2010}\right)\right)^2}{2\sigma^2_{Korea\ N}}$$

where $\emptyset = 0$ if the B_{2010} iteration of the optimization was within the 95% confidence limits of the 2010 survey estimate, and $\emptyset = 1$ if the B_{2010} iteration was outside the 95% confidence limits of the 2010 survey estimate. (Again, equivalently substitute *Spain N* for *Korea N*, and / or survey 2013 for survey 2010). The third penalty term was for $K \geq B_1$ (Prager 1994), and the fourth penalty term was for $B_{2015} \geq$ maximum sustainable yield (MSY). The third and fourth penalty terms were likewise calculated as log squared differences and triggered by multipliers $\emptyset = 0$ or 1 according to whether the condition was met.

The Schaefer production model was optimized in R programming code with a Nelder-Mead algorithm (Nash and Varadhan 2011), on both Korean and Spanish CPUE indices and the four penalty functions. The larger number of Korean data automatically gave greater weight to the Korean index. To estimate parameter variability the model was run though a Markov Chain Monte Carlo (MCMC) with

5×10^6 iterations of which the first 20,000 were discarded as burn-in, and every tenth iteration was retained to mitigate autocorrelation. The set of 498,000 retained MCMC iterations was used to generate 95% confidence intervals for each of the optimization parameters K, B_1, r, $q_{Korea\ N}$ and $q_{Spain\ N}$, and for MSY calculated as (Hilborn and Walters 1992):

$$\mathrm{MSY} = \frac{\mathrm{rK}}{4}.$$

Table 5.1. For the fishery north of 51ºS latitude*, yearly total skate catches under target license (F/R), yearly total skate catches under other licenses, and standardized skate CPUE index of Korean and Spanish target trawls. Skate target and non-target licenses were not discriminated before 1994.

Year	Catch (tonnes)		CPUE (t/hr)	
	target	non-target	Korean target trawl	Spanish target trawl
1989	812.92		0.33	-
1990	787.03		0.47	-
1991	5806.63		0.39	-
1992	3314.25		0.27	-
1993	5465.51		0.28	-
1994	2186.32	1932.34	0.35	-
1995	3623.42	862.35	0.30	0.09
1996	1927.08	791.01	0.23	-
1997	1976.42	593.86	0.33	-
1998	226.63	396.65	0.42	-
1999	3467.83	417.58	0.38	-
2000	2511.36	549.27	0.33	-
2001	3406.68	542.06	0.40	-
2002	2194.42	495.94	0.44	-
2003	3137.54	479.57	0.43	-
2004	3881.38	473.34	0.43	-
2005	4396.01	594.41	0.51	-
2006	2711.47	1229.93	0.50	-
2007	3527.83	1300.19	0.63	0.45
2008	2280.21	1067.41	0.54	0.49
2009	2932.08	1916.39	0.62	0.62
2010	2725.08	2040.46	0.67	0.44
2011	2572.93	2781.54	0.59	0.34
2012	3094.04	2377.99	0.77	0.60
2013	2223.73	2478.56	0.60	0.39
2014	2953.40	2128.40	0.65	0.84
2015	2365.28	3187.47	0.74	0.38

* Skate-license fishing has been restricted to north of 51ºS latitude since 1996. Target catches before 1996, and non-target catches before and since 1996 listed in the table are thus not total catches of skate.

The assessment of total skate biomass can potentially mask changes in assemblage composition, with species more vulnerable to fishing pressure replaced by more resilient species (Dulvy et al. 2000, Ruocco et al. 2012). Agnew et al. (2000), Wakeford et al. (2005), and Winter et al. (2015) examined species composition trends in the Falkland Islands skate fishery. For the current stock assessment, CPUE time-series trends were updated and examined for the six species of interest described in Winter et al. (2015): *B. albomaculata*, *B. brachyurops*, *Z. chilensis*, *B. griseocauda*, *B. multispinis* and *B. scaphiops*. Skate CPUE were calculated from all trawl stations under skate license (or inferred to be skate-targeting prior to 1994; FIFD 2013), north of 51°S, that had observer reports of catch by species. CPUE trends were calculated according to methods slightly simplified from Winter et al. (2015), with CPUE per station GAM-standardized for latitude, longitude, month, depth and nation (Korea or Spain), and the inter-annual trends smoothed using locally-weighted regression (LOESS). Variability of the trends was estimated by randomly resampling with replacement the yearly stations and recalculating the LOESS for each resample. Resampling was iterated 5000× for each species. In several (particularly early) years, some stations recorded various amounts of both identified skate species and the unidentified code 'RAY'. For these stations the unidentified RAY was then assigned to the identified species as the lesser of either the proportion of identified species among themselves or the ratio of each identified species to the unidentified RAY. The latter option was mainly to prevent large amounts of unidentified RAY being assigned to single identified species at a station. For variability estimation, stations with both identified skate species and RAY were additionally randomized at each iteration by setting the proportional assignment for an identified species to a random uniform draw between zero and 2× the ratio of the identified species to the unidentified RAY (up to a maximum of the total amount of unidentified RAY). Stations that reported only RAY and no identified skate species were excluded altogether as it would be incorrect to record these as having zero catch of any one skate species.

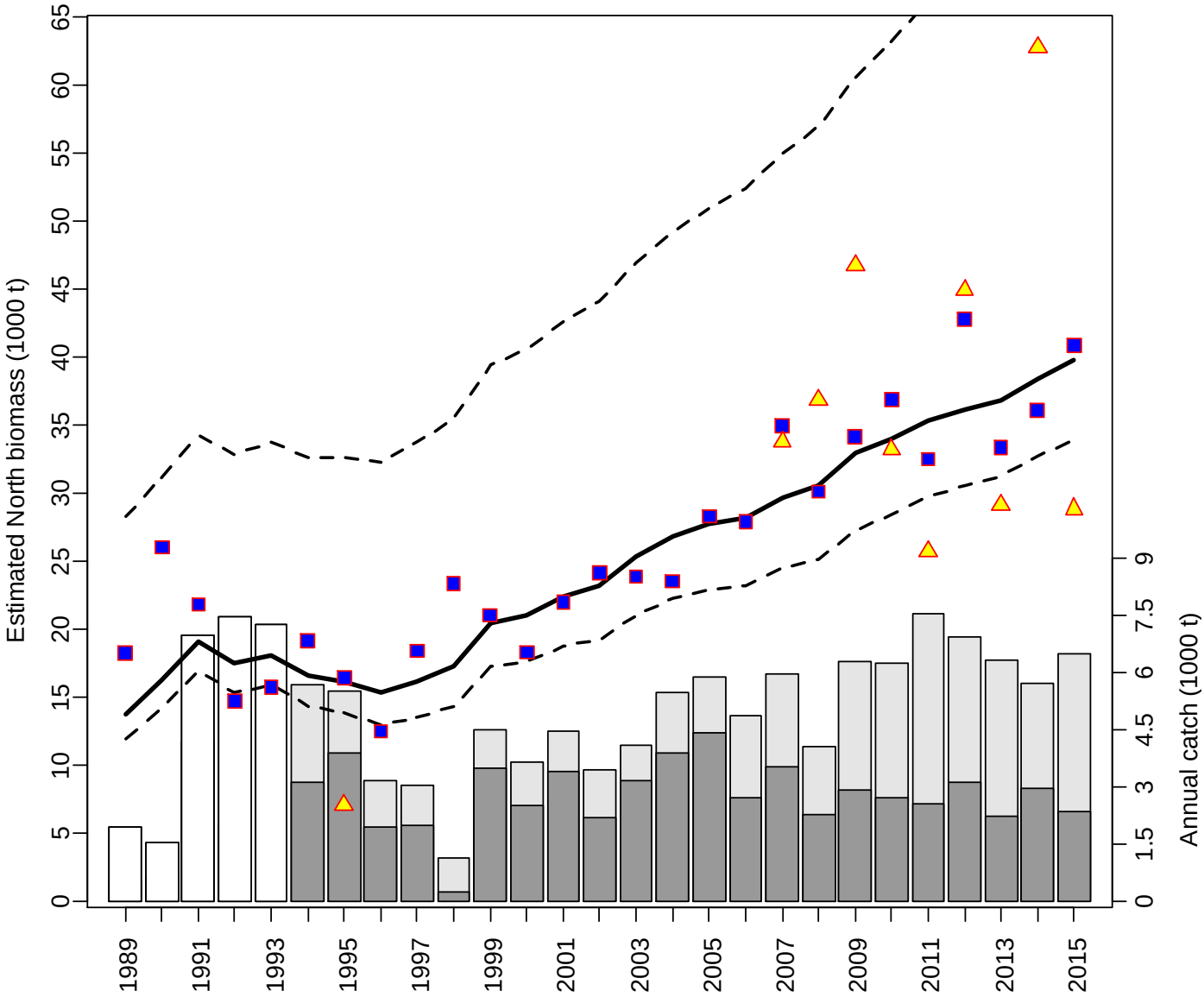

Figure 2. F/R-licensed skate catches (dark grey bars), non-target-licensed skate catches (light grey bars), indiscriminate license catches (white bars), estimated biomass of the northern skate stock ± 95% confidence intervals (black lines), and CPUE indices the biomass time series was optimized on: Korean target trawls (blue squares) and Spanish target trawls (yellow triangles). The figure is formatted for comparison with Figure 3A in Wakeford et al. (2005).

5.4. Results

Skate catch north of 51°S was 5552.75 t in 2015, the highest since 1991. While target catch was unexceptional, the non-target skate catch north of 51°S was the highest on record since the start of separate skate licensing in 1994 (Table 1). Total skate catch (north + south) was the third-highest since 1993, after 2011 and 2012 (Figure 2). The proportion of target skate catch vs. total skate catch (north and south) was 36.5% in 2015, a sharp drop from the year before but higher than in 2013 and 2011. The Korean target trawl standardized CPUE in 2015 was the 2nd highest on record after

2012, at 0.74 t hr^{-1}. The Spanish target trawl standardized CPUE (used for the first time in this assessment) included one vessel fishing skate 12 days in 1995, then no fishing effort again until 2007. In contrast to the high Korean CPUE, the Spanish CPUE in 2015 was the second-lowest since 2007 at 0.38 t hr^{-1} (Table 1).

Production model fit parameters for total skate biomass north of 51 ºS are summarized in Table 2 together with their 95% confidence intervals from the MCMC. Notwithstanding the addition of the Spanish CPUE index, a similar outcome as in previous assessments was obtained: very wide bounding of the carrying capacity K and heavily right-skewed biomass estimates. The optimum skate biomass estimate for 2015 was 39,733 tonnes, and the maximum sustainable yield estimate 6,726 tonnes.

Table 5.2. Optimized Schaefer production model parameters obtained with the combination of Korean and Spanish target trawl CPUE indices, plus resulting estimates of year 2015 biomass north of 51 ºS latitude and MSY. 95% confidence intervals from MCMC iteration of the production model.

Parameter	CPUE target trawl indices	
	optimum	95% conf. int.
K	99,283	80,872 - 1,500,828
B_{1989}	13,780	11,867 - 28,225
r	0.271	0.134 - 0.304
q_{Korea}	1.81 e^{-5}	0.94 e^{-5} - 2.11 e^{-5}
q_{Spain}	1.33 e^{-5}	0.65 e^{-5} - 1.70 e^{-5}
B_{2015}	39,733	33,838 - 81,133
MSY	6,726	5,907 - 60,079

The time series of skate species catch data extended from 1993 to 2015, with data absent in years 1998, 1999, 2005 and 2008 (Table 3). *B. albomaculata* (RAL) and *B. brachyurops* (RBR) continued the increasing CPUE trends that had been noted in Winter et al. (2015), albeit with high variability in recent years (Figure 3). *Z. chilensis* (RFL) CPUE increased consistently through 2013, then followed with two low years in 2014 and 2015. The resulting downturn of the LOESS CPUE trend (Figure 3) was statistically significant by the criterion that a horizontal line would intersect the lower and upper 95% confidence intervals (Swartzman et al. 1992). *B. griseocauda* (RGR) CPUE likewise decreased in 2014 and 2015 to the lowest levels since 2004 (Table 3), but the downturn of the LOESS trend did not meet the criterion of being statistically significant (so far; through 2015, Figure 3). Both of the two less abundant species *B. multispinis* (RMU) and *B. scaphiops* (RSC) had lower CPUE in 2014 and 2015, resulting in a plateau for RMU and a statistically significant decrease for RSC (Figure 3).

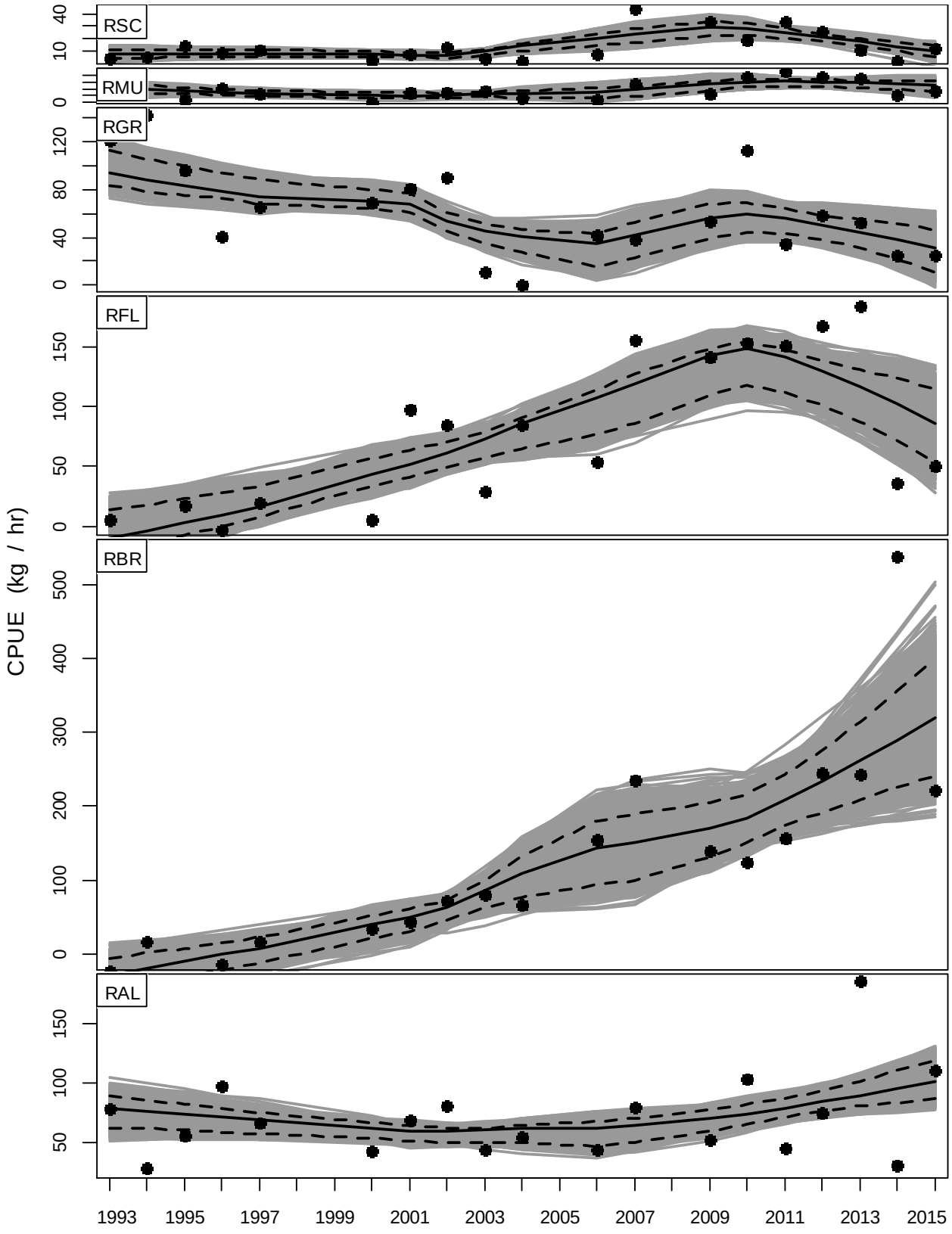

Figure 5.3. LOESS trends (solid black lines) and 95% confidence intervals (broken black lines) of standardized CPUE by species, 1993 to 2015. Confidence intervals are derived from the randomized iterations (grey lines). Empirical estimates (black circles) correspond to Table 5.3.

Table 5.3. GAM standardized CPUE (kg hr^{-1}) per year per species from observer catch data; N = number of observer-sampled stations. Standardized CPUE values correspond to the black circles on Figure 3. Note that the standardization (with residual error added back) resulted in some negative values in some years. These were not corrected, to maintain the relative changes of the inter-annual trends.

Year	N	RAL	RBR	RFL	RGR	RMU	RSC
1989	0	-	-	-	-	-	-
1990	0	-	-	-	-	-	-
1991	0	-	-	-	-	-	-
1992	0	-	-	-	-	-	-
1993	35	78.9	-23.0	5.4	121.8	16.0	4.6
1994	11	28.2	15.8	-18.8	142.5	-9.7	5.8
1995	19	56.5	-33.8	17.2	96.0	2.0	14.6
1996	53	97.6	-14.2	-2.8	40.8	11.0	9.2
1997	60	67.1	16.0	19.4	66.2	6.7	11.4
1998	0	-	-	-	-	-	-
1999	0	-	-	-	-	-	-
2000	76	42.7	33.7	5.6	69.5	0.0	3.4
2001	72	68.6	42.9	97.4	80.5	7.4	8.0
2002	69	80.8	73.1	84.5	90.2	7.5	14.1
2003	54	44.8	79.3	29.4	11.5	8.0	5.5
2004	57	54.8	66.1	84.8	-0.3	3.4	2.9
2005	0	-	-	-	-	-	-
2006	29	44.4	155.6	54.6	41.4	2.2	7.9
2007	35	79.7	235.6	155.6	37.8	13.5	43.4
2008	0	-	-	-	-	-	-
2009	50	52.7	138.6	141.1	54.1	6.4	33.4
2010	57	103.1	123.5	153.9	113.7	19.0	19.9
2011	55	45.2	155.9	151.3	34.5	22.8	34.2
2012	70	75.2	244.0	167.9	58.6	18.5	26.6
2013	33	184.7	242.1	184.5	52.2	18.1	11.3
2014	29	30.6	539.1	37.0	25.3	5.5	2.7
2015	43	111.0	221.2	51.0	24.7	8.6	12.6

5.5. Conclusions

Total skate CPUE in the commercial skate-target fishery continued to show an increasing trend in 2015, ongoing since 1996 (Figure 2). The resulting lack of contrast in the time series obtained an imprecise optimization of the Schaefer production model, particularly for carrying capacity K (Table 2). Carrying capacity may be especially unstable in a production model as cumulative changes in reproductive parameters, juvenile and adult survival, growth, and predator and prey interactions contribute to fluctuations in carrying capacity over time (Quinn 2003). However, the optimum model parameters and MSY estimate of this assessment were generally similar to previous years' estimates (e.g., FIFD 2015); indicative that total skate

biomass in the Falkland Islands zone appears stable. The ratio of catchability coefficients between Spanish and Korean vessels from joint model optimization (Table 2: 1.33 / 1.81 = 0.737) was higher than - but comparable to - the estimate of 0.600 made after the 2013 skate survey (Pompert et al. 2014).

Use of combined CPUE indices for assessment of the multi-species skate assemblage (Wakeford et al. 2005) remains a potential source of error. Maunder et al. (2006) noted that CPUE is not proportional to community abundance if q (catchability coefficient) is not similar for all species being combined. The species with the highest catchability may contribute a greater proportion to the combined CPUE, and represent the population that is most depleted. Given this issue, for the current skate assessment the examination of individual species' CPUE trends was reprised from Winter et al. (2015), with one year's older data (1993) and two years' more recent data (2014-2015). For several species, the CPUE trend is now less positive than indicated up to 2013 (Winter et al. 2015). In particular, the long increasing trend of *Z. chilensis*, a vulnerable species according to the IUCN (Kyne et al. 2007), has reversed. The recovery of *B. griseocauda*, an endangered species (McCormack et al. 2007), appears to have stalled. Continuing surveillance of skate species trends in the Falkland Islands fishery will be required.

5.6. References

Agnew, D.J., Nolan, C.P., Pompert, J. 1999. Management of the Falkland Islands skate and ray fishery. In: Case studies of the Management of Elasmobranch Fisheries (R. Shotton, ed.), FAO, Rome, pp. 268-284.

Agnew, D.J., Nolan, C.P., Beddington, J.R., Baranowski, R. 2000. Approaches to the assessment and management of multispecies skate and ray fisheries using the Falkland Islands fishery as an example. Canadian Journal of Fisheries and Aquatic Sciences 57: 429-440.

Arkhipkin, A., Brickle, P., Laptikhovsky, V., Pompert, J., Winter, A. 2012. Skate assemblage on the eastern Patagonian Shelf and Slope: structure, diversity and abundance. Journal of Fish Biology 80:1704-1726.

Arkhipkin, A., Winter, A., Pompert, J. 2010. Cruise Report, ZDLT1-10-2010, Skate Biomass survey. Fisheries Dept., Directorate of Natural Resources, Falkland Islands Government, 43 p.

Dulvy, N.K., Metcalfe, J.D., Glanville, J., Pawson, M.G., Reynolds, J.D. 2000. Fishery stability, local extinctions, and shifts in community structure in skates. Conservation Biology 14: 283-293.

FIFD. 2013. Vessel Units, Allowable Effort, and Allowable Catch 2014. Fisheries Dept., Directorate of Natural Resources, Falkland Islands Government, 49 p.

FIFD. 2015. Vessel Units, Allowable Effort, and Allowable Catch 2016. Fisheries Dept., Directorate of Natural Resources, Falkland Islands Government, 44 p.

Hilborn, R., Mangel, M. 1997. The Ecological Detective. Monographs in Population Biology 28, Princeton University Press, 315 p.

Hilborn, R., Walters, C.J. 1992. Quantitative Fisheries Stock Assessment. Chapman and Hall, New York, 570 p.

Kyne, P.M., Lamilla, J., Licandeo, R.R., San Martín, M.J., Stehmann, M.F.W., McCormack, C. 2007. Zearaja chilensis. The IUCN Red List of Threatened Species. Version 2014.3. At www.iucn.redlist.org/details/63147/0.

Laptikhovsky, V., Winter, A., Brickle, P., Arkhipkin, A. 2011. Vessel units, allowable effort, and allowable catch 2012. Technical Document, FIG Fisheries Department, 27 p.

Maunder, M.N., Sibert, J.R., Fonteneau, A., Hampton, J., Kleiber, P., Harley, S.J. 2006. Interpreting catch per unit effort data to assess the status of individual stocks and communities. ICES Journal of Marine Science 63: 1373-1385.

McCormack, C., Lamilla, J., San Martín, M.J., Stehmann, M.F.W. 2007. Bathyraja griseocauda. The IUCN Red List of Threatened Species. Version 2014.3. At www.iucn.redlist.org/details/63113/0.

Nash, J.C., Varadhan, R. 2011. optimx: A replacement and extension of the optim() function. R package version 2011-2.27. http://CRAN.R-project.org/package=optimx

Payá, I., Schuchert, P., Dimmlich, W., Brickle, P. 2008. Vessel Units, Allowable Effort, and Allowable Catch 2009. Fisheries Dept., Directorate of Natural Resources, Falkland Islands Government, 29 p.

Pompert, J., Brewin, P., Winter, A., Blake, A. 2014. Scientific Cruise ZDLT1-11-2013. Fisheries Dept., Directorate of Natural Resources, Falkland Islands Government, 72 p.

Prager, M.H. 1994. A suite of extensions to a nonequilibrium surplus-production model. Fishery Bulletin 92: 374-389.

Punt, A. E. 1990. Is B_1 = K an appropriate assumption when applying an observation error production-model estimator to catch-effort data? South African Journal of Marine Science 9: 249-259.

Quinn II, T.J. 2003. Ruminations on the development and future of population dynamics models in fisheries. Natural Resource Modeling 16: 341-392.

Ruocco, N.L., Lucifora, L.O., Díaz de Astarloa, J.M., Menni, R.C., Mabragaña, E., Giberto, D.A. 2012. From coexistence to competitive exclusion: can overfishing change the outcome of competition in skates? Latin American Journal of Aquatic Research 40: 102-112.

Schaefer, M.B. 1954. Some aspects of the dynamics of populations important to the management of commercial marine fisheries. Bulletin of the IATTC 1: 27-56.

Swartzman, G., Huang, C., Kaluzny, S. 1992. Spatial analysis of Bering Sea groundfish survey data using generalized additive models. Canadian Journal of Fisheries and Aquatic Sciences 49: 1366-1378.

Wakeford, R.C., Agnew, D.J., Middleton, D.A.J., Pompert, J.H.W., Laptikhovsky, V.V. 2005. Management of the Falkland Islands multispecies ray fishery: Is species-specific management required? Journal of Northwest Atlantic Fishery Science 35: 309-324.

Winter, A., Pompert, J. 2014. Re-evaluation of skate catch weight reports with reference to the use of conversion factors. Fisheries Dept., Directorate of Natural Resources, Falkland Islands Government, 31 p.

Winter, A., Pompert, J., Arkhipkin, A., Brewin, P. 2015. Interannual variability in the skate assemblage on the South Patagonian shelf and slope. Journal of Fish Biology 87: 1449-1468.